수의학박사 학위논문

Development of basic assisted reproductive technologies for Selachimorpha

상어에서의 기초 보조생식기술 연구

2022 년 2 월

서울대학교 대학원

수의학과 수의병인생물학 및 예방수의학 전공

김 상 화

Development of basic assisted reproductive technologies for Selachimorpha

By

Sang Wha Kim

February, 2022

Major in Veterinary Pathobiology and Preventive Medicine

Department of Veterinary Medicine

Graduate School of Seoul National University

Development of basic assisted reproductive technologies for Selachimorpha

By

Sang Wha Kim

Supervisor: Professor Se Chang Park, D.V.M., Ph.D.

A dissertation submitted to the faculty of the Graduate School of Seoul National University in partial fulfillment of the requirements for the degree of Doctor of Philosophy in Veterinary Pathobiology and Preventive Medicine

February, 2022

Major in Veterinary Pathobiology and Preventive Medicine
Department of Veterinary Medicine
Graduate School of Seoul National University

Development of basic assisted reproductive technologies for Selachimorpha

상어에서의 기초 보조생식기술 연구

지도교수: 박 세 창

이 논문을 수의학박사 학위논문으로 제출함

2021 년 10 월

서울대학교 대학원

수의학과 수의병인생물학 및 예방수의학 전공

김 상 화

김상화의 수의학박사 학위논문을 인준함

2022 년 1 월

위 원 장	윤 화 영	(인)
부위원장	박 세 창	(인)
위 원	김 지 형	(인)
위 원	한 지 은	(인)
위 원	전 진 우	(인)

ABSTRACT

Development of basic assisted reproductive technologies for Selachimorpha

Sang Wha Kim
Major in Veterinary Pathobiology and Preventive Medicine
Department of Veterinary Medicine
The Graduate School of Seoul National University

Shark is a generic term for fish species belonging to the Class Chondrichthyes Superorder Selachimorpha and is a representative animal group that has successfully survived to date among early vertebrates. As they appeared in the early stages of vertebrate formation and thus contain the history of evolution, sharks are important subject of evolutionary biological studies in various aspects such as immunology, reproductive biology, and cancer biology. In addition, sharks play an important role in ecological point of view because they are the apex predators of the marine food chain and are contributing to maintain a balanced and stable ecosystem. It has already been revealed through several previous studies that if the number of sharks become seriously reduced, the entire food chain of the relevant area can collapse. Sharks are thus also called as keystone species because of their high importance.

The problem is that sharks are currently in critical danger of extinction. According to the IUCN Red List, about 37% of chondrocytes are classified into “vulnerable (VU),” “endangered (EN),” and “critically endangered (CR)” groups, facing serious extinction. Decline of population had been perceived since the 1970s, and the biggest contributing factor has been pointed out as fishing, led by the shark's fin industry. Accordingly, conservational efforts have been carried out worldwide to reduce shark fishing, but their endangered status has not been easily improved due to their uniquely slow breeding rate.

Artificial intervention by human is indispensable for the conservation of critically endangered animal species. Assisted reproductive technology has already been developed and applied to conservational works for various endangered species

such as white cranes, Przewalski's horses, elephants, and northern white rhinos. However, in the case of sharks, access to the animals is not easy, so few studies have been conducted thus far. Therefore, in this paper, a series of studies on assisted reproductive technology were conducted to contribute to the shark conservation. First, basic imaging atlas was established, and then shark semen cryopreservation protocol, hormone induced ovulation protocol, and hormone induced semen sampling protocol were developed.

1. As imaging analysis techniques are the basis of veterinary approaches, this study established detailed imaging atlas in sharks using computed tomography (CT) and magnetic resonance imaging (MRI) methods for the first time. Whole-body CT and MRI scans were performed with three young banded houndsharks (*Triakis scyllium*) of around 1 m in total body length, and each individual was cryosectioned into transverse, sagittal, and dorsal planes to compare and analyze with the images from CT and MRI scans. Atlas was established by classifying various organs and tissues in detail. However, it was impossible to confirm the reproductive system as the study was conducted on immature individuals.

2. Experiments were conducted on five male banded houndsharks (*Triakis scyllium*). One hour after 0.2 mL/kg of Ovaprim® administration, the shark's abdomen was gently massaged and the secondary cloudy portion of semen was sampled through urogenital papilla. The composition of an activating extender capable of maximizing the motility of stationary spermatozoa was established,

which was designated as SSAE-1. To establish a cryopreservation protocol optimized for banded houndshark semen, a total of 8 extender solutions, 3 extension ratios, 15 cryoprotectants, 4 equilibration periods, 3 cooling rates, and 3 thawing temperatures were tested. The optimized protocol (Kim's protocol) was as follows: extender, filtered seawater; extension ratio, 1:3; cryoprotectant, egg yolk 10% + ethylene glycol 10%; equilibration period, 10 min; cooling rate, 3 cm, 3 min; thawing temperature, 30℃, 10 s. The resulting post-thaw spermatozoa motility was 2.03%.

3. Experiments were conducted on the ovoviviparous shark banded houndshark (*Triakis scyllium*) and the placental shark (*Triaenodon obesus*) to confirm the applicability of salmon-derived gonadotropin-releasing hormone analogue (sGnRHa, Ovaprim®) throughout shark species with various breeding strategies. Prior to the experiment, normal blood sex hormone concentrations of females and males were identified in each of the species, and used as the base line for further experimental analysis. In both species, it was confirmed that Ovaprim® successfully induced changes in concentration of estradiol, progesterone, and testosterone in the blood, follicular maturation and ovulation in females, and semen release in males. The optimized injection protocols of Ovaprim® for future application to artificial insemination were as follows: male banded houndshark: 0.2 mL/kg administration and semen sampling 1 hour after administration; female banded houndshark: 0.2 mL/kg first administration and 0.5 mL/kg second administration with 24 hours of gap time;

male whitetip reef shark: 0.2 mL/kg administration and semen sampling right after administration; female whitetip reef shark: 0.2 mL/kg first administration and 0.2 mL/kg or 0.3 mL/kg second administration with 24 hours of gap time.

Key words: shark, assisted reproductive technology, computed tomography, magnetic resonance imaging, semen cryopreservation, hormone-induced ovulation, *Triakis scyllium*, *Triaenodon obesus*.

Student number: 2019-39492

CONTENTS

CHAPTER III

Use of synthetic salmon GnRH and domperidone (Ovaprim®) in sharks: preparation for *ex-situ* conservation

LIST OF FIGURES

CHAPTER I

CHAPTER II

CHAPTER III

LIST OF TABLES

CHAPTER II

CHAPTER III

ABBREVIATIONS

3D	Three-dimensional
AET	Activating extender test
AFGP	Antifreeze glycoprotein
AFP	Antifreeze protein
AI	Artificial insemination
ARRIVE	Animal Research: Reporting of *In Vivo* Experiments
ART	Assisted reproductive technology
BSA	Bovine serum albumin
CT	Computed tomography
DICOM	Digital imaging and communications in medicine
DMSO	Dimethyl sulfoxide
DO	Dissolved oxygen
DOM	Duration of motility
ECLIA	Electrochemiluminescence immunoassay
EG	Ethylene glycol
EY	Egg yolk
FOV	Field of view
FSW	Filtered seawater
GnRH	Gonadotropin-releasing hormone
HAI	Hormone-induced artificial insemination

IM	Intramuscular
IUCN	International Union of Conservation of Nature
MB	Modified Beltsville poultry semen extender
MB-EM	Elasmobranch-modified MB
MH	Modified Hank's balanced salt solution
MH-EM	Elasmobranch-modified MH
MPR	Multiplanar reconstruction
MRI	Magnetic resonance imaging
MS-222	Tricaine methanesulfonate
MT	Modified Tsvetkova's extender
MT-EM	Elasmobranch-modified MT
NH_3	Ammonia
NO_2^-	Nitrite
NO_3^-	Nitrate
OT	Original Tsvetkova's extender
OT-EM	Elasmobranch-modified OT
SA	Surface area
SCT	Semen cryopreservation test
sFOV	Scan field of view
sGnRHa	Salmon-derived gonadotropin-releasing hormone analogue
SR	Shark Ringer solution

SSAE	Spermatozoa activating extender
T	Tesla
T2W	T2-weighted
TBL	Total body length
TMAO	Trimethylamine oxide
TR	Repetition time
V	Volume

CHAPTER I

Cross-sectional anatomy, computed tomography, and magnetic resonance imaging of the banded houndshark (*Triakis scyllium*)

This manuscript has been published in *Sci. Rep.* 11:1165 (2021).

Abstract

Due to their important phylogenetic position among extant vertebrates, sharks are an invaluable group in evolutionary developmental biology studies. A thorough understanding of shark anatomy is essential to facilitate these studies and documentation of this iconic taxon. With the increasing availability of cross-sectional imaging techniques, the complicated anatomy of both cartilaginous and soft tissues can be analyzed non-invasively, quickly, and accurately. The aim of this study is to provide a detailed anatomical description of the normal banded houndshark (*Triakis scyllium*) using computed tomography (CT) and magnetic resonance imaging (MRI) along with cryosection images. Three banded houndsharks were scanned using a 64-detector row spiral CT scanner and a 3T MRI scanner. All images were digitally stored and assessed using open-source Digital Imaging and Communications in Medicine viewer software in the transverse, sagittal, and dorsal dimensions. The banded houndshark cadavers were then cryosectioned at approximately 1-cm intervals. Corresponding transverse cryosection images were chosen to identify the best anatomical correlations for transverse CT and MRI images. The resulting images provided excellent detail of the major anatomical structures of the banded houndshark. The illustrations in the present study could be considered as a useful reference for interpretation of normal and pathological imaging studies of sharks.

Keywords: Banded houndshark, *Triakis scyllium*, magnetic resonance imaging, computed tomography, cross-sectional anatomy

1. Introduction

The past half-century has seen a sharp decline in the population of sharks due to indiscriminate fishing, and they are now facing a severe extinction crisis (Lack and Sant, 2011; Barker and Schluessel, 2005; Baum and Blanchard, 2010; IUCN, 2018). Sharks are apex predators and keystone species, playing an important role in maintaining the marine ecosystem. Thus, extinction of sharks in certain areas is expected to lead to marine food chain collapses, which could result in a sharp reduction in the marine food resources available for human beings (Heithaus et al., 2012; Ferretti et al., 2010; Myers et al., 2007). As a result, the importance of protecting endangered shark species has been recognized worldwide, and efforts to study these species to understand and protect them are being made by various groups, including aquariums, fishery industries, and biologists (Myers et al., 2007; Dulvy et al., 2017; Summers et al., 2004; Stevens et al., 2000; Dulvy et al., 2014; Davidson et al., 2016).

With the increasing availability of cross-sectional imaging techniques such as computed tomography (CT) and magnetic resonance imaging (MRI), the complicated and sophisticated anatomy of both skeletal and soft tissues can be analyzed non-invasively, quickly, and accurately (Lauridsen et al., 2011; Dirnhofer et al., 2006; Kot et al., 2018; Furukawa et al., 2004). CT and MRI have often been used not only for humans but also for various animal species (Lauridsen et al., 2011; Gumpenberger and Henninger, 2001; Preziosi et al., 2005; Van Bonn et al., 2001).

Some of these studies were conducted on sharks and involved diverse fields such as physiology, anatomy, developmental biology, archaeology, and evolutionary biology (Summers et al., 2004; Jambura et al., 2019; Abel et al., 2010; Wroe et al., 2008; Timm and Fish, 2012; Kamminga et al., 2017; Mollen et al., 2012; Mara et al., 2015; Geraghty et al., 2012; Moyer et al., 2015).

Although a wide variety of studies have been performed on sharks (Meng and Li, 1992), official publications describing the basic anatomy of sharks particularly in CT and/or MRI evaluations are currently unavailable. Accurate evaluation of CT and MRI images requires precise knowledge of the anatomy and physiology of the animal. In this regard, the development of accurate atlases for certain species by comparing CT and MRI images with actual cryosections is one of the primary steps that should be established by researchers and veterinarians (Samii et al., 1998). Normal atlases of CT and MRI findings in various animals have already been set up in order to facilitate accurate image analysis (Samii et al., 1998; Alonso-Farre et al., 2014; Alonso-Farre et al., 2015; Ibrahim et al., 2019; Wyman et al., 1978; Feeney et al., 1991; Smallwood and George, 1993a; Smallwood and George, 1993b; Valente et al., 2007). In the same context, precise atlases of CT and MRI findings in shark species should also be established.

The banded houndshark (*Triakis scyllium*) is a relatively small-sized shark that is easily found in Korean water. They inhabit the Northwest Pacific Ocean and are classified as the “least concern” group by the International Union for Conservation

of Nature (IUCN) red list (IUCN, 2018; Compagno, 1984). The purpose of this study is to set up a detailed atlas of the banded houndshark by comparing CT and MRI images with actual cryosections. To the best of my knowledge, this is the first study reporting delicate comparison of CT, MRI, and cryosection findings for shark anatomy.

2. Materials and methods

2.1. Animals

Three banded houndsharks were obtained commercially from Seoul, the Republic of Korea. The banded houndsharks were 1 male (total body length (TBL): 90 cm, age: estimated as 3.4 years) and 2 females (TBL: 91 cm, age: estimated as 3.3 years; TBL: 102 cm, age: estimated as 4.1 years) with body lengths ranging from 90 to 102 cm. Ages of the sharks were estimated based on their TBL and it was judged that the sharks were about to be sexually mature (Fujinami and Tanaka, 2013). All animals were selected by a veterinarian (SWK) based on the lack of external evidence of trauma and disease. The banded houndsharks were euthanized via tricaine methanesulfonate overdose (500 ppm) right before imaging examinations in order to minimize post-mortem changes.

2.2. Magnetic resonance imaging (MRI)

MRI examinations were performed using a 3-Tesla (T) MRI scanner (Achieva, Philips Healthcare, The Netherlands). A head coil was used to receive the signal using fast spin echo sequences in the T2-weighted (T2W) mode, in which signals from loosely bound protons (e.g., fluids) were enhanced:

[1] Transverse images were obtained with the following parameters: echo time (TE), 90 ms; repetition time (TR), 4920.8 ms; pixel bandwidth, 180 Hz; flip angle, 90°, and field of view (FOV), 123 × 123 mm with reconstructed spacing, 0.17 × 0.17 mm. Slice thickness was 2 mm.

[2] Sagittal images were obtained with the following parameters: TE, 90 ms; TR, 4870.9 ms; pixel bandwidth, 215 Hz; flip angle, 90°, and FOV, 76 × 76 mm with reconstructed spacing, 0.20 × 0.20 mm. Slice thickness was 3 mm.

[3] Dorsal images were obtained with the following parameters: TE, 70 ms; TR, 3865.9 ms; pixel bandwidth, 236 Hz; flip angle, 90°, and FOV, 81 × 81 mm with reconstructed spacing, 0.23 × 0.23 mm. Slice thickness was 1.5 mm.

2.3. Computed tomography (CT)

CT images were acquired with a 64-detector row spiral CT scanner (Aquilion, Toshiba Medical Systems, Nasu, Japan). The CT examination was performed at 120 kV and 80-100 mA with a 1-mm slice thickness. The scan field of view (sFOV) ranged from 20.3 to 30.2 cm. The transverse image datasets were acquired using the

soft tissue and bone algorithm. CT images in the dorsal and sagittal dimensions were obtained using the multiplanar reconstruction (MPR) function. MRI and CT images were assessed using open-source Digital Imaging and Communications in Medicine (DICOM) viewer software (Horos Project, version 3.3.6; www.horosproject.org).

2.4. Cryosectioning

All specimens were frozen (-22°C) in the ventral recumbency position until cryosectioning could be carried out. The banded houndsharks were sectioned using an electrical band saw along the transverse plane at approximately 1-cm intervals. Slices were numbered, cleaned, and photographed on both sides. Fourteen transverse section levels were selected. For each section level, the corresponding transverse MRI and CT images were chosen to identify the best anatomical correlation. Lines corresponding to these levels were superimposed on three-dimensional reconstructed images of a banded houndshark (**Figure 1**).

2.5. Three-dimensional (3D) reconstruction

3D reconstructions of the skeletons were made on acquired CT data sets using intensity-based segmentation methods of the inbuilt software of 64-detector row spiral CT scanner (Aquilion, Toshiba Medical Systems, Nasu, Japan). The reconstructed skeletons were visualised after excluding remaining residual soft tissue structures. 3D reconstructions of major organs were made on MRI data sets using intensity-based and manual segmentation methods of an open-source DICOM

viewer - InVesalius 3.0 (CTI - Center for Information and Technology Renato Archer, Campinas, São Paulo, Brazil).

2.6. Ethical approval

The study was approved by the Seoul National University Institutional Animal Care and Use Committee (approval number: SNU-190925-2). All experiments were performed in accordance with the IACUC guidelines and regulations. This study was also performed in accordance with the Animal Research: Reporting of In Vivo Experiments (ARRIVE) guidelines: to reflect the scarcity of banded houndshark over 90 cm TBL in the fish markets of the Republic of Korea, sample size was decided to three; to minimize the potential confounders, both male and female sharks were used; to show the developmental stages, TBL and estimated age of each shark were provided.

3. Results

In the present study, CT and MRI allowed identification of a broad selection of anatomical structures and correlated well with the corresponding cryosections of the banded houndshark. Clinically relevant anatomical structures are labeled in Figures 2–24. Figures 2–15 (transverse images), Figures 16–18 (sagittal images), and Figures 19–24 (dorsal images) present the findings in cranial to caudal, right to left,

and dorsal to ventral progression, respectively. Three-dimensional (3D) reconstructed images of CT and MRI data sets showing major skeletons and organs of the banded houndshark were presented in **Figure 25**. Transverse images of MRI and CT are shown continuously in Supplementary Video S1 and Supplementary Video S2, respectively, to make up for the shortcomings of discontinuous cross-sectional images.

3.1. Transverse images

Figures 2 – 15.

3.2. Sagittal images

Figures 16 – 18.

3.3. Dorsal images

Figures 19 – 24.

4. Discussion

The MRI signal intensity is proportional to the hydrogen density of the structures, ensuring excellent definition of soft tissues, organs, and cavitary structures in banded houndsharks. These structures included major muscles; cardiovascular system

structures, including the atrium, ventricle, and major arteries and veins; digestive system structures, including the stomach, gall bladder, and valvular intestine; excretory system structures, including the kidney; nervous system structures, including the cerebrum, optic lobe, and thalamus. Due to the absence of hydrogen atoms, most of the cartilaginous skeletons in banded houndsharks did not provide sufficient magnetic resonance signal and showed a hypointense (black/dark grey) pattern. Nonetheless, some cartilaginous structures, such as the jaws and coracoid bar, could still be observed due to the contrast between the cartilage and the adjacent soft tissues.

In contrast to MRI, excellent discrimination of cartilaginous structures was evident in the CT images. The higher electron density of cartilages caused increased attenuation compared to soft tissue, making them appear more whitish in the CT images. The cartilage margins were better defined by means of CT than cryosections or MRI, particularly in assessing joint structures. Soft tissues were vaguely distinguished using CT examinations due to their similar attenuation properties. Nevertheless, attenuation differences between lipid-rich tissues (e.g., liver) and muscles (e.g., stomach and valvular intestine) were shown in varying shades of grey allowing definition of some organs in the visceral cavity.

CT and MRI offer considerable advantages over traditional radiographic approaches on identification of the anatomical structures of sharks. In traditional radiography, images are presented as superimposed two-dimensional projections of

three-dimensional structures, which result in limitation to exhibit high conspicuity. The tomographic nature of CT and MRI allows organs to be examined in thin sections, eliminating superimposition of overlying structures that may hinder the specific interpretation of anatomical structures.

Another major advantage of CT and MRI is the ability to reformat the datasets in any imaging plane or as 3D projections, allowing better understanding of the spatial relationships of anatomical structures in sharks. These techniques have added detail of the anatomical structures and can be used as an anatomic reference for imaging studies of the banded houndshark and other shark species. It is recommended to reduce CT / MRI slice thickness as much as possible in order to achieve excellent quality and high detail of 3D reconstructed images, since increasing slice thicknesses may require more interpolation between slices when rendering 3D images, which results in a loss of resolution (Ford and Decker, 2016).

Due to their important phylogenetic position among extant vertebrates, sharks are an invaluable group in evolutionary developmental biology studies. However, the presence of high levels of urea accelerates the decomposition of shark flesh (Kandoran et al., 1965). Moreover, because of its cartilaginous nature, shark skeleton has a high tendency to warp, crack, and shrink during specimen preparation (Enault et al., 2016). These factors represent major difficulties in preserving anatomical data from sharks. In the present study, CT and MRI were used to identify and document soft tissues and cartilaginous structures in banded houndsharks. The non-invasive

nature of CT and MRI prevented the irretrievable destruction of specimens during traditional dissection. The spatial relationships among organs, soft tissues, and cartilage can be selectively observed *in situ* in their natural locations (Montie et al., 2011; Lautenschlager et al., 2014). After examinations, all images are permanently recorded in the DICOM format and could be recalled at will. The images are digitally transferable, which can also facilitate discussion and opinion sharing among professionals worldwide even if the specimens cannot be physically provided.

Banded houndshark is a relatively small-sized shark species that can be adequately fit into the bore of medical CT and MRI used in the present study. However, to the best of the authors' knowledge, only the head of large-sized shark species has been subjected to imaging examination possibly because of limited gantry size (Mollen et al., 2012; Tomita et al., 2011; Wroe et al., 2008). Sharks with body girth larger than the maximum diameter of FOV of medical CT and MRI may also induce out-of-field artifacts, anatomical structures that lies beyond the FOV may be truncated. With the rapid advancement of medical imaging technologies, wide bore CT and MRI have become available for large animals (Nakamae et al., 2018; Porter et al., 2016; Kraitchman et al., 2017). Although the current availability of wide bore CT and MRI scanners are limited and the set up cost is high, the use of wide bore CT and MRI may offer a feasible alternative for imaging examination of large-sized shark species in future.

5. Conclusions

The illustrations in the present study are the first to provide a comprehensive atlas, using CT and MRI, to evaluate the anatomical structures of the banded houndshark. Both imaging modalities provide good contrast for the anatomical structures of the banded houndshark. With the rapid advancement and increasing availability of medical imaging technologies, CT and MRI are enhancing the knowledge of the anatomy of sharks together with dissected and necropsy materials. The findings of the present study could be considered as a useful reference of normal tomographic anatomy of sharks and used for the interpretation of normal and pathological imaging studies of sharks in future.

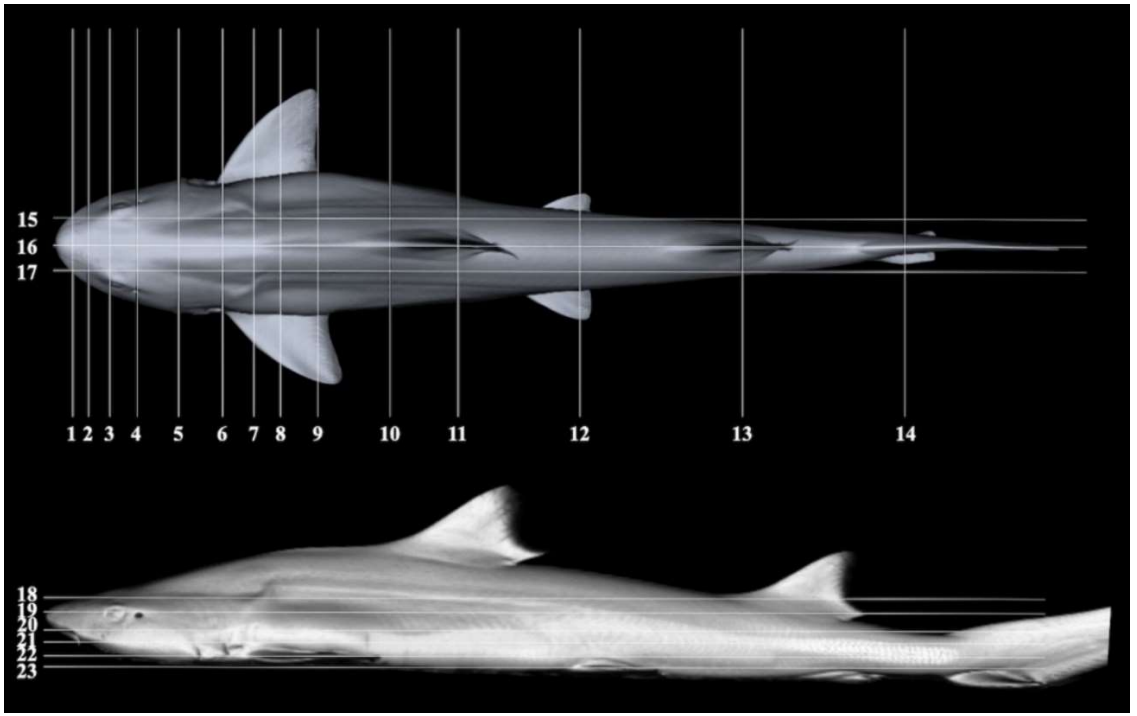

Figure 1. Three-dimensional surface reconstructions of a banded houndshark (*Triakis scyllium*) from computed tomography (CT) scans, indicating approximate levels of transverse, sagittal, and dorsal sections corresponding to Figures 2–24. Slices 1–4 are approximately 2 cm intervals, slices 4–9 are approximately 5 cm intervals, slices 9–11 are approximately 6 cm intervals, slices 11–14 are approximately 12 cm intervals, slices 15–17 are approximately 3 cm intervals, and slices 18–23 are approximately 1 cm intervals.

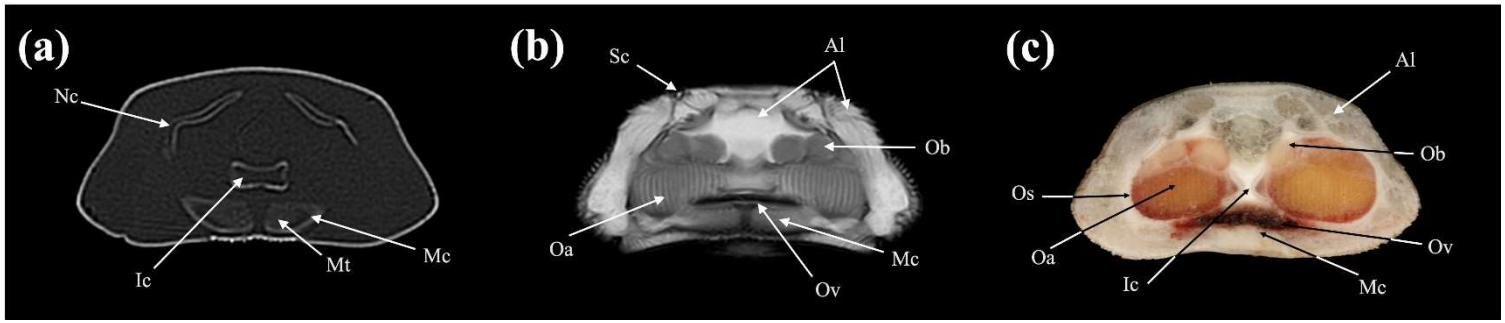

Figure 2. Transverse (a) CT, (b) MR, and (c) cryosection images of a banded houndshark (*Triakis scyllium*) at level 1 of Figure 1. Abbreviations: Al = Ampullae of Lorenzini; Ic = Internasal cartilage; Mc = Meckel's cartilage; Ms = Median septum; Te = Teeth; Nc = Nasal capsule cartilage; Oa = Olfactory lamellae; Ob = Olfactory bulb; Os = Olfactory sac; Ov = Oral cavity; Sc = Supraorbital canal.

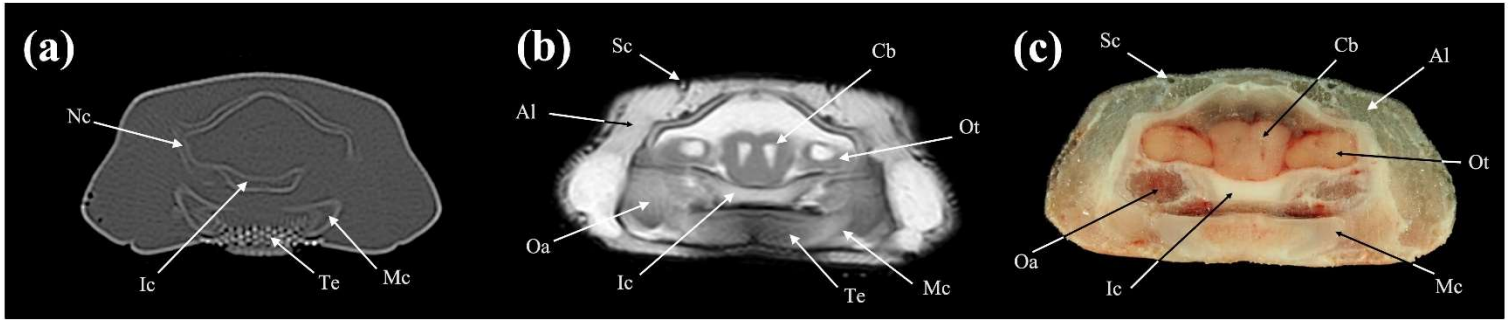

Figure 3. Transverse (a) CT, (b) MR, and (c) cryosection images of a banded houndshark (*Triakis scyllium*) at level 2 of Figure 1. Abbreviations: Al = Ampullae of Lorenzini; Cb = Cerebrum; Ic = Internasal cartilage; Mc = Meckel's cartilage; Te = Teeth; Nc = Nasal capsule cartilage; Oa = Olfactory lamellae; Ot = Olfactory tract; Sc = Supraorbital canal.

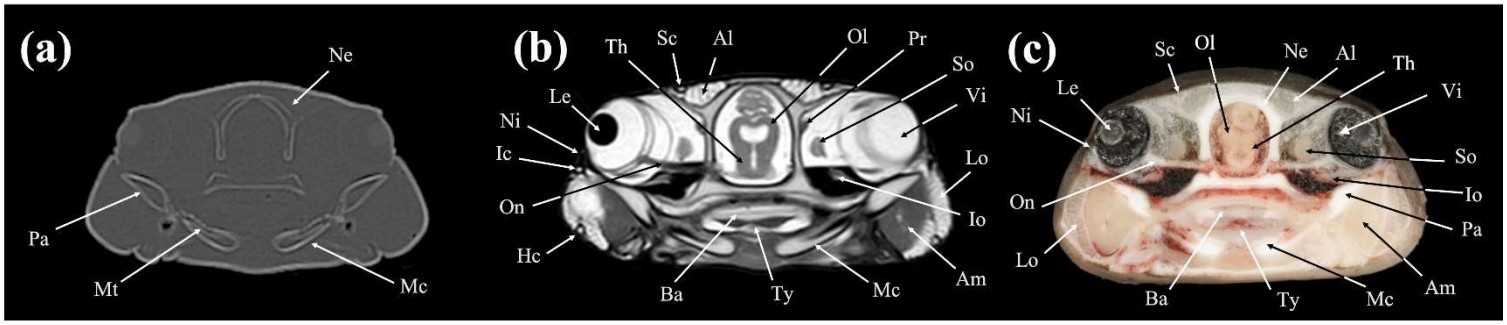

Figure 4. Transverse (a) CT, (b) MR, and (c) cryosection images of a banded houndshark (*Triakis scyllium*) at level 3 of Figure 1. Abbreviations: Al = Ampullae of Lorenzini; Am = Adductor mandibularis; Ba = Basihyal cartilage; Hc = Hyomandibular canal; Ic = Infraorbital canal; Io = Inferior obliquus; Le = Lens; Mc = Meckel's cartilage; Mt = Mandibular teeth; Ne = Neurocranium; Ni = Nictitating fold; Ol = Optic lobe; On = Optic nerve; Pa = Palatoquadrate; Pr = Posterior rectus; Sc = Supraorbital canal; So = Superior obliquus; Th = Thalamus; Ty = Thyroid; Vi = Vitreous humor.

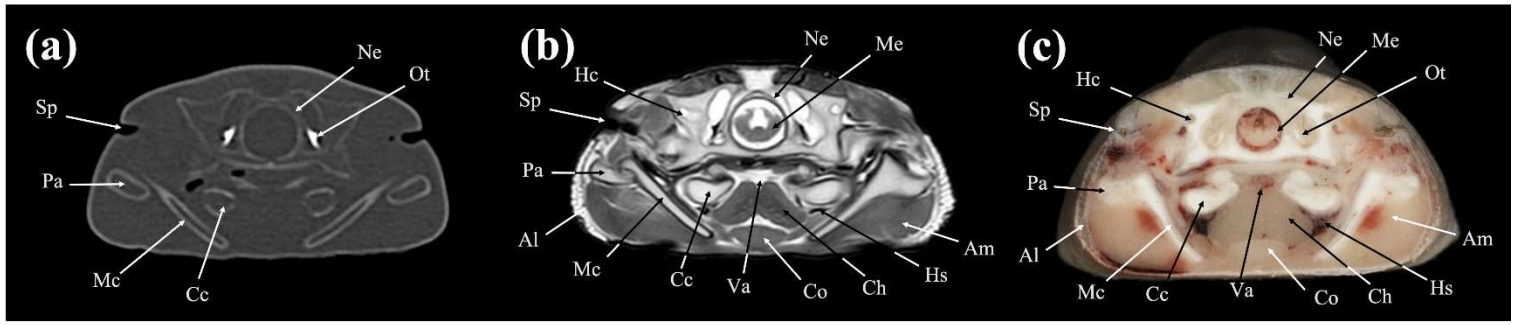

Figure 5. Transverse (a) CT, (b) MR, and (c) cryosection images of a banded houndshark (*Triakis scyllium*) at level 4 of Figure 1. Abbreviations: Al = Ampullae of Lorenzini; Am = Adductor mandibularis; Cc = Ceratohyal cartilage; Ch = Coracohyoideus; Co = Coracomandibularis; Hc = Horizontal semicircular canal; Hs = Hyoidean sinus; Me = Medulla Oblongata; Mc = Meckel's cartilage; Ne = Neurocranium; Ot = Otolith; Pa = Palatoquadrate; Sp = Spiracle; Va = Ventral aorta.

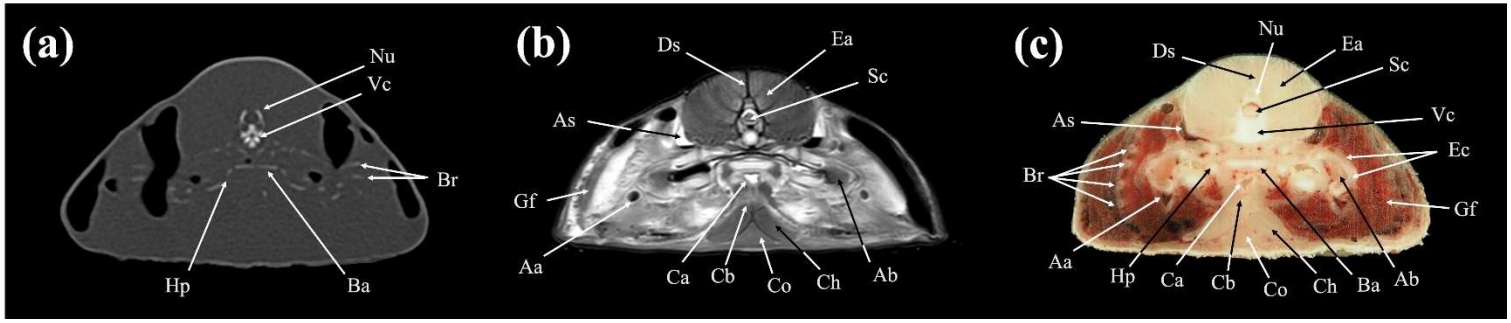

Figure 6. Transverse (a) CT, (b) MR, and (c) cryosection images of a banded houndshark (*Triakis scyllium*) at level 5 of Figure 1. Abbreviations: Aa = Afferent branchial artery; Ab = Adductor branchial; As = Anterior cardinal sinus; Ba = Basibranchial; Br = Branchial rays; Ca = Conus arteriosus; Cb = Coracobranchialis; Ch = Coracohyoideus; Co = Coracomandibularis; Ds = Dorsal skeletogenous septum; Ea = Epaxial; Ec = Epibranchial and ceratobranchial cartilage; Gf = Gill filament; Hp = Hypobranchial cartilage; Nu = Neural arch; Vc = Vertebral centrum.

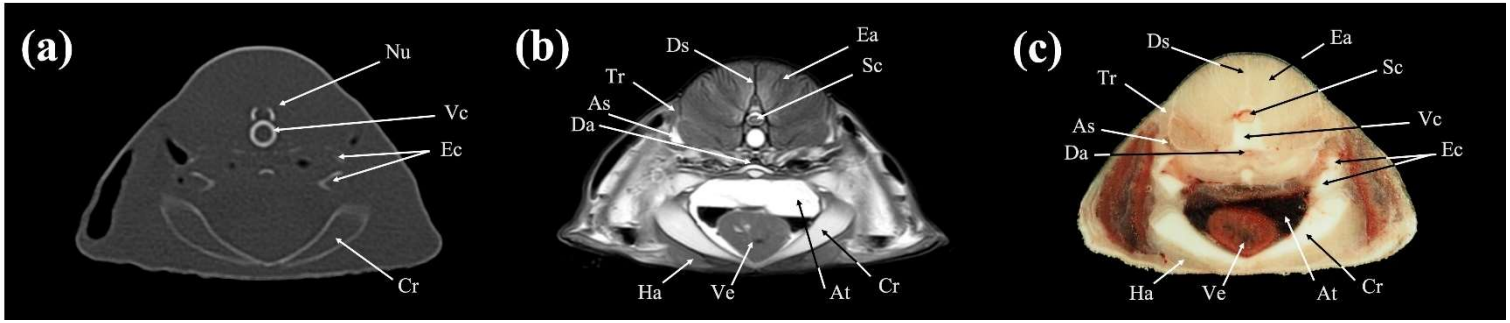

Figure 7. Transverse (a) CT, (b) MR, and (c) cryosection images of a banded houndshark (*Triakis scyllium*) at level 6 of Figure 1. Abbreviations: As = Anterior cardinal sinus; At = Atrium; Cr = Coracoid bar; Da = Dorsal aorta; Ds = Dorsal median septum; Ea = Epaxial; Ec = Epibranchial and ceratobranchial cartilage; Ha = Hypaxial; Sc = Spinal cord; Tr = Trapezius; Ve = Ventricle; Vc = Vertebral centrum.

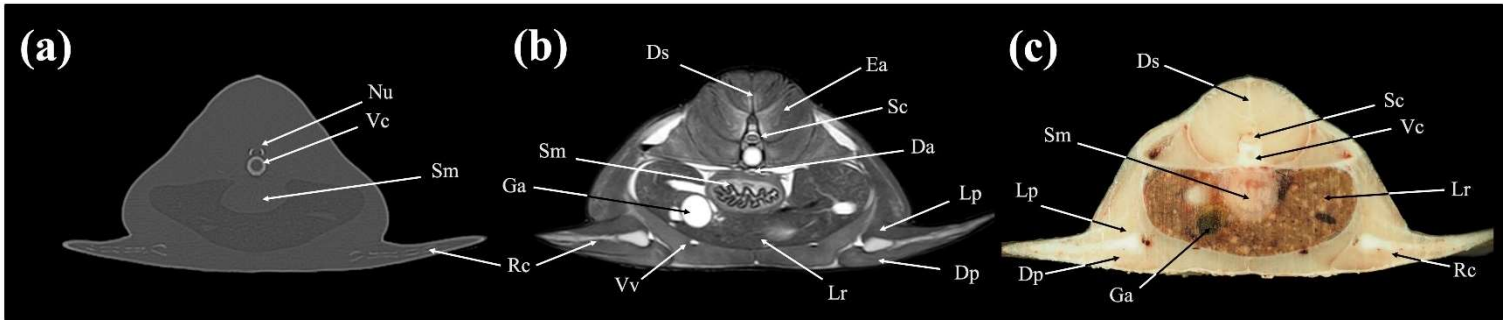

Figure 8. Transverse (a) CT, (b) MR, and (c) cryosection images of a banded houndshark (*Triakis scyllium*) at level 7 of Figure 1. Abbreviations: Da = Dorsal aorta; Dp = Depressor pectoralis; Ds = Dorsal median septum; Ea = Epaxial; Ga = Gall bladder; Ha = Hypaxial; Lp = Levator pectoralis internus; Nu = Neural arch; Lr = Liver; Rc = Radial cartilage; Sc = Spinal cord; Sm = Stomach; Vc = Vertebral centrum; Vv = Ventral abdominal vein.

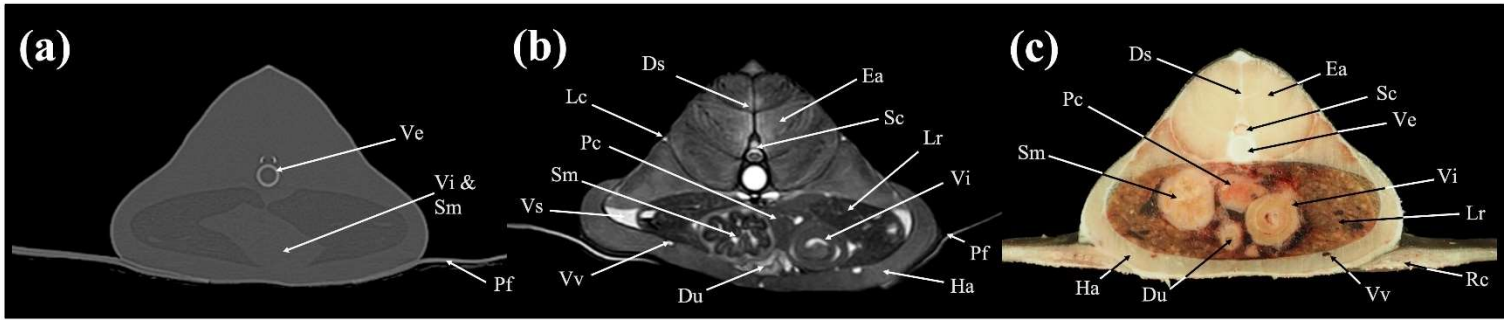

Figure 9. Transverse (a) CT, (b) MR, and (c) cryosection images of a banded houndshark (*Triakis scyllium*) at level 8 of Figure 1. Abbreviations: Ds = Dorsal median septum; Du = Duodenum; Ea = Epaxial; Ha = Hypaxial; Id = Inclinator dorsalis; Kd = Kidney; Lc = Lateral line canal; Lr = Liver; Pc = Pancreas; Pf = Pectoral fin; Rc = Radial cartilage; Sc = Spinal cord; Sm = Stomach; Ve = Vertebra; Vi = Valvular intestine; Vs = Visceral cavity; Vv = Ventral abdominal vein.

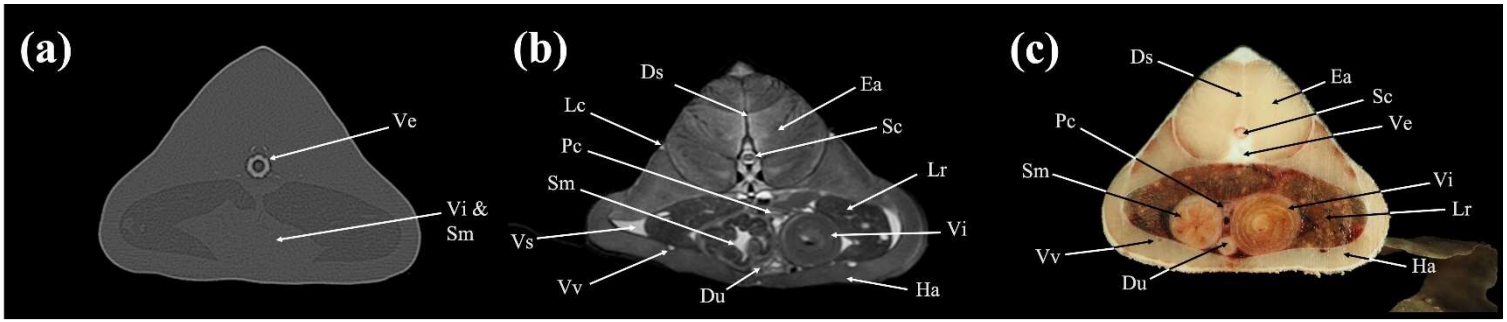

Figure 10. Transverse (a) CT, (b) MR, and (c) cryosection images of a banded houndshark (*Triakis scyllium*) at level 9 of Figure 1. Abbreviations: Ds = Dorsal median septum; Du = Duodenum; Ea = Epaxial; Ha = Hypaxial; Id = Inclinator dorsalis; Kd = Kidney; Lc = Lateral line canal; Lr = Liver; Pc = Pancreas; Rc = Radial cartilage; Sc = Spinal cord; Sm = Stomach; Ve = Vertebra; Vi = Valvular intestine; Vs = Visceral cavity; Vv = Ventral abdominal vein.

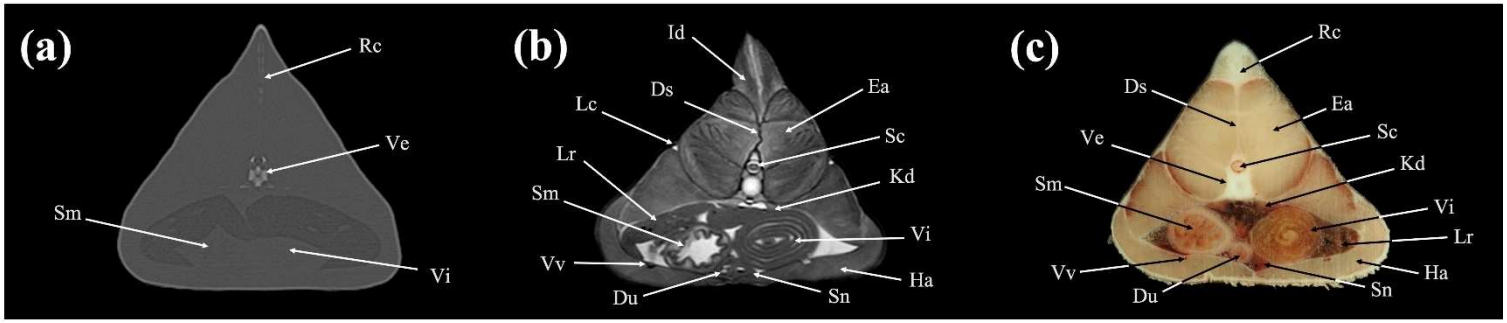

Figure 11. Transverse (a) CT, (b) MR, and (c) cryosection images of a banded houndshark (*Triakis scyllium*) at level 10 of Figure 1. Abbreviations: Ds = Dorsal median septum; Du = Duodenum; Ea = Epaxial; Ha = Hypaxial; Id = Inclinator dorsalis; Kd = Kidney; Lc = Lateral line canal; Lr = Liver; Rc = Radial cartilage; Sc = Spinal cord; Sm = Stomach; Sn = Spleen; Ve = Vertebra; Vi = Valvular intestine; Vv = Ventral abdominal vein.

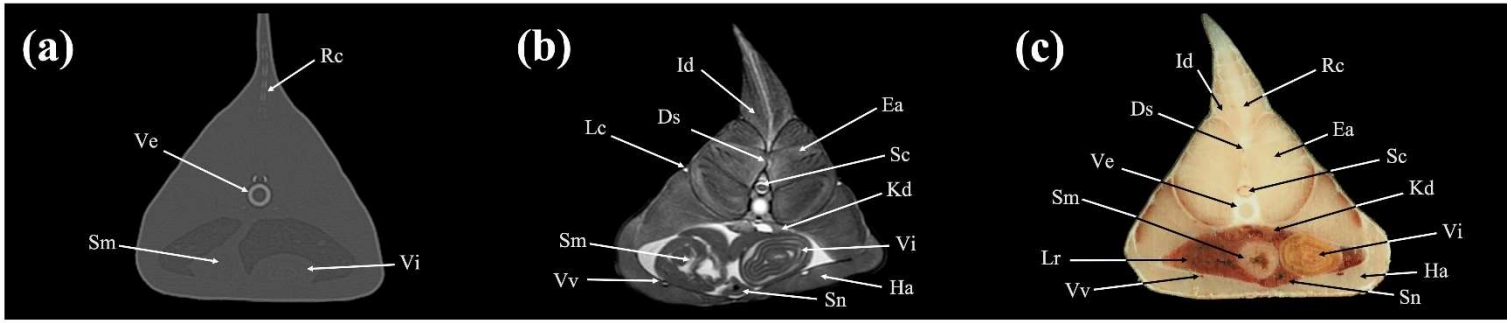

Figure 12. Transverse (a) CT, (b) MR, and (c) cryosection images of a banded houndshark (*Triakis scyllium*) at level 11 of Figure 1. Abbreviations: Ds = Dorsal median septum; Ea = Epaxial; Ha = Hypaxial; Id = Inclinator dorsalis; Kd = Kidney; Lc = Lateral line canal; Lr = Liver; Rc = Radial cartilage; Sc = Spinal cord; Sm = Stomach; Sn = Spleen; Ve = Vertebra; Vi = Valvular intestine; Vv = Ventral abdominal vein.

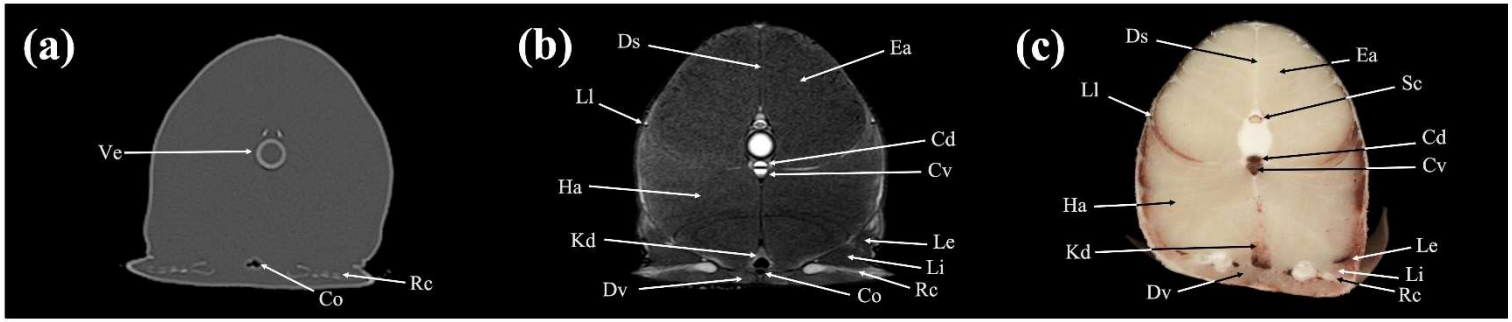

Figure 13. Transverse (a) CT, (b) MR, and (c) cryosection images of a banded houndshark (*Triakis scyllium*) at level 12 of Figure 1. Abbreviations: Cd = Caudal artery; Co = cloaca; Cv = Caudal vein; Ds = Dorsal skeletogenous septum; Dv = Depressor ventralis; Ea = Epaxial; Ha = Hypaxial; Kd = Kidney; Le = Levator ventralis externus; Li = Levator ventralis internus; Ll = Lateral line canal; Rc = Radial cartilage; Sc = Spinal cord.

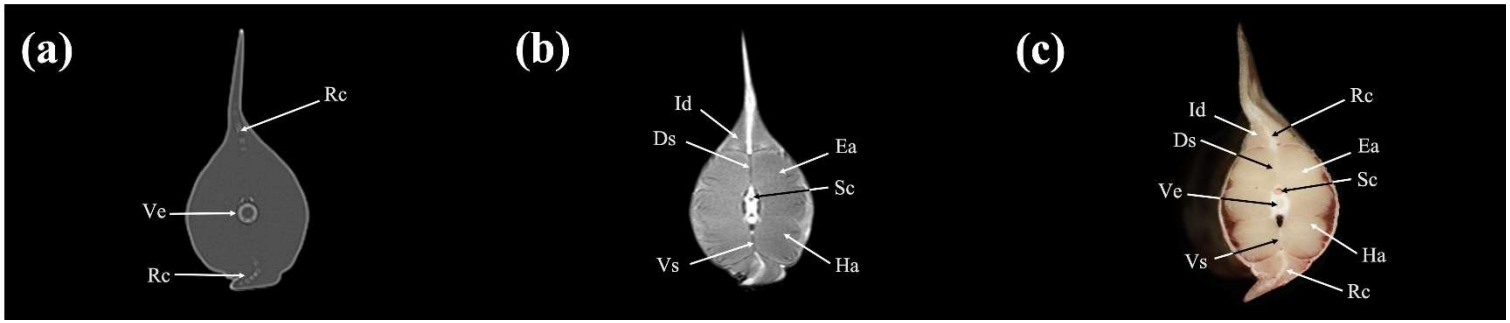

Figure 14. Transverse (a) CT, (b) MR, and (c) cryosection images of a banded houndshark (*Triakis scyllium*) at level 13 of Figure 1. Abbreviations: Ds = Dorsal skeletogenous septum; Ea = Epaxial; Ha = Hypaxial; Id = Inclinator dorsalis; Rc = Radial cartilage; Sc = Spinal cord; Ve = Vertebra; Vs = Ventral skeletogenous septum.

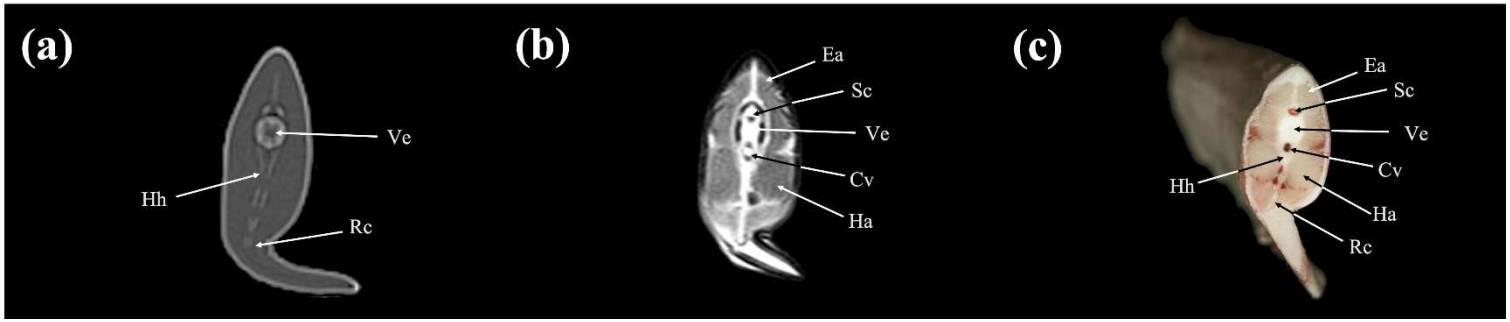

Figure 15. Transverse (a) CT, (b) MR, and (c) cryosection images of a banded houndshark (*Triakis scyllium*) at level 14 of Figure 1. Abbreviations: Cv = Caudal vessel; Ea = Epaxial; Ha = Hypaxial; Hh = Haemal arch; Rc = Radial cartilage; Sc = Spinal cord; Ve = Vertebra.

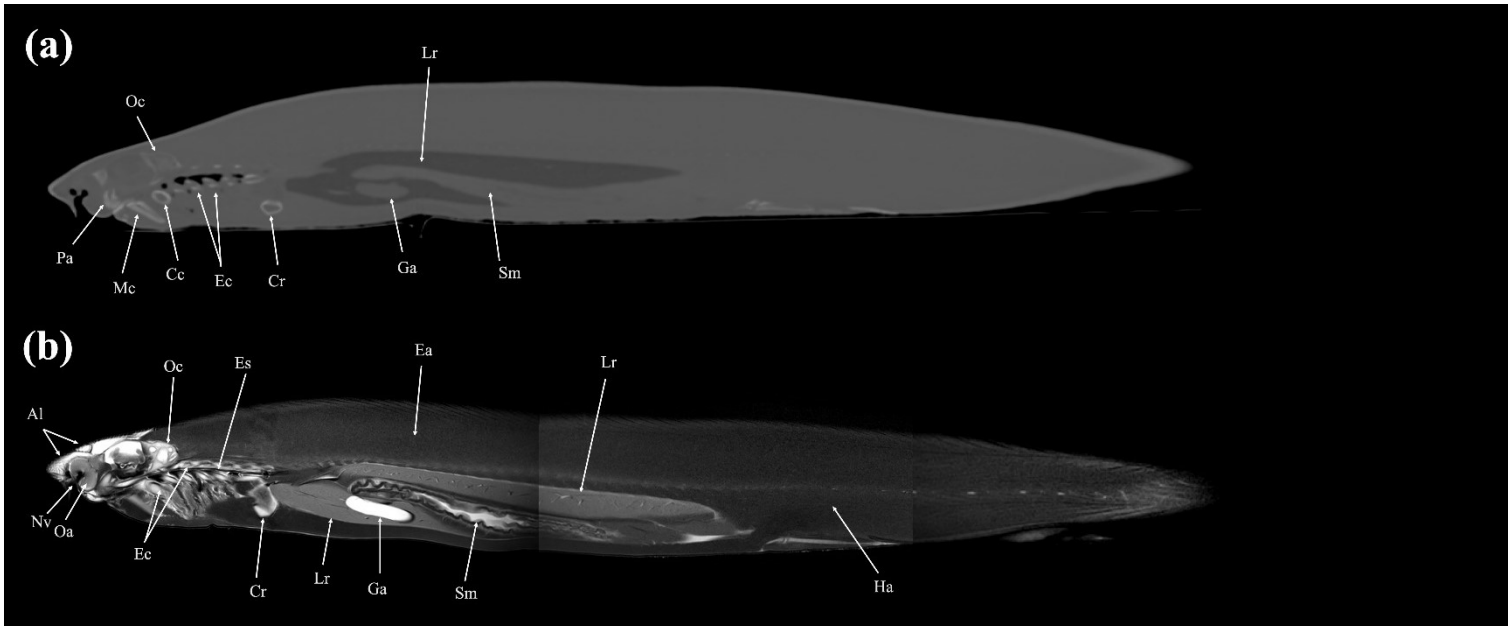

Figure 16. Sagittal (a) CT and (b) MR images of a banded houndshark (*Triakis scyllium*) at level 15 of Figure 1. Abbreviations: Al = Ampullae of Lorenzini; Cc = Ceratohyal cartilage; Cr = Coracoid bar; Ec = Epibranchial and ceratobranchial cartilage; Es = Esophagus; Ga = Gall bladder; Mc = Meckel's cartilage; Oa = Olfactory lamellae; Oc = Otic capsule; Pa = Palatoquadrate; Sm = Stomach; Nv = Nasal cavity.

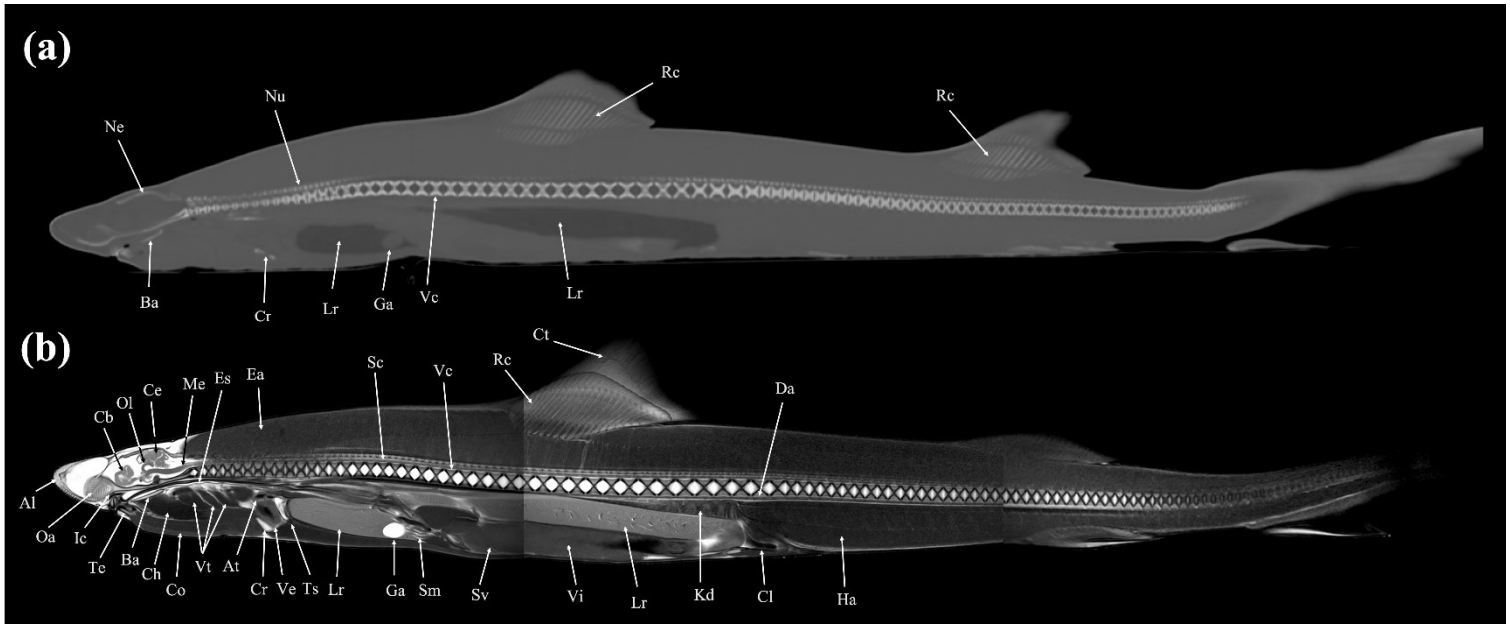

Figure 17. Mid-sagittal (a) CT and (b) MR images of a banded houndshark (*Triakis scyllium*) at level 16 of Figure 1. Abbreviations: Al = Ampullae of Lorenzini; At = Atrium; Ba = Basihyal cartilage; Cb = Cerebrum; Ce = Cerebellum; Cl = cloaca; Co = Coracomandibularis; Cr = Coracoid bar; Ch = Coracohyoideus; Ct = Ceratotrichia; Da = Dorsal aorta; Ea = Epaxial; Es = Esophagus; Ga = Gall bladder; Ha = Hypaxial; Ic = Internasal cartilage; Kd = Kidney; Lr = Liver; Me = Medulla oblongata; Ne = Neurocranium; Nu = Neural arch; Oa = Olfactory lamellae; Ol = Optic lobe; Rc = Radial cartilage; Sc = Spinal cord; Te = Teeth; Ts = Transverse septum; Vi = Valvular intestine; Ve = Ventricle; Vt = Ventral constrictors; Vc = Vertebral centrum; Sm = Stomach; Sv = Spiral valve.

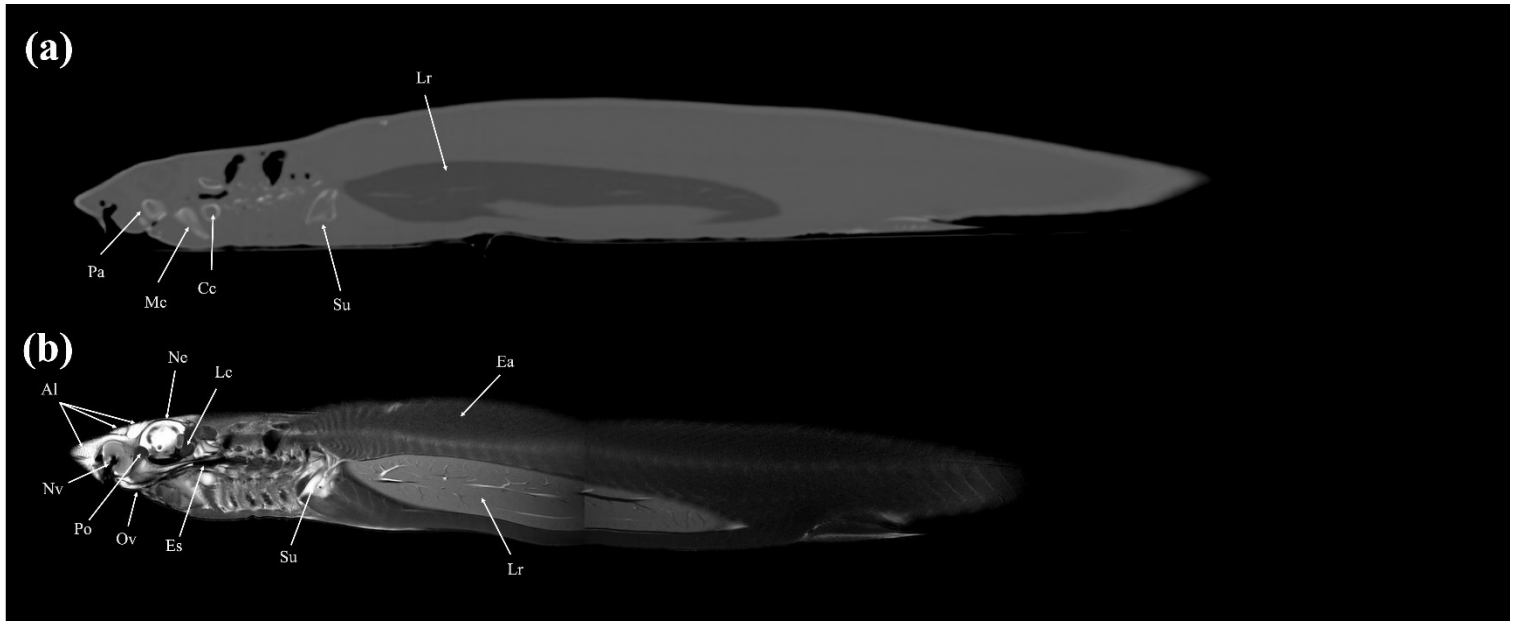

Figure 18. Sagittal (a) CT and (b) MR images of a banded houndshark (*Triakis scyllium*) at level 17 of Figure 1. Abbreviations: Al = Ampullae of Lorenzini; Am = Adductor mandibularis; Ba = Basihyal cartilage; Cc = Ceratohyal cartilage; Es = Esophagus; Hc = Hyomandibular canal; Ic = Infraorbital canal; Io = Inferior obliquus; Lc = Levator cranium maxillae; Le = Lens; Mc = Meckel's cartilage; Mp = Metapterygium; Mt = Mandibular teeth; Ne = Neurocranium; Ni = Nictitating fold; Ol = Optic lobe; Op = Optic nerve; Ov = Oral cavity; Pa = Palatoquadrate; Po = Preorbitalis; Pr = Posterior rectus; Sc = Supraorbital canal; Su = Scapular cartilage; So = Superior obliquus; Th = Thalamus; Ty = Thyroid; Vi = Vitreous humor.

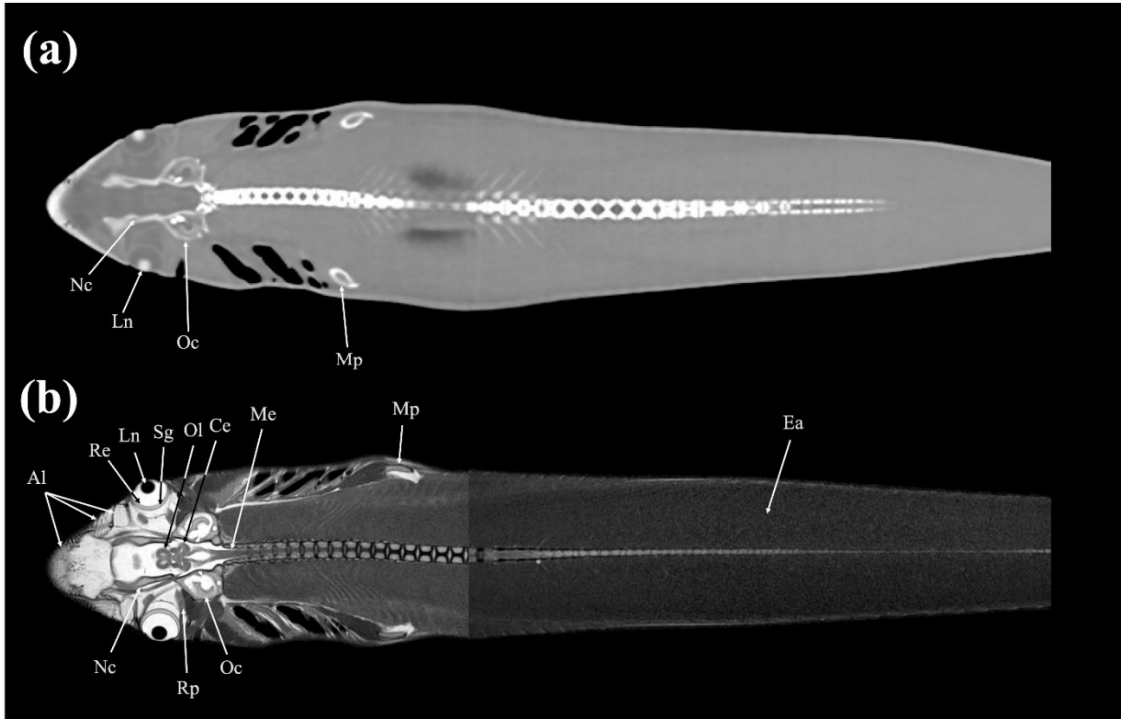

Figure 19. Dorsal (a) CT and (b) MR images of a banded houndshark (*Triakis scyllium*) at level 18 of Figure 1. Abbreviations: Al = Ampullae of Lorenzini; Ce = Cerebellum; Ea = Epaxial; Sg = Scleral cartilage; Ln = Lens; Me = Medulla oblongata; Mp = Metapterygium; Nc = Neurocranium; Oc = Otic capsule; Ol = Optic lobe; Re = Retina; Rp = Rectus posterior.

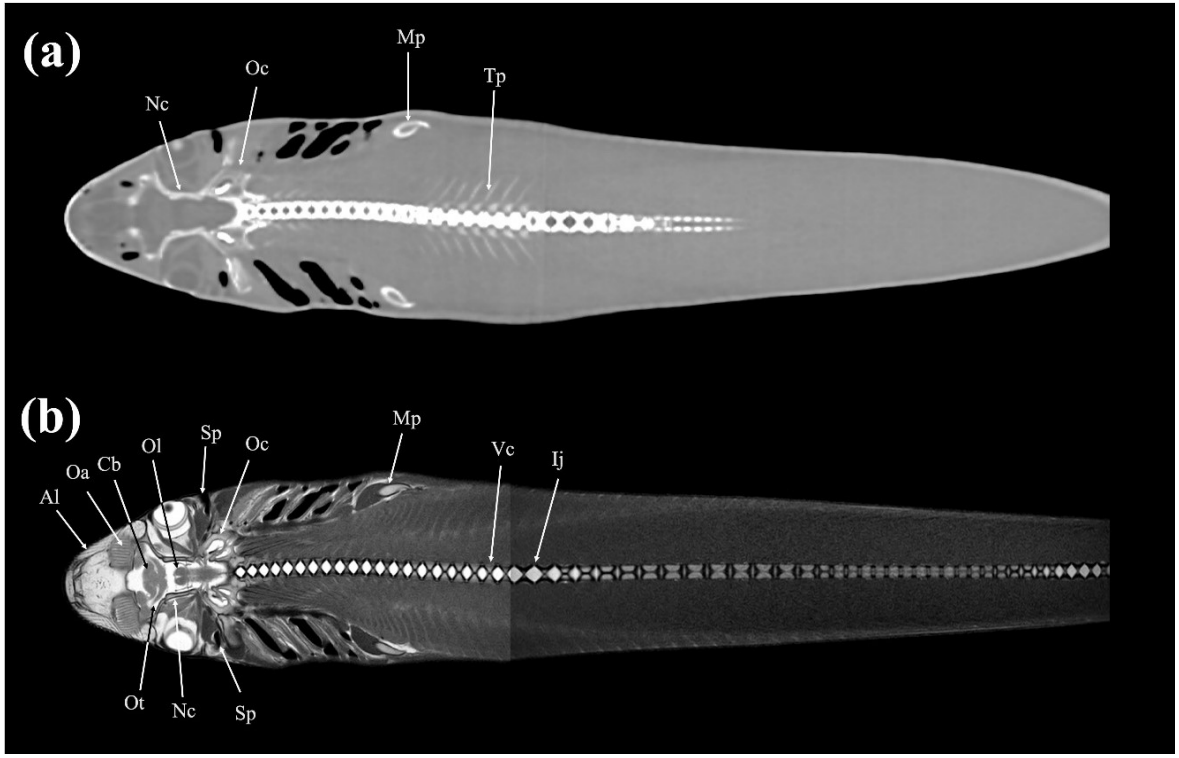

Figure 20. Dorsal (a) CT and (b) MR images of a banded houndshark (*Triakis scyllium*) at level 19 of Figure 1. Abbreviations: Al = Ampullae of Lorenzini; Cb = Cerebrum; Ij = Intervertebral junction; Mp = Metapterygium; Nc = Neurocranium; Oa = Olfactory lamellae; Oc = Otic capsule; Ol = Optic lobe; Ot = Olfactory tract; Sp = Spiracle; Tp = Transverse process; Vc = Vertebral centrum.

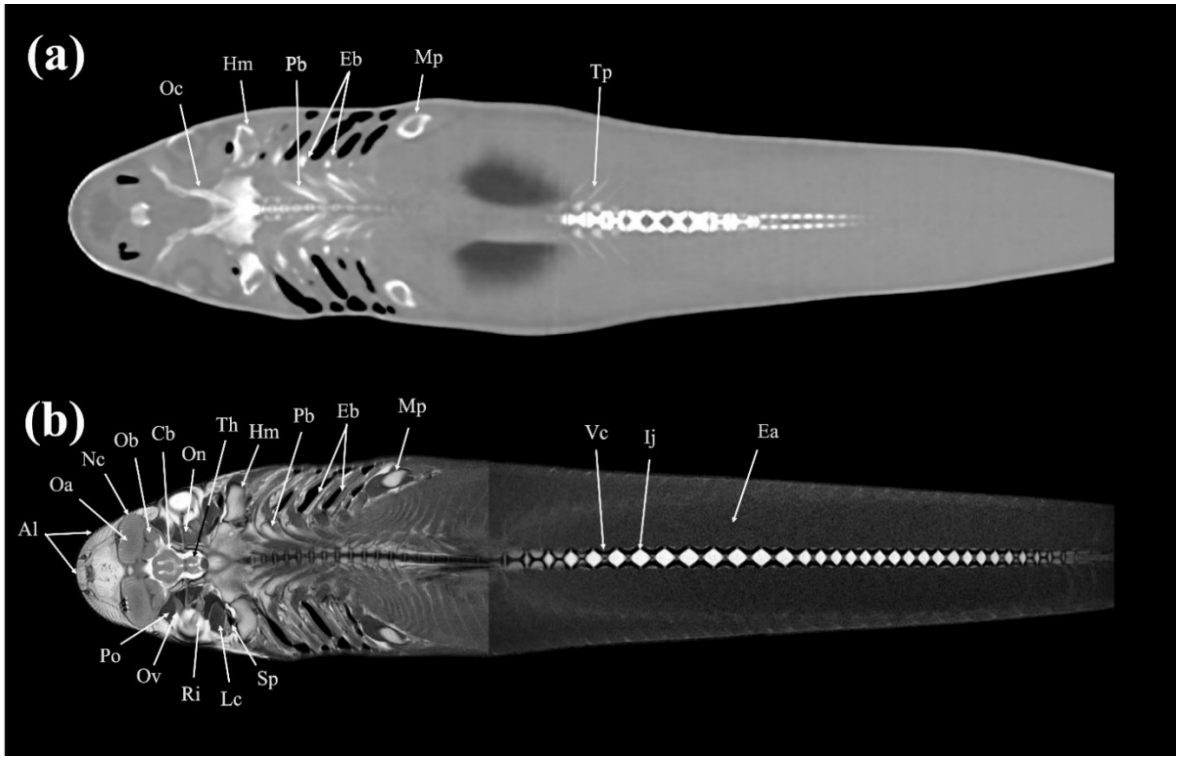

Figure 21. Dorsal (a) CT and (b) MR images of a banded houndshark (*Triakis scyllium*) at level 20 of Figure 1. Abbreviations: Al = Ampullae of Lorenzini; Cb = Cerebrum; Ea = Epaxial; Eb = Epibranchial; Hm = Hyomandibular; Ij = Intervertebral joint; Lc = Levator cranium maxillae; Mp = Metapterygium; Nc = Nasal capsule; Oa = Olfactory lamellae; Ob = Olfactory bulb; Oc = Optic capsule; On = Optic nerve; Ov = Obliquus ventralis; Pb = Pharyngobranchial; Po = Preorbitalis; Ri = Rectus inferior; Sp = Spiracle; Th = Thalamus; Vc = Vertebral centrum.

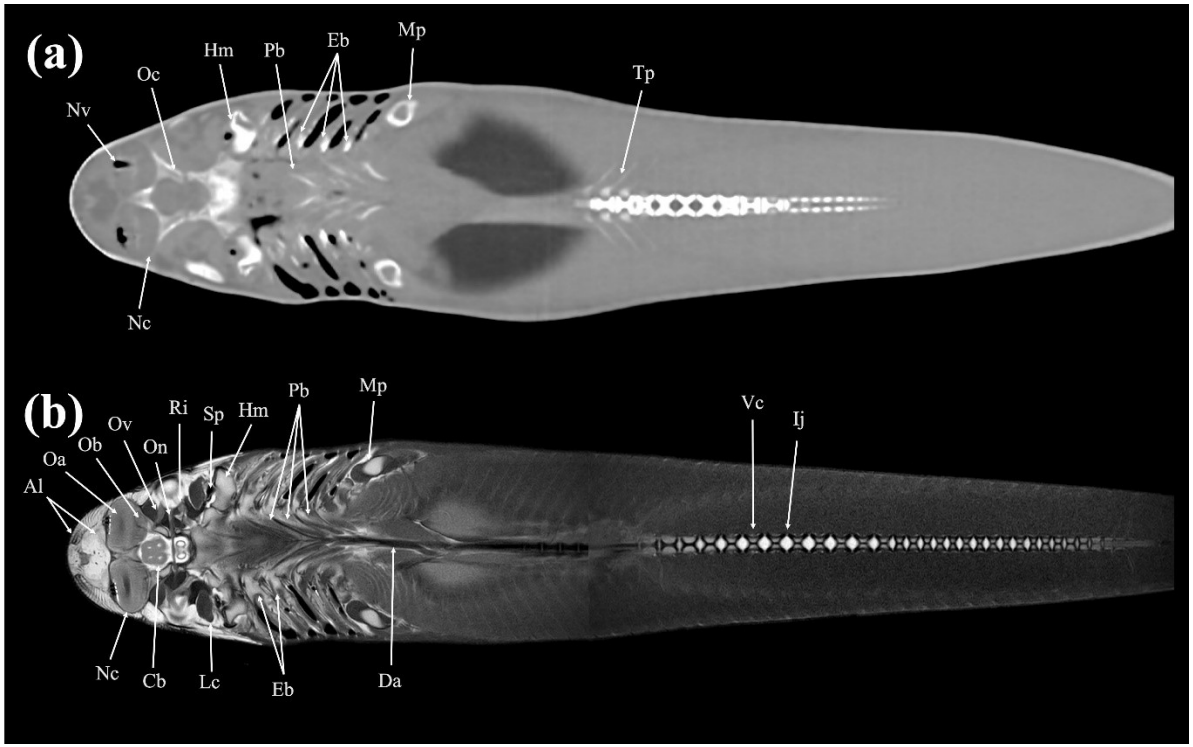

Figure 22. Dorsal (a) CT and (b) MR images of a banded houndshark (*Triakis scyllium*) at level 21 of Figure 1. Abbreviations: Al = Ampullae of Lorenzini; Cb = Cerebrum; Da = Dorsal aorta; Eb = Epibranchial; Hm = Hyomandibular; Ij = Intervertebral junction; Lc = Levator cranium maxillae; Mp = Metapterygium; Nc = Nasal capsule; Nv = Nasal cavity; Oa = Olfactory lamellae; Ob = Olfactory bulb; Oc = Optic capsule; On = Optic nerve; Ov = Obliquus ventralis; Pb = Pharyngobranchial; Tp = Transverse process; Ri = Rectus inferior; Sp = Spiracle; Vc = Vertebral centrum.

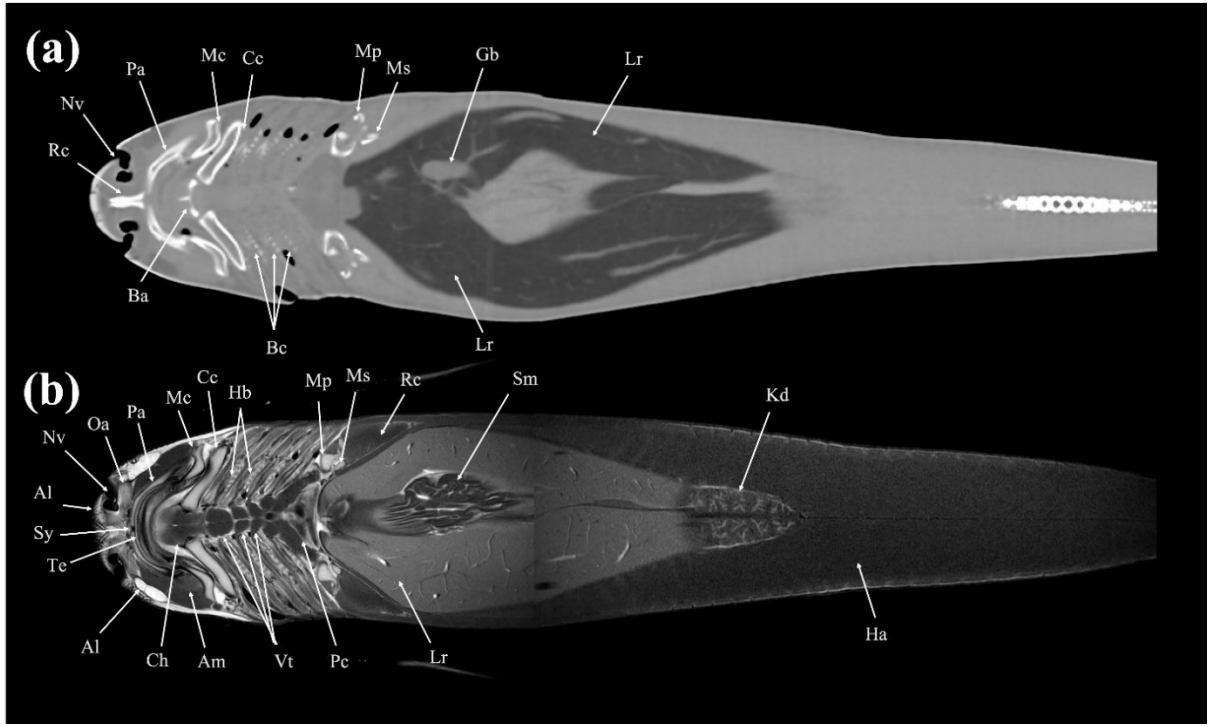

Figure 23. Dorsal (a) CT and (b) MR images of a banded houndshark (*Triakis scyllium*) at level 22 of Figure 1. Abbreviations: Al = Ampullae of Lorenzini; Am = Adductor mandibularis; Ba = Basihyal cartilage; Bc = Branchial cartilage; Cc = Ceratohyal cartilage; Ch = Coracohyoideus; Ha = Hypaxial; Hb = Hypobranchial; Gb = Gall bladder; Kd = Kidney; Lr = Liver; Mc = Meckel's cartilage; Ms = Mesopterygium; Mp = Metapterygium; Nv = Nasal cavity; Oa = Olfactory lamellae; Pa = Palatoquadrate; Pc = Pericardial cavity; Vt = Ventral constrictors; Rc = Rostral cartilage; Te = Teeth; Sm = Stomach; Sy = Symphysis.

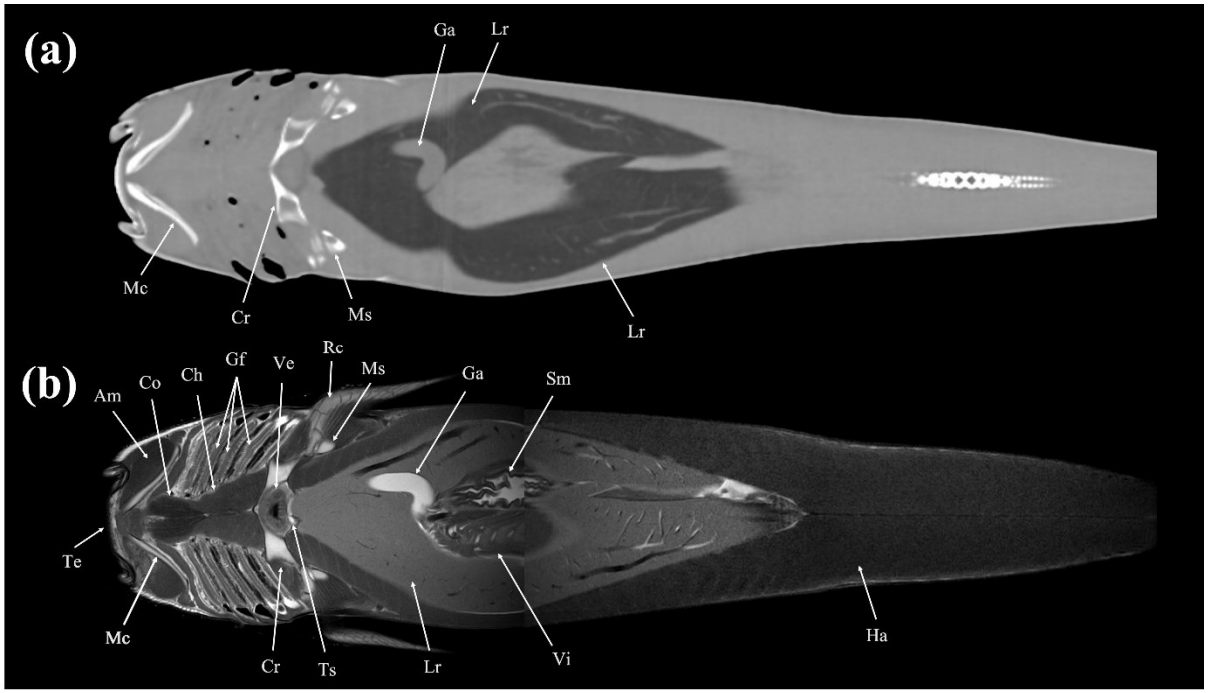

Figure 24. Dorsal (a) CT and (b) MR images of a banded houndshark (*Triakis scyllium*) at level 23 of Figure 1. Abbreviations: Am = Adductor mandibularis; Co = Coracomandibularis; Cr = Coracoid bar; Ch = Coracohyoideus; Ga = Gall bladder; Gf = Gill filament; Ha = Hypaxial; Lr = Liver; Mc = Meckel's cartilage; Ms = Mesopterygium; Rc = Radial cartilage; Sm = Stomach; Te = Teeth; Ts = Transverse septum; Ve = Ventricle; Vi = Valvular intestine.

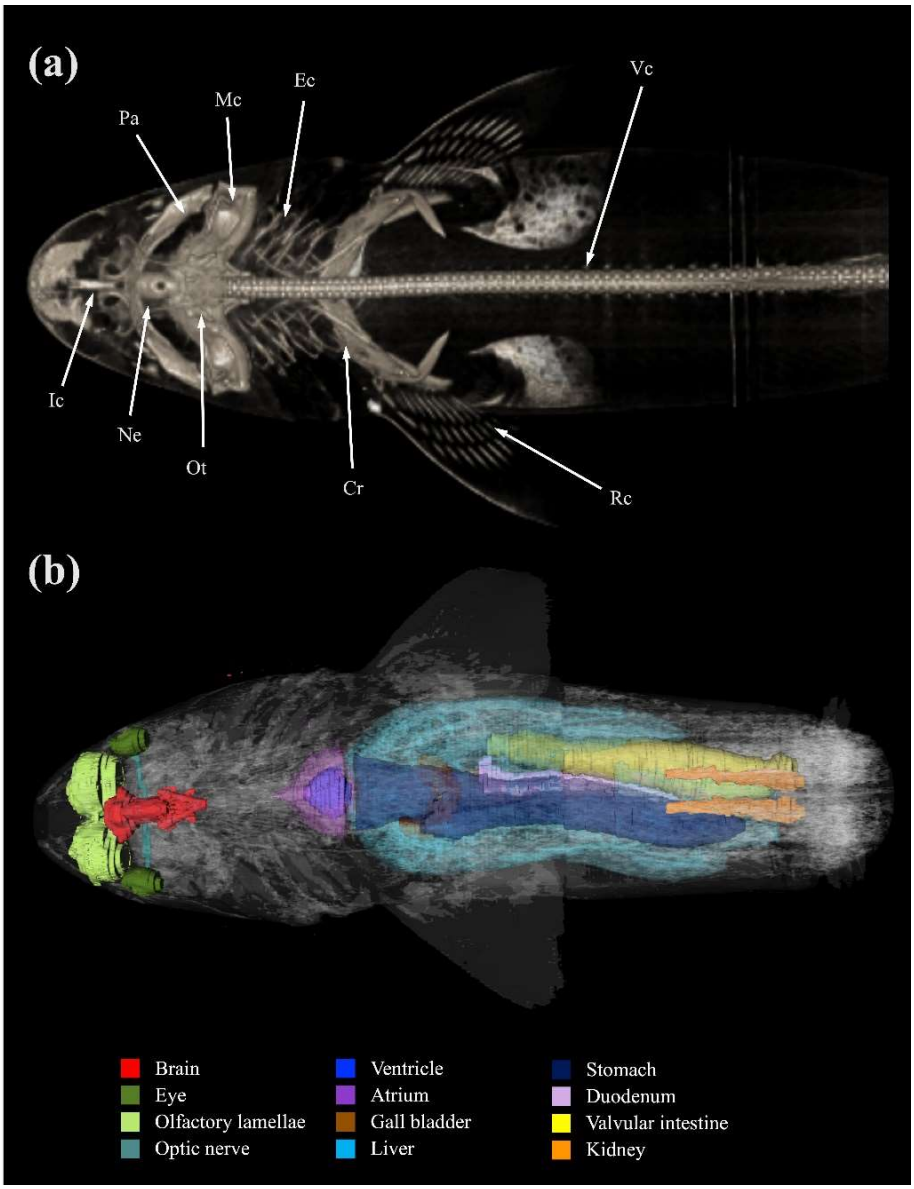

Figure 25. Three-dimensional reconstructed images of (a) CT and (b) MRI showing major skeletal structures and organs respectively of a banded houndshark (*Triakis scyllium*). Abbreviations: Cr = Coracoid bar; Ec = Epibranchial and ceratobranchial cartilage; Ic = Internasal cartilage; Mc = Meckel's cartilage; Ne = Neurocranium; Ot = Otolith; Pa = Palatoquadrate; Rc = Radial cartilage; Vc = Vertebral centrum.

References

Abel, R.L., Maclaine, J.S., Cotton, R., Xuan, V.B., Nickels, T.B., Clark, T.H., et al. (2010). Functional morphology of the nasal region of a hammerhead shark. *Comp. Biochem. Physiol. Part A Mol. Integr. Physiol.* 155(4), 464–475.

Alonso-Farré, J.M., Gonzalo-Orden, M., Barreiro-Vázquez, J.D., Ajenjo, J.M., Barreiro-Lois, A., Llarena-Reino, M. et al. (2014). Cross-Sectional Anatomy, Computed Tomography and Magnetic Resonance Imaging of the Thoracic Region of Common Dolphin (*Delphinus delphis*) and Striped Dolphin (*Stenella coeruleoalba*). *Anat.* 43, 221–229.

Alonso-Farré, J.M. Gonzalo-Orden, M., Barreiro-Vázquez, J.D., Barreiro-Lois, A., André, M., Morell, M., et al. (2015). Cross-sectional Anatomy, Computed Tomography and Magnetic Resonance Imaging of the Head of Common Dolphin (*Delphinus delphis*) and Striped Dolphin (*Stenella coeruleoalba*). *Anat*. 44, 13–21.

Barker, M.J., Schluessel, V. (2005). Managing global shark fisheries: suggestions for prioritising management strategies. *Aquat. Conserv.* 15, 325–347.

Baum, J.K., Blanchard, W. (2010). Inferring shark population trends from generalized linear mixed models of pelagic longline catch and effort data. *Fish Res.* 102, 229–239.

Compagno, L.J.V. (1984). Sharks of the world: an annotated and illustrated catalogue of shark species known to date. *FAO Species Catalogue* 4, 432.

Davidson, L.N.K., Krawchuk, M.A., Dulvy, N.K. (2016). Why have global shark and ray landings declined: improved management or overfishing? *Fish Fish*. 17(2), 438–458.

Dirnhofer, R., Jackowski, C., Vock, P., Potter, K., Thali, M.J. (2006). VIRTOPSY: Minimally Invasive, Imaging-guided Virtual Autopsy. *Radiographics*. 26(5), 1305–1334.

Dulvy, N.K., Simpfendorfer, C.A., Davidson, L.N.K., Fordham, S.V., Bräutigam, A., Sant, G., et al. (2017). Challenges and Priorities in Shark and Ray Conservation, *Curr. Biol.* 27(11), R565–R572.

Dulvy, N.K., Fowler, S.L., Musick, J.A., Cavanagh, R.D., Kyne, P.M., Harrison, L.R., et al. (2014). Extinction risk and conservation of the world's sharks and rays. *eLife* 3, e00590.

Enault, S., Auclair, C., Adnet, S., Debiais-Thibaud, M. (2016). A complete protocol for the preparation of chondrichthyan skeletal specimens. *J. Appl. Ichthyol*. 32(3), 409–415.

Feeney, D.A., Fletcher, T.F., Hardy, R.M. (1991). Atlas of correlative imaging anatomy of the normal dog/Ultrasound and computed tomography. 1st ed. (WB Saunders).

Ferretti, F., Worm, B., Britten, G.L., Heithaus, M.R., Lotze, H.K. (2010). Patterns and ecosystem consequences of shark declines in the ocean. *Ecol. Lett.* 13, 1055–1071.

Ford, J.M., Decker, S.J. (2016). Computed tomography slice thickness and its effects on three-dimensional reconstruction of anatomical structures. *J. Forensic Radiol. Imaging.* 4, 43–46.

Fujinami, Y., Tanaka, S. (2013). Age, growth and reproduction of the banded houndshark *Triakis scyllium* around the tip of the Izu Peninsula, Japan. *Nippon Suisan Gakk.* 79(6), 968–976.

Furukawa, A., Saotome, T., Yamasaki, M., Maeda, K., Nitta, N., Takahashi, M., et al. (2004). Cross-sectional Imaging in Crohn Disease. *Radiographics*, 24(3), 689–702.

Geraghty, P.T., Jones, A.L., Stewart, J., Macbeth, W.G. (2012). Micro-computed tomography: an alternative method for shark ageing. *J. Fish Biol.* 80(5), 1292–1299.

Gumpenberger, M., Henninger, W. (2001). The use of computed tomography in avian and reptile medicine. *Semin. Avian Exot. Pet. Med.* 10(4), 174–180.

Heithaus, M.R., Wirsing, A.J., Dill, L.M. (2012). The ecological importance of intact top-predator populations: a synthesis of 15 years of research in a seagrass ecosystem. *Mar. Freshwater. Res.* 63(11), 1039–1050.

Ibrahim, A.A.H., Adam, Z.E., Tawfiek, M.G. (2019). Cross-sectional anatomy, magnetic resonance imaging and computed tomography of fetlock joint in camel. *J. Vet. Med. Res*. 26(2), 258–270.

IUCN (International Union for Conservation of Nature). The IUCN Red List of Threatened Species 2018. http://www.iucnredlist.org [Accessed November 11, 2019]

Jambura, P.L., Kindlimann, R., López-Romero, F., Marramà, G., Pfaff, C., Stumpf, S., et al. (2019). Micro-computed tomography imaging reveals the development of a unique tooth mineralization pattern in mackerel sharks (Chondrichthyes; Lamniformes) in deep time. *Sci. Rep.* 9, 9652.

Kamminga, P., Bruin, P.W.D., Geleijns, J., Brazeau, M.D. (2017). X-ray computed tomography library of shark anatomy and lower jaw surface models. *Sci. Data.* 4, 170047.

Kandoran, M.K., Govindan, T.K., Suryanarayana Rao, S.V. (1965). Some aspects of curing of sharks and rays. *Fish Technol.* 2(2), 193–197.

Kot, B.C.W., Chan, D.K.P., Yuen, A.H.L., Tsui, H.C.L. (2018). Diagnosis of atlanto-occipital dissociation: Standardised measurements of normal craniocervical relationship in finless porpoises (genus Neophocaena) using postmortem computed tomography. *Sci Rep*. 8, 8474.

Kraitchman, D., Kamel, I., Weiss, C., Georgiades, C. (2017). Elucidation of percutaneously accessible lymph nodes in swine: a large animal model for interventional lymphatic research. *J. Vasc. Interv. Radiol.* 28, 451–456.

Lack, M., Sant, G. (2011). The future of sharks: a review of action and inaction. TRAFFIC International and the Pew Environment Group.

https://www.pewtrusts.org/~/media/legacy/uploadedfiles/peg/publications/report/the20future20of20sharkspdf.pdf

Lauridsen, H., Hansen, K., Wang, T., Agger, P., Andersen, J.L., Knudsen, P.S., et al. (2011). Inside Out: Modern Imaging Techniques to Reveal Animal Anatomy. *PLoS One*. 6(3), e17879.

Lautenschlager, S., Bright, J.A., Rayfield, E.J. (2014). Digital dissection-using contrast-enhanced computed tomography scanning to elucidate hard- and soft-tissue anatomy in the Common Buzzard Buteo buteo. *J. Anat.* 224, 412–431.

Mara, K.R., Motta, P.J., Martin, A.P., Hueter, R.E. (2015). Constructional morphology within the head of hammerhead sharks (sphyrnidae). *J. Morphol.* 276(5), 526–539.

Meng, Q., Li, W. (1992). Monographs of Fishes of China. No. 3 Anatomy of Shark and Skate (PL: Ocean Publishing).

Mollen, F.H., Wintner, S.P., Iglésias, S.P., Sommeran, S.R.V., Jagt, J.W.M. (2012). Comparative morphology of rostral cartilages in extant mackerel sharks (Chondrichthyes, Lamniformes, Lamnidae) using CT scanning. *Zootaxa*. 3340(1), 29–43.

Mollen, F.H., Wintner, S.P., Iglesias, S.P., Van Sommeran, S.R., Jagt, J.W. (2012). Comparative morphology of rostral cartilages in extant mackerel sharks (Chondrichthyes, Lamniformes, Lamnidae) using CT scanning. *Zootaxa*. 3340, 29–43.

Montie, E.W., Manire, C.A., Mann, D.A. (2011). Live CT imaging of sound reception anatomy and hearing measurements in the pygmy killer whale, Feresa attenuata. *J. Exp. Biol*. 214, 945–955.

Moyer, J.K., Hamilton, N.D., Seeley, R.H., Riccio, M.L., Bemis, W.E. (2015). Identification of shark teeth (Elasmobranchii: Lamnidae) from a historic fishing station on Smuttynose Island, Maine, using computed tomography imaging. *Northeast Nat.* 22(3), 585–597.

Myers, R.A., Baum, J.K., Shepherd, T.D., Powers, S.P., Peterson, C.H. (2007). Cascading Effects of the Loss of Apex Predatory Sharks from a Coastal Ocean. *Science.* 315, 1846–1850.

Nakamae, Y., Ishihara, A., Itoh, M., Yanagawa, M., Sasaki, N., Yamada, K. (2018). Displacement of the large colon in a horse with enterolithiasis due to changed positions observed by computed tomography. *J. Equine. Sci.* 29, 9–13.

Porter, E.G., Winter, M.D., Sheppard, B.J., Berry, C.R., Hernandez, J.A. (2005). Correlation of articular cartilage thickness measurements made with magnetic resonance imaging, magnetic resonance arthrography, and computed tomographic arthrography with gross articular cartilage thickness in the equine metacarpophalangeal joint. *Vet. Radiol. Ultrasound.* 57, 515–525.

Preziosi, R., Gridelli, S., Borghetti, P., Diana, A., Parmeggiani, A., Fioravanti, M.L., et al. (2005). Spinal deformity in a sandtiger shark, Carcharias taurus Rafinesque: a clinical–pathological study. *J. Fish Dis.* 29(1), 49–60.

Samii, V.F., Biller, D.S., Koblik, P.D. (1998). Normal cross-sectional anatomy of the feline thorax and abdomen: comparison of computed tomography and cadaver anatomy. *Vet. Radiol. Ultrasound.* 39(6), 504–511.

Smallwood, J.E., George, T.F. (1993a). Anatomic atlas for computed tomography in the mesaticephalic dog: Thorax and cranial abdomen. *Vet. Radiol.* 34, 65–84.

Smallwood, J.E., George, T.F. (1993b). Anatomic atlas for computed tomography in the mesaticephalic dog: Caudal abdomen and pelvis. *Vet. Radiol.* 34, 143–167.

Stevens, J.D., Bonfil, R., Dulvy, N.K., Walker, P.A. (2000). The effects of fishing on sharks, rays, and chimaeras (chondrichthyans), and the implications for marine ecosystems. *Ices. J. Mar. Sci.* 57(3), 476–494.

Summers, A.P., Ketcham, R.A., Rowe, T. (2004). Structure and function of the horn shark (Heterodontus francisci) cranium through ontogeny: Development of a hard prey specialist. *J. Morphol.* 260(1), 1–12.

Timm, L.L., Fish, F.E. (2012). A comparative morphological study of head shape and olfactory cavities of sharks inhabiting benthic and coastal/pelagic environments. *J. Exp. Mar. Biol. Ecol.* 414–415, 75–84.

Tomita, T., Sato, K., Suda, K., Kawauchi, J., Nakaya, K. (2011) Feeding of the Megamouth Shark (Pisces: Lamniformes: Megachasmidae) predicted by its hyoid arch: a biomechanical approach. *J. Morphol*. 272, 513–524.

Valente, A.L.S., Cuenca, R., Zamora, M., Parga, M.L., Lavin, S., Alegre, F., et al. (2007). Computed tomography of the vertebral column and coelomic structures in the normal loggerhead sea turtle (*Caretta caretta*). *Vet. J.* 174(2), 362–370.

Van Bonn, W., Jensen, E., Brook, F. (2001). “Radiology, computed tomography, and magnetic resonance imaging” in CRC Handbook of Marine Mammal Medicine, ed. L. A. Dierauf, F. M. D. Gulland (CRC Press Inc.), 557–591.

Wroe, S., Huber, D.R., Lowry, M., McHenry, C., Moreno, K., Clausen, P., et al. (2008). Three-dimensional computer analysis of white shark jaw mechanics: how hard can a great white bite? *J. Zool.* 276, 336–342.

Wyman, A.C., Lawson, T.L., Goodman, L.R. (1978). “Transverse anatomy of the human thorax, abdomen and pelvis” in An atlas of anatomic radiologic computed tomographic and ultrasonic correlation. 1st ed. (Little, Brown and Co.).

CHAPTER II

Preliminary study for banded houndshark (*Triakis scyllium*) semen cryopreservation: preparing for the *ex-situ* conservation of endangered shark species

Abstract

In modern times, overfishing by humans has resulted in sharks becoming critically endangered. *Ex-situ* conservation is especially important for sharks because their reproduction rates are very slow. To establish shark semen cryopreservation protocol for *Triakis scyllium*, an optimum activating extender solution named shark spermatozoa activating extender 1 was utilized. The final cryopreservation protocol established was as follows: extender, filtered seawater; extension ratio, 1:3; cryoprotectant, egg yolk 10% + ethylene glycol 10%; equilibration period, 10 min; cooling rate, 3 cm, 3 min; thawing temperature, 30℃, 10 s. The resulting post-thaw spermatozoa motility was 2.03%. Although this is a low level of post-thaw spermatozoa motility, the results of this study provide a basis for future studies, which can derive the conditions and directions of tests to improve post-thaw spermatozoa motility levels.

Key words: cryopreservation, *ex-situ* conservation, spermatozoa, shark, *Triakis scyllium*

1. Introduction

Sharks have survived many mass extinction events over the last 450 million years. However, over the last 40–50 years, overfishing by humans has led to a recent decline in the populations of many shark species, and consequently, their risk for extinction has greatly increased (Lack and Sant, 2011; Stevens et al., 2000). Of the shark species on the International Union for Conservation of Nature (IUCN) Red List, 27.9% are classified as “vulnerable,” “endangered,” or “critically endangered” (IUCN, 2020). Given this trend, it is obvious that it is only a matter of time before these sharks face actual extinction. As sharks are keystone species that exist at the top of ocean food chains and play essential roles for maintaining the balance of marine ecosystems, previous investigations have shown that the number of edible fish species would drop sharply if sharks were to become extinct (Myers et al., 2007). The conservation of endangered shark species is, thus, essential, not only for the sharks and their ecosystems, but also for the sustainable management of human food resources from the seas and oceans (Myers et al., 2007).

As the shark extinction crisis has become serious, securing conservation technologies has become inevitable, and one of the last options for critically endangered species is *ex-situ* conservation. Inducing ovulation and increasing their populations through artificial insemination (AI) is a typical *ex-situ* conservation method. Artificial insemination studies have previously been conducted to conserve various endangered species, not only with terrestrial animals, but also with various

piscine species, including lake sturgeon (*Acipenser fulvescens*), golden mahseer (*Tor putitora*), long whiskers catfish (*Mystus guillo*), and Pabda catfish (*Ompok pabda*) (Thongtip et al., 2009; Blanco et al., 2009; Ogale et al., 1997; Mijkherjee et al., 2002; Ogale et al., 2002; Hermes et al., 2007; Hildebrandt et al., 2007; Devi et al., 2009).

Semen cryopreservation is an important assisted reproductive technology (ART) that is often used alongside AI, as when species numbers plummet worldwide, it can help maintain sufficient levels of genetic diversity. Furthermore, of the various cell types, spermatozoa have previously been identified as the easiest targets for cryopreservation (Martinez-Paramo et al., 2017). It is much easier to move cryopreserved spermatozoa than it is to move the organism itself for reproduction.

However, despite the need, only a few studies have been conducted on securing ARTs for sharks. Only two studies on AI and one study on hormone-induced AI were reported in sharks so far (Masuda et al., 2003; Masuda et al., 2005; Kim et al., 2020). There has only been one study published to date on semen cryopreservation in elasmobranchs, which focused on the stingray *Urolophus paucimaculatus* (Daly et al., 2011; Daly et al., 2017), but none have been published on sharks. Once a shark semen cryopreservation protocol has been established, AI can be performed by exchanging the semen between aquariums around the world. Furthermore, by creating a cryobank or a sperm bank, genetic pools can be secured beyond the constraints of space and time (Wildt et al., 1997; Kumar, (Wildt et al., 1997; Kumar,

2012). The spread of disease can also be prevented if enough care is taken in the process (Martinez-Paramo et al., 2009).

Triakis scyllium (banded houndshark) is a shark species that belongs to the order Carcharhiniformes and family Triakidae. They are small sharks with an adult body length of less than 1.5 m, show aplacental viviparity, and seasonally breed in the wild. Their main prey are benthic invertebrates and fish, and the sharks are found in the Northwest Pacific Ocean and are commonly caught in the waters of the Republic of Korea, Japan, and Taiwan (Compagno, 1984). Of the species in the order Carcharhiniformes, *T. scyllium* is relatively small, which makes it easy to handle. It is one of the most accessible shark species in the Republic of Korea. However, they are classified as “endangered” in the IUCN Red List (Rigby et al., 2021).

To obtain sufficient sample sizes in wildlife studies, various constraints must be addressed, including limited study periods, sample scarcity, or insufficient funding (Morrison et al., 2008). In shark research, it is particularly difficult to obtain sufficient sample sizes in a similar vein. However, even with such difficulty, it is not impossible to acquire a *T. scyllium* population for research. Though wild bycaught *T. scyllium* in fish markets are mostly immature, they can be raised in aquariums for a few years, during which they can become mature enough for breeding. Therefore, *T. scyllium* was chosen as the subject species for this study to establish a preliminary semen cryopreservation protocol in sharks.

To the best of my knowledge, this is the first report on shark spermatozoa cryopreservation. This study aimed to set up a semen cryopreservation protocol in the endangered *T. scyllium* and establish foundational information that can be utilized long-term for developing an applicable protocol for future conservation practices of endangered shark species.

2. Materials and methods

2.1. Sharks and their husbandry

Male *T. scyllium* with total body lengths longer than 90 cm were primarily screened for sexual maturity (Fujinami and Tanaka, 2013), and moved to Aqua Planet Jeju. Sharks large enough for this experiment were those that had been raised in an aquarium for more than six years, and five sharks were gathered for the experiment and named M001–M005, respectively. Their body weights, lengths, and clasper sizes were measured accurately. To determine sexual maturity more precisely, clasper calcification, elongation, and bending and rhipidion formation were checked (**Table 1**) (Clark and Von Schmidt, 1965). Overall, the sharks demonstrated good activity levels and appetites.

The sharks were contained in a nine-ton seawater tank that received water directly from the coastal water of Jeju Island after filtration and temperature control.

During the experiment, the water quality was maintained at a pH of 7.0 ± 0.0; temperature, 22.0 ± 0.2℃; salinity, 40.2 ± 1.0 ppt; specific gravity, 1.0 ± 0.0; dissolved oxygen, 8.6 ± 0.3 ppm; NO_2^-, 0.006 ± 0.002 ppm; NO_3^-, 2.3 ± 0.3 ppm; NH_3, 0.0 ± 0.0 ppm. Sharks were fed squid, whiteleg shrimp, and mackerel three times a week, and the Mazuri Vita-Zu® Shark/Ray II Tablet (Purina Mills LCC, USA) once a week. The experiments began after an acclimation period of more than a month.

2.2. Semen collection and activation

2.2.1. Semen collection

As a previous study showed that the largest quantity of semen could be sampled 1 h post intramuscular injection with Ovaprim® [(D-Arg6, Pro9NEt)-sGnRH + domperidone] (0.2 mL/kg), semen sampling was done accordingly in subsequent experiments (**Figure 1**) (Kim et al., 2020).

Semen sampling was performed under sedation using MS-222 (pH adjusted to 7.0 with $NaHCO_3$) at 45 to 55 ppm. To obtain semen without feces contamination, the whole urogenital papilla was inserted into the tip of the syringe without a needle, and a slight negative pressure was applied while gently massaging the abdomen of the shark. In shark semen samples, the primary portion is clear liquid, which does not contain spermatozoa, followed by a cloudy portion with a high concentration of spermatozoa. When semen is ejected from the urogenital papilla, the primary portion

of the liquid inevitably mixes with urine, and consequently, only the cloudy secondary portion of the semen was sampled to avoid urine contamination in a strategy similar to that used in the semen sampling of other animals (Barber, 2016).

2.2.2. Activating extender tests (AETs)

Activating extender test (AET)-1 and AET-2 were conducted to determine the composition of an optimal solution. The spermatozoa activating extender candidates for AET-1 were based on a literature study and included modified Tsvetkova's extender (MT), modified Beltsville poultry semen extender (MB), modified Hank's balanced salt solution (MH), and shark Ringer solution (SR) (Daly et al., 2011; Suquet et al., 2000; Lockwood, 1961; Glogowski et al., 2002). The candidates MT, MB, and MH were further modified by adding trimethylamine oxide (TMAO) and urea based on the shark's body fluid concentrations (**Table 2**); these were then designated as MT-EM, MB-EM, and MH-EM, as EM stands for "elasmobranch modification". Next, AET-1 was conducted using the semen sample of the largest volume from the five males. Fresh semen was diluted to 1:10 with each activating extender solution and kept at 21℃ during the motility test. Activating extender solution of the best capability was selected.

To improve the activation capabilities, AET-2 was planned as described in **Table 3**. Two new activating extender solution candidates for AET-2 were made and identified as shark spermatozoa activating extender (SSAE)-1 and SSAE-2.

Spermatozoa motility was recorded on video and analyzed for both AET-1 and AET-2 (Nussdorfer et al., 2018). The semen was diluted at a ratio of 1:10 using each activating extender solution, and the video was recorded at a ×400 magnification using an optical microscope (Olympus CX31, Japan). A total of five viewpoints were recorded in one slide, including center and marginal sites, and at least 100 spermatozoa were counted to determine the proportion with total motility. In every motility analysis, total motility, including that of both progressive and non-progressive spermatozoa, was measured. The temperature of the semen and activating extender solutions was maintained at 21°C. Every experiment was done in triplicate. Simple descriptive comparisons were performed since statistical analysis was impossible due to an insufficient study population, which is a common occurrence in experiments with sharks.

2.3. Semen quality check

The volume, concentration, morphology, total motility, and duration of motility (DOM) of the five sharks' semen were analyzed using the selected activating extender solution from AET-2. The best semen was selected after the quality check and used for the subsequent cryopreservation experiments.

To analyze the spermatozoa concentrations, the semen was diluted to 1:100 with filtered seawater (FSW) and counted using a disposable hemocytometer. The FSW was seawater from the shark tank, filtered with a 0.22 μm Millex-GV syringe filter

(Merck Millipore, Darmstadt, Ger-many). For the morphology analysis, the semen was diluted to 1:10 with FSW, and the proportions of the spermatozoa with normal morphologies were determined. Total motility was checked on a 3 h basis, and the time from dilution in the activating extender solution to when total motility reached zero was the DOM. During the experiments, the semen and activating extender solutions was maintained at 21°C.

2.4. Semen cryopreservation

2.4.1. Primary experiment strategy

To determine the best protocol for the primary semen cryopreservation test (SCT-1), the following six independent factors were tested: extender solution (α), extension ratio (β), type and concentration of cryoprotectant (γ), equilibration period (δ), cooling rate (ε), and thawing temperature (ζ). Starting with a default protocol where α = SR, β = (1:3), γ = 10% dimethyl sulfoxide (DMSO), δ = 1 min, ε = 5 cm (height above the liquid nitrogen surface), and ζ = 21°C, which was decided based on information from marine teleosts (Suquet et al., 2000), α was changed for all n_α levels while the other five factors were fixed at the levels in the default protocol. Then, β was changed for all n_β levels while the other five factors were fixed as in the default protocol. This process was repeated for all factors. This approach formed a subset consisting of $n_\alpha + n_\beta + n_\gamma + n_\delta + n_\varepsilon + n_\zeta$ experiments from the entire set of $n_\alpha \times n_\beta \times$

$n_\gamma \times n_\delta \times n_\varepsilon \times n_\zeta$ experiments. The subset implies a fine grain enumeration of experimental conditions in the proximal distance from the reference protocol.

The cryopreservation extender solution has a different purpose than that of the activating extender solution, since the spermatozoa needs to minimize its ATP usage before being frozen (Suquet et al., 2000). Therefore, all the extender candidates in SCT-1 were retested. In addition, the elasmobranch-modified Original Tsvetkova's extender (OT-EM) that did not contain NaCl (Minamikawa and Morisawa, 1996) was tested. SR without NaCl was also compared with normal SR (**Table 4**). After equilibration, 300 μL of the semen solution was placed into 0.5 mL medium straws (Minitüb, Tiefenbach, Germany) and sealed. The cooling rate varied, as the samples were cooled 3, 5, and 9.5 cm above the liquid nitrogen surface for 3 min and then directly placed into the liquid nitrogen tank. The cryopreserved semen was kept for 17 h and then thawed for 10 s. Then, the semen was maintained at 21℃, and the post-thaw semen quality was checked. A total of 32 experiments with different conditions were tested in triplicate (**Table 5**).

2.4.2. Secondary experiment strategy

The secondary semen cryopreservation test (SCT-2) was established to compare the extension ratios of 1:3 and 1:5 (experiment IDs 1 and 9) as the differences between the motile spermatozoa counts were negligible in SCT-1. The experiments with the extension ratios of 1:3 and 1:5 were named "experiment 2-1" and "experiment 2-2",

respectively. All the other conditions were selected from SCT-1 based on a simple comparison of the experimental results: extender, FSW; cryoprotectant, egg yolk (EY) 10% + ethylene glycol (EG) 10%; equilibration period, 10 min; cooling rate, 3 cm (3 min); thawing temperature, 30℃ (10 s).

2.4.3. Post-thaw semen quality check

The cryopreserved samples were thawed after 17 h, and the semen quality was checked for both SCT-1 and SCT-2. The cryopreserved 0.5 mL medium straws were thawed in water at temperatures corresponding to each experimental condition for 10 s. Frozen-thawed semen samples were immediately diluted to 1:5 with the previously selected activating extender solution. The samples were maintained at 21℃ using the water bath, and the total motility was checked every 12 h to determine the DOM, as previous records showed DOMs of more than 60 h. The total spermatozoa number was calculated by multiplying the spermatozoa concentrations and the volume (6 μL).

2.5. Three-dimensional modeling

The spermatozoon of *T. scyllium* was modeled in three-dimensions (3D) using Autodesk® Inventor® Professional 2019 (Autodesk Inc., San Rafael, CA, USA) based on the size and shape observed in this experiment to understand its geometric features. For comparison, human spermatozoon was also modeled in 3D, as its size and shape have been previously investigated (Tsvetkova et al., 1996). The volume

(V), surface area (SA), and SA:V ratio of each spermatozoon were calculated using the same software.

2.6. Institutional review board statement

This study was approved by the Seoul National University Institutional Animal Care and Use Committee (approval number: SNU-181218-2). All the experiments were performed in accordance with the relevant guidelines and regulations.

3. Results

3.1. Spermatozoa morphology and kinetics

The spermatozoa of *T. scyllium* were observed with an optical microscope, both with and without staining (**Figure 2**). Each cell was composed of a helical head with many gyres, a long midpiece, and a flagellum, showing common features of other sharks' spermatozoa (Minamikawa and Morisawa, 1996). From measuring the length of the head, midpiece, and flagellum of 100 randomly chosen spermatozoa using MOTIC Image Plus 2.0 (Motic China Group Co., LTD, Xiamen, China), the average sizes were determined to be as follows: head, 32.7 ± 1.7 μm; midpiece, 8.3 ± 0.4 μm; flagellum, 54.6 ± 2.9 μm.

3.2. Optimal shark spermatozoa activating extender solution

3.2.1. Activating extender test 1

Out of the five sharks tested, the largest volume of semen was collected from M001. Since the composition of the optimal SSAE solution was not yet determined, the semen quality of each shark could not be accurately verified. Thus, AET-1 was performed using the semen from M001. Total motility (both progressive and non-progressive) was measured after 1:10 dilutions with the five different activating extender solutions, and the results were as follows: MB-EM, 9.01%; MH-EM, 0.00%; MT-EM, 0.00%; SR, 57.35%; FSW, 18.18%.

3.2.2. Activating extender test 2

Semen from M005 was used in AET-2 since it provided the largest sample volume for the test (M001: 1 mL; M002: 1.5 mL; M003: 0.75 mL; M004: 2.7 mL; M005: 4 mL). As the source of the semen used was changed from that used in AET-1 (i.e., M001), the SR solution was tested again for comparison. Since it has been previously determined that Na^+ concentration is one of the most important factors for spermatozoa activation in *T. scyllium* and that pH has no significant effect on motility, the main purpose of AET-2 was to improve the performance of the solution by adjusting the Na^+ concentrations (Rurangwa et al., 2004). In addition, TMAO and dextrose were added to the solution, as hexose has previously been shown to serve as an important factor in maintaining spermatozoa motility (Rurangwa et al., 2004).

As a result, the total motility of the M005 semen was as follows: SR, 91.82%; SSAE-1, 99.02%; SSAE-2, 79.78%.

3.3. Semen quality test

The semen quality check results from all five sharks are presented in **Table 6**. M003 had the highest concentration of spermatozoa (3.70×10^{11}/L), while M004 had the highest percentage of spermatozoa with normal morphologies (99.5%). M005 had the highest total motility levels (98.90%), and M001 had the greatest DOM (60 h). The largest volumes of semen obtained with AET-1 and 2 were from M001 and M005, respectively. Since the most important criterion of the post-thaw semen quality is motility, the spermatozoa from M004 and M005 were chosen for use in the subsequent experiments.

3.4. Semen cryopreservation

3.4.1. Semen cryopreservation test 1

In each experiment, the same semen pool had to be used to compare each candidate under the same condition. Since the amount of semen from a single shark was not enough to test various experimental conditions in triplicate at one time, semen from two sharks were mixed to obtain a sufficient volume. In this regard, the semen samples from M004 and M005 were mixed and used for SCT-1 and SCT-2. The

qualities of the semen used for each experiment can be found in **Table 7**, and the results of SCT-1 are in **Table 8**.

3.4.2. Semen cryopreservation test 2

The results of SCT-2 were as follows: experiment ID 2-1 (extension ratio 1:3), 2.03% total motility and 36 h DOM; experiment ID 2-2 (extension ratio 1:5), 1.64% total motility and 36 h DOM. The total motility values from SCT-1 and SCT-2 are plotted together in **Figure 3**.

3.5. Three-dimensional modeling

As the features of the shark spermatozoon are unique relative to those of other vertebrates, human and shark spermatozoa were modeled in 3D to compare and understand the geometric characteristics of the shark spermatozoon (**Figure 4**). The results for the V, SA, and SA:V ratio were as follows: shark, V = 9.4 μm^3 (relative error = 0.5%), SA = 96.2 μm^2 (relative error = 0.5%), SA:V ratio = 10.3; human, V = 25.3 μm^3 (relative error = 0.4%), SA = 87.5 μm^2 (relative error = 0.1%), SA:V ratio = 3.5. Thus, the SA:V ratio of the shark spermatozoon is approximately three times greater than that of the human spermatozoon.

4. Discussion

The sharks used in this study were collected from the largest aquariums in South Korea (Aqua Planets Ilsan, 63, and Jeju). Though *T. scyllium* are commonly caught off the coast of Korea, almost all the sharks caught are immature and less than 70 cm in total body length. Sufficiently mature *T. scyllium* were only available in the aquariums since they had been raised for more than six years after capture, and the number used in this study was virtually the maximum in Korea. Although it was not possible to secure enough samples for statistical analysis due to the time, physical, and environmental constraints of this project, which are limitations of wildlife research in general (Morrison et al., 2008), this study pressed ahead as it is meaningful as a study of sharks and as preliminary research for further studies.

4.1. Seasonality

The breeding history of the sharks shows that they have pregnancies regardless of the season, which indicates the loss of seasonality. This is thought to be due to the water temperature of fish tanks, since it is very stably maintained year-round and fluctuates less than 2℃. Based on the fact that annual water temperature changes in the aquarium were insignificant and that the sharks in this experiment had been kept indoors for more than six years, with irregular pregnancies, the loss of seasonality is probable. In fact, loss of seasonality has already been reported in indoor-bred fish, including sharks (Schaller, 2006). Although each shark can be at a different stage of

the reproductive cycle due to such a situation, a comparative evaluation of protocols was possible since the experiments were conducted using the same semen pool in SCT-1 and SCT-2. Nonetheless, in future studies, post-thaw motility may increase if the cryopreservation protocol is applied to suitably matured semen during the mating season.

The induction of semen was needed because of the loss of seasonality in the sharks, and Ovaprim® worked well for the purpose of this study. Ovaprim® is one of the most successfully used chemicals for teleost reproduction induction, as its safety and effectiveness have been proven over time (Yanong et al., 2009). It contains synthetic salmon gonadotropin-releasing hormone (GnRH), which facilitates the release of stored gonadotropins, and domperidone, which acts as a dopamine D2 receptor antagonist. Together, they facilitate germ cell maturation and release in fish bodies. Though there has only been one study on Ovaprim® application in elasmobranchs (Kim et al., 2020), this study also showed that Ovaprim® is effective for reproduction induction with male *T. scyllium*.

4.2. Spermatozoa morphology and kinetics

The metric characteristics of spermatozoa provide important information since they are species specific (Tanaka et al., 1995). Though the morphologies of spermatozoa in various shark species have been studied to date, metric information on *T. scyllium* spermatozoa has not been reported yet (Temple-Smith et al., 2018; Hamlett, 2005;

Rowley et al., 2019). The spermatozoon showed a peculiar helix shape with 10–12 gyres, and the average sizes of head length, midpiece length, and flagellum length showed values within the ranges of those of 25 shark species identified by Rowley et al. (2019). Compared with the features of other vertebrate spermatozoa, the shark spermatozoon was found to have a relatively higher head-to-total length ratio (Fig. 5).

Microscopic observations of shark spermatozoa showed that the speed of movement in passing through mucus was faster than that in low viscosity extension solutions. The time taken for a single spermatozoon to travel the length of its own head was found to be 2.1 s in the extension solution and 0.8 s in the mucus. The shark spermatozoa made drill-like, rotational, and forward movements at the same time, using their flagella as the driving force. Their helical heads worked like the thread of a screw, allowing them to pass through semi-solid materials such as mucus, and this mechanism allows for faster movement in mucus than in a liquid with a lower viscosity.

Spermatozoa must generate energy for moving flagella, and a constant supply of energy sources such as fructose, glucose, or pyruvate and discharge of waste materials are required (Pitnick et al., 2009). Minamikawa and Morisawa (1996) found that the glucose concentration of female uterine fluid is higher than that of semen in *T. scyllium*. Spermatozoa maintain high motility in uterine plasma, but their motility significantly decreases in artificial uterine plasma with lower glucose

concentrations. As glucose is commonly used as an energy source for spermatozoa in other vertebrates, hexoses, including glucose, can be used as an energy source for spermatozoon motility during migration through the female reproductive tract (Pitnick et al., 2009). In this regard, a high SA:V ratio can act as a factor for efficient energy source absorption and waste product excretion in a spermatozoon. In the case of sharks, there are even cases where spermatozoa survive in the female reproductive tract for more than two years, during which efficient material exchange with the surrounding environment can confer a favorable advantage for cell survival (Misro and Ramya, 2012).

4.3. Spermatozoa activation

Spermatozoa were entangled with each other, forming a packet, and did not show much motility when freshly sampled. They started to display motility when they were diluted and untangled using the proper activating extender solution. The shark Ringer solution, which contained a higher Na^+ concentration than that of the other activating extenders in AET-1, induced the best motility. It also had a buffer system that contained Na^+. These findings are consistent with the results of a previous study that identified the importance of Na^+ concentration in the activation of *T. scyllium* semen (Rurangwa et al., 2004). Since the motilities of the M001 and M005 spermatozoa in the SR were markedly different (M005: 91.82%; M001: 57.35%), the semen quality was confirmed to vary between individuals. In AET-2, SSAE-1 showed a higher motility of 98.90% than that in SR, while SSAE-2 showed a lower

motility of 79.78%. The only difference between SSAE-1 and SSAE-2 was their Na^+ concentrations. The appropriate Na^+ concentration for semen activation is closer to 500 mM since the SSAE-1 contained 500 mM of Na^+, which is consistent with the results of a previous study by Minamikawa and Morisawa (1996). Based on the AET-1 and AET-2 results, SSAE-1 was selected as the optimal SSAE solution. The chosen activating extender was able to induce the total motility of spermatozoa up to 99.02%, which makes the solution worth using in subsequent studies in the future.

4.4. Semen cryopreservation

In this study, motility was selected as one of the factors representing the quality of post-thaw spermatozoa. This is based on the characteristic that the motility of spermatozoa reflects their viability and fertilizing capacity well, showing a positive relationship (Storrie et al., 2008; Aas et al., 1991; Rurangwa et al., 2004). The total motility of the frozen-thawed spermatozoa using the default protocol was very low, at 0.002%, and it could thus be inferred that it was not suitable for shark semen. This resulted in overall very low motility of less than 1% with SCT-1. Among the various conditions tested, DMSO and glycerol resulted in the decrease in motility in a dose-dependent way. Higher concentration resulted in less motility in the spermatozoa, which was not able to be statistically confirmed due to the lack of the number of sharks but could be observed through simple comparisons. As cryoprotectants, DMSO and glycerol had little contribution to survival rates and even made the motility lower at their higher concentrations. The selection of DMSO as the

cryoprotectant of the default protocol is one of the reasons for the overall decline in motility in SCT-1. The equilibration period also appears to have contributed to the lower overall spermatozoa motility with SCT-1, as the default time was 1 min, which was an insufficient amount of time for the various cryoprotectants to be absorbed. However, despite all these factors, every total motility value varied, and it was possible to verify the best candidates of SCT-1 and SCT-2 using simple numerical comparisons and conclude the best combination, which is named as Kim's protocol, as follows: extender, FSW; extension ratio, 1:3; cryoprotectant, EY 10% + EG 10%; equilibration period, 10 min; cooling rate, 3 cm (3 min); thawing temperature, 30℃ (10 s). Although the initial total motility of the semen used in SCT-2 was 3.62% lower than that used in SCT-1, the post-thaw total motility increased by more than 10 times into the 2% range, which indicates that this combination contributes to the cryopreservation of shark semen.

Many studies have been conducted on semen cryopreservation in diverse teleost species and post-thaw motility rate or post-thaw motility recovery (ratio of the fresh semen's motility rate and post-thaw semen's motility rate) have also been reported (Cabrita et al., 2010). There are many species that show remarkably high levels of post-thaw motility. Silver carp and Malaba grouper are two of the examples as they show post-thaw motility values close to 100% (Alvarez et al., 2008; Gwo and Ohta et al., 2008). There are also some cases of low post-thaw motility such as Arctic char (10–25%), shortnose stur-geon (16%), or zebrafish (12.1%) (Mansour et al., 2006;

Horvath et al., 2008; Morris et al., 2008). However, the post-thaw motility is not necessarily linked directly to the fertility rate artificially inseminating using cryopreserved semen. For example, in the case of the Arctic char mentioned earlier, despite the 10–25% of post-thaw motility rate, the fertility rate is high at 62.2% (Mansour et al., 2006). Silver carp, on the other hand, reported a fertility rate of 50.6%, which is relatively lower than its post-thaw motility of nearly 100%. Sharks do not have data on the post-thaw motility of semen required for fecundation yet, due to the lack of study on their semen cryopreservation and AI trial with frozen semen. This should be studied precisely by follow-up studies as actual fecundation is one the most important parts of ART.

Fish spermatozoa are immotile in testis and become activated after ejaculation by various factors (Cabrita et al., 2010). In the case of extender solutions used before freezing, the goal is not to activate spermatozoa that are still immotile right after ejaculation but to keep the cells stable so that post-thaw spermatozoa show the best motility and DOM when activated. The energy sources available to spermatozoa are limited to some extent, which can be seen by the inverse reduction of DOM when the motility increases due to increased metabolic rates with rising water temperatures (Cabrita et al., 2010). When cryopreserving spermatozoa, these limited energy sources are desired to be used for improving motility and DOM in post-thaw conditions, not to be consumed before freezing. For this reason, the purpose of using an extender solution in the cryopreservation protocol differs from that of the

activating extender solution. Filtered seawater, which was previously used as a control sub-stance to compare with the other extension solutions in SCT-1, was considered as an extension solution candidate since it performed better than the other extenders. Shark semen is highly likely to enter the female body in a mixture with seawater, not only because the female cloaca and uterus are open to the outside but also because male sharks use seawater in their siphon sacs to ejaculate the semen (Alvarez et al., 2008). Consequently, shark spermatozoa are stable in seawater. In fact, the internal osmolarity of sharks is adjusted to the osmolarity of seawater because of urea and TMAO. Since the extender used for cryopreservation needs to maintain spermatozoa in a stable state, the SCT-1 results concluded that FSW was the most appropriate extender, which is logical, considering the facts presented above.

When performing cryopreservation, both spermatozoa and cryopreservation medium are frozen and thawed and this results in damages in various locations on the cells. This includes reduction of membrane integrity, protein leakage and degradation, mitochondrial damage, etc. This consequently reduces the motility, viability, and fertilizing ability of spermatozoa (Gwo and Ohta, 2008). Many substances are used as cryoprotectants to reduce these damages, and EG, glycerol, DMSO, bovine serum albumin (BSA), and EY used in this study have been commonly used as cryoprotectants in the cryopreservation of semen in teleost (Suquet et al., 2000). Among them, cryoprotectants selected for shark semen in this

study were EY and EG, which provided a good protective effect. Not only did DMSO show a toxic effect as a default cryoprotectant, but testing the concentrations of EY and EG with protective effects of up to only 10% contributed to the low post-thaw motility in this study. Further studies to confirm the effects of various EY and EG concentrations, including higher concentrations, on post-thaw spermatozoa total motility are needed. Testing various concentrations of EY and EG and equilibration times may determine a combination that increases the post-thaw spermatozoa survival rate. In addition, EY derived from species other than chickens can also be considered. EY is one of the most common non-penetrating cryoprotectants used with other species and is known to lower the freezing point of the medium and reduce extracellular ice crystal formation (Mansour et al., 2006). In this experiment, chicken eggs were used, as they were easy to obtain. However, since there is a risk of exposure to pathogens from different species and since the composition of the EY varies from species to species, shark EY needs to be tested as a cryoprotectant in future studies (Horvath et al., 2008). In addition to the cryoprotectants used in this study, fish semen cryopreservation uses a variety of substances such as antifreeze protein (AFP), antifreeze glycoprotein (AFGP), seminal plasma proteins, antioxidants to improve the quality of post-thaw spermatozoa (Gwo and Ohta, 2008; Morris et al., 2008; Xin et al., 2018; Dadras et al., 2017; Gilbert et al., 1972). Reflecting the directionality of these recent studies, more diverse cryoprotectants can also be attempted in further study.

In this study, the experimental temperature was set to 21℃ except for the thawing period. This was to set as a similar temperature to the shark's breeding environment and its body temperature, which was based on the fact that sharks are ectothermic animals. Previous studies have shown that spermatozoa's motility rate, swimming speed, flagellum beat frequency, and ATP consumption speed show positive correlations with temperature, and DOM shows a negative correlation with temperature (Cabrita et al., 2010). Accordingly, if the quality of spermatozoa is measured under different temperature conditions from the 21℃ set in this study, changes in the values are expected to be observed. Depending on the motility and DOM values that have changed under various temperature conditions, it is also necessary to determine in further study which conditions will result in higher fertility when used for AI.

From the perspective of the whole experimental design, it can be speculated that exploring the direction vector from the default protocol to Kim’s protocol in future experiments will further improve spermatozoa motility, assuming that the response surface is smooth. Further research should be conducted to improve post-thaw total motility. Further studies with different conditions or progressive methodologies should also be conducted to improve post-thaw motility, such as adding a variety of cryoprotectants, changing cryoprotectants’ concentrations, changing measurement temperatures, or trying new technologies like vitrification (Xin et al., 2020).

5. Conclusions

Sharks are apex predators and keystone species in marine ecosystem food chains. However, owing to human activities, they have recently experienced rapid population decreases and now face an extinction crisis and require improved conservation efforts. Semen cryopreservation, along with AI, is one of the most important ART techniques that can help endangered species. This study presents a preliminary cryopreservation protocol for shark semen using the semen of *T. scyllium*. Using the protocol that was selected in this study, Kim's protocol, a post-thaw total motility of 2.03% was achieved. As this study clearly demonstrates the direction required for further research, additional experiments must be conducted to find an optimum combination that can further enhance post-thaw motility.

Table 1. Biological data of the *Triakis scyllium* used for the experiments. All data were measured before the experiment started. ①: Length from the cloaca opening to the tip of the left clasper; ②: Length from the notch between the left pelvic fin and the clasper to the tip of the left clasper; ③: Length from the caudal end of the left pelvic fin to the tip of the left clasper.

Organism ID	**Body length** (cm)	**Body weight** (kg)	**Clasper**					
			Length ① (cm)	**Length ②** (cm)	**Length ③** (cm)	**Calcification**	**Bending**	**Rhipidion formation**
M001	160.0	14.8	17.5	12.0	6.5	C	B	R
M002	98.0	3.1	13.0	10.0	5.5	C	B	R
M003	100.0	3.4	12.5	9.0	5.5	C	B	R
M004	100.0	3.1	13.0	9.0	5.5	C	B	R
M005	137.5	8.9	16.5	11.0	6.5	C	B	R

* C: calcified; B: bending; R; rhipidion formed

Table 2. Composition of solution candidates for activating extender test 1.

Constituent (mM)	MT-EM	MB-EM	MH-EM	SR
NaCl	-	92.4	1368.9	280.0
KCl	0.3	-	53.6	6.0
$CaCl_2$	-	-	-	5.0
$MgCl_2$	-	-	-	3.0
$MgCl_2 \cdot 6H_2O$	-	1.7	-	-
Dextrose	-	-	-	5.0
Glucose	-	-	55.5	-
Sucrose	23.4	-	-	-
Fructose	-	27.8	-	-
TMAO	103.8	103.8	103.8	-
Urea	359.6	359.6	359.6	350.0
Sodium glutamate	-	51.3	-	-
Sodium acetate	-	31.6	-	-
$NaHCO_3$	-	-	-	8.0
NaH_2PO_4	-	-	4.0	1.0
Na_2SO_4	-	-	-	0.5
$K_2HPO_4 \cdot 3H_2O$	-	55.6	-	-
Potassium citrate	-	2.1	-	-
KH_2PO_4	-	4.8	4.4	-
TES	-	8.5	8.5	-
Tris	30.0	-	-	-

* MT-EM: elasmobranch-modified Tsvetkova's extender; MB-EM: elasmobranch-modified Beltsville poultry semen extender; MH-EM: elasmobranch-modified Hank's balanced salt solution; SR: shark Ringer solution; TMAO: trimethylamine oxide; TES: N-tris[hydroxymethyl]methyl-1-aminoethane sulfonic acid

Table 3. Composition of solution candidates for activating extender test 2.

Constituent (mM)	SR	SSAE-1	SSAE-2
NaCl	280.0	500.0	1000.0
KCl	6.0	6.0	6.0
$CaCl_2$	5.0	5.0	5.0
$MgCl_2$	3.0	3.0	3.0
Dextrose	5.0	25.0	25.0
Urea	350.0	359.6	359.6
TMAO	-	103.8	103.8
$NaHCO_3$	8.0	8.0	8.0
NaH_2PO_4	1.0	1.0	1.0
Na_2SO_4	0.5	0.5	0.5

* TMAO: trimethylamine oxide; SR: shark Ringer solution; SSAE-1: shark spermatozoa activating extender 1; SSAE-2: shark spermatozoa activating extender 2

Table 4. Composition of solutions used for the primary semen cryopreservation test (SCT-1).

Constituent (mM)	OT-EM	SR-MOD
Sucrose	23.4	-
Trimethylamine oxide	103.8	-
Urea	359.6	350.0
$KHCO_3$	-	-
Reduced glutathione	-	-
Bovine serum albumin	-	-
Tris	118.0	-
KCl	-	6.0
$CaCl_2$	-	5.0
$MgCl_2$	-	3.0
Dextrose	-	5.0
$NaHCO_3$	-	8.0
NaH_2PO_4	-	1.0
Na_2SO_4	-	0.5

* OT-EM: elasmobranch-modified Original Tsvetkova's extender; SR-MOD: modified shark Ringer solution

Table 5. Experimental conditions for the primary semen cryopreservation test (SCT-1). All experiments were done in triplicate.

Experiment ID	Extender	Extension ratio	Cryoprotectant	Equilibration period (min)	Cooling rate (cm)	Thawing temp (℃)
1	SR	1:3	DMSO 10%	1	5	21
2	SR-MOD	1:3	DMSO 10%	1	5	21
3	OT-EM	1:3	DMSO 10%	1	5	21
4	MT-EM	1:3	DMSO 10%	1	5	21
5	MB-EM	1:3	DMSO 10%	1	5	21
6	MH-EM	1:3	DMSO 10%	1	5	21
7	SSAE-1	1:3	DMSO 10%	1	5	21
8	SR	1:1	DMSO 10%	1	5	21
9	SR	1:5	DMSO 10%	1	5	21
10	SR	1:3	DMSO 5%	1	5	21
11	SR	1:3	DMSO 15%	1	5	21
12	SR	1:3	Glycerol 5%	1	5	21
13	SR	1:3	Glycerol 10%	1	5	21
14	SR	1:3	Glycerol 15%	1	5	21
15	SR	1:3	EG 5%	1	5	21
16	SR	1:3	EG 10%	1	5	21
17	SR	1:3	EG 15%	1	5	21
18	SR	1:3	EY 10% + EG 10%	1	5	21
19	SR	1:3	EY 10% + Glycerol 10%	1	5	21
20	SR	1:3	EY 10% + DMSO 10%	1	5	21
21	SR	1:3	BSA 10% + EG 10%	1	5	21
22	SR	1:3	BSA 10% + Glycerol 10%	1	5	21
23	SR	1:3	BSA 10% + DMSO 10%	1	5	21
24	SR	1:3	DMSO 10%	5	5	21
25	SR	1:3	DMSO 10%	10	5	21
26	SR	1:3	DMSO 10%	20	5	21
27	SR	1:3	DMSO 10%	1	3	21
28	SR	1:3	DMSO 10%	1	9.5	21
29	SR	1:3	DMSO 10%	1	5	10
30	SR	1:3	DMSO 10%	1	5	30
Ctrl1	FSW	1:3	DMSO 10%	1	5	21
Ctrl2	SR	1:3	-	1	5	21

* SR: shark Ringer solution; SR-MOD: modified shark Ringer solution; OT-EM: elasmobranch-modified Original Tsvetkova's extender; MT-EM: elasmobranch-modified Tsvetkova's extender; MB-EM: elasmobranch-modified Beltsville poultry semen extender; MH-EM: elasmobranch-modified Hank's balanced salt solution; SSAE-1: shark spermatozoa activating extender 1; FSW: filtered seawater; DMSO: dimethyl sulfoxide; EG: ethylene glycol; EY: egg yolk; BSA: bovine serum albumin

Table 6. Quality of the semen from the five *Triakis scyllium*. Motility and duration of motility (DOM) were measured after activated with shark spermatozoa activating extender 1 (SSAE-1).

Organism ID	Concentration (10^{11}/L)	Morphology (%)	Motility (%)	DOM (hours)
M001	2.96	98.8	35.22	60
M002	2.81	94.6	22.86	15
M003	3.70	97.6	35.29	24
M004	2.59	99.5	93.53	45
M005	3.62	95.2	98.90	51

* DOM: duration of motility

Table 7. Semen quality used for the primary and secondary semen cryopreservation tests (SCT-1 and SCT-2). Spermatozoa were activated with shark spermatozoa activating extender 1 (SSAE-1).

Organism ID	Experiment #	Total volume	Concentration	Motility
M004, M005	SCT-1	7 ml	4.542×10^{11}/L	92.74%
	SCT-2	2 ml	1.114×10^{11}/L	89.12%

Table 8. Frozen-thawed motility and duration of motility (DOM) from the primary semen cryopreservation test (SCT-1). Default protocol: Extender SR; extension ratio 1:3; cryoprotectant DMSO 10%; equilibration period 1 min; cooling rate 5 cm, 3 min; thawing temperature 21℃, 10 s. Motility was calculated as a percentage of the spermatozoa that were motile after being thawed. Values are the averages of triplicate experiments. DOM was measured as the duration from the thawing of the spermatozoa to the time when the motility of more than 2 out of 3 groups became 0%. Motility was measured every 12 h.

Experiment ID	Treat	Motility (%)	DOM (hours)
1	Default protocol	0.0015	24
2	Extender: SR-MOD	0.0000	0
3	Extender: OT-EM	0.0000	0
4	Extender: MT-EM	0.0000	0
5	Extender: MB-EM	0.0000	0
6	Extender: MH-EM	0.0046	12
7	Extender: SSAE-1	0.0041	12
8	Extension ratio: 1:1	0.0000	0
9	Extension ratio: 1:5	0.0010	12
10	Cryoprotectant: DMSO 5%	0.0030	24
11	Cryoprotectant: DMSO 15%	0.0000	0
12	Cryoprotectant: Glycerol 5%	0.0068	24
13	Cryoprotectant: Glycerol 10%	0.0000	0
14	Cryoprotectant: Glycerol 15%	0.0007	12
15	Cryoprotectant: EG 5%	0.0189	60
16	Cryoprotectant: EG 10%	0.0362	132
17	Cryoprotectant: EG 15%	0.0014	12
18	Cryoprotectant: EY 10% + EG 10%	0.0637	120
19	Cryoprotectant: EY 10% + Glycerol 10%	0.0032	12
20	Cryoprotectant: EY 10% + DMSO 10%	0.0261	60
21	Cryoprotectant: BSA 10% + EG 10%	0.0000	0
22	Cryoprotectant: BSA 10% + Glycerol 10%	0.0000	0
23	Cryoprotectant: BSA 10% + DMSO 10%	0.0007	0
24	Equilibration period: 5 min	0.0004	0
25	Equilibration period: 10 min	0.1405	96

26	Equilibration period: 20 min	0.0237	24
27	Cooling rate: 3 cm	0.0152	12
28	Cooling rate: 9.5 cm	0.0000	0
29	Thawing temperature: 10℃	0.0254	12
30	Thawing temperature: 30℃	0.1233	96
Ctrl1	Extender: FSW	0.0271	36
Ctrl2	Cryoprotectant: n/a	0.0007	12

* SR: shark Ringer solution; SR-MOD: modified shark Ringer solution; OT-EM: elasmobranch-modified Original Tsvetkova's extender; MT-EM: elasmobranch-modified Tsvetkova's extender; MB-EM: elasmobranch-modified Beltsville poultry semen extender; MH-EM: elasmobranch-modified Hank's balanced salt solution; SSAE-1: shark spermatozoa activating extender 1; FSW: filtered seawater; DMSO: dimethyl sulfoxide; EG: ethylene glycol; EY: egg yolk; BSA: bovine serum albumin

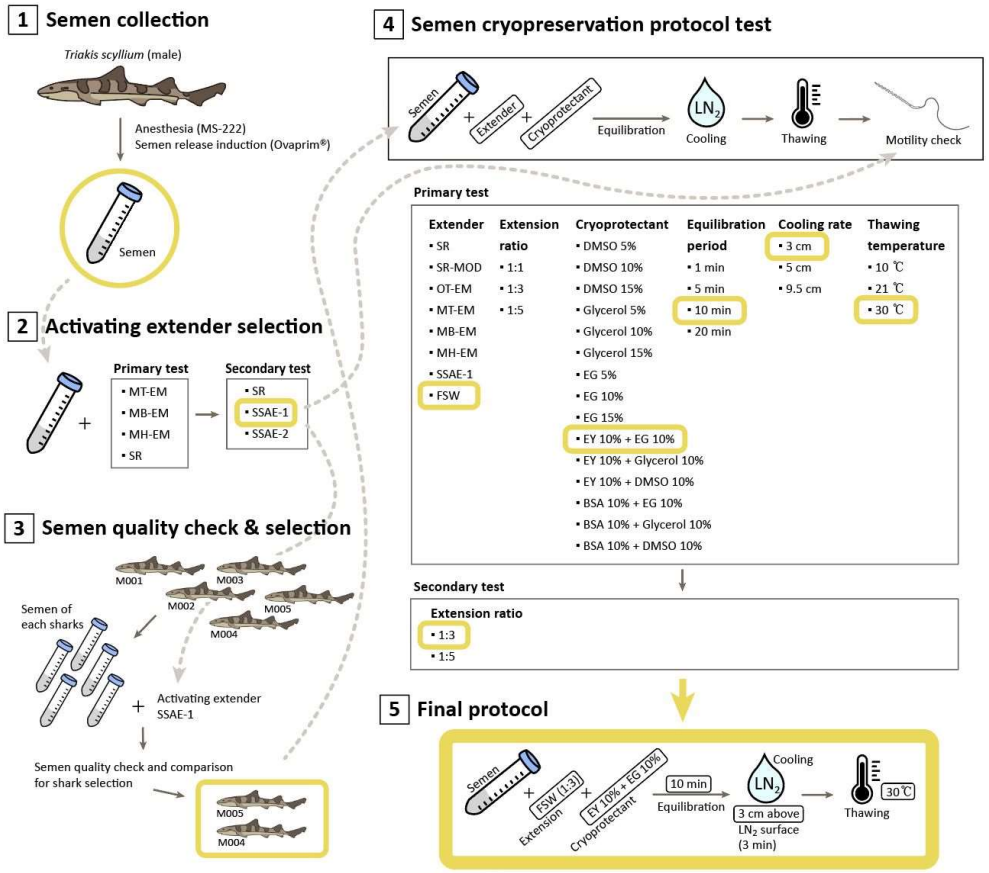

Figure 1. Scheme of the experiment with results. SR: shark Ringer solution; SR-MOD: modified shark Ringer solution; OT-EM: elasmobranch-modified Original Tsvetkova's ex-tender; MT-EM: elasmobranch-modified Tsvetkova's extender; MB-EM: elasmobranch-modified Beltsville poultry semen extender; MH-EM: elasmobranch-modified Hank's balanced salt solution; SSAE: shark spermatozoa activating extender; FSW: filtered seawater; DMSO: dimethyl sulfoxide; EG: ethylene glycol; EY: egg yolk; BSA: bovine serum albumin; LN_2: liquid nitrogen.

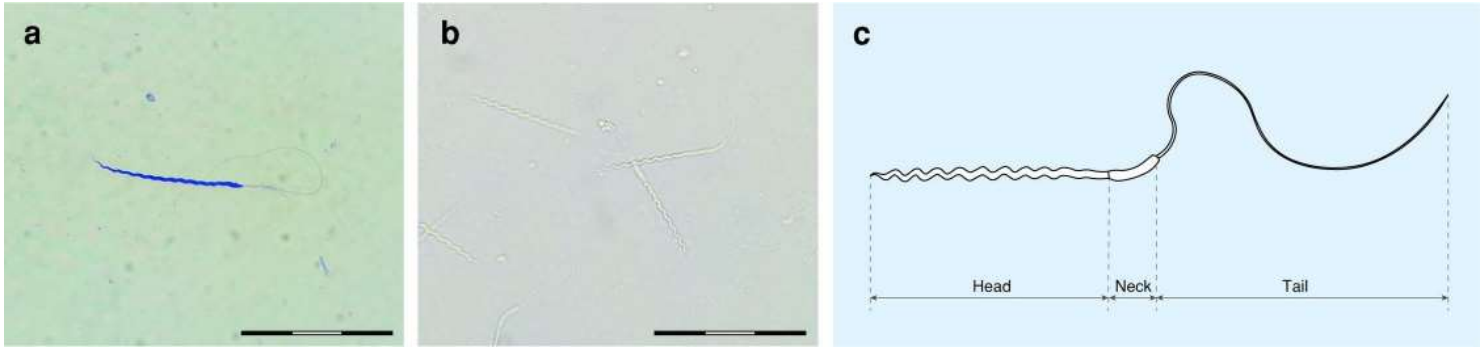

Figure 2. Morphology of the spermatozoon from *Triakis scyllium*. (a) Diff-Quick stained spermatozoon observed with an optical microscope (400×); (b) Non-stained spermatozoa diluted with filtered seawater and observed with an optical microscope (400×); (c) Schematic morphology of the spermatozoon. Scale bars: 30 μm.

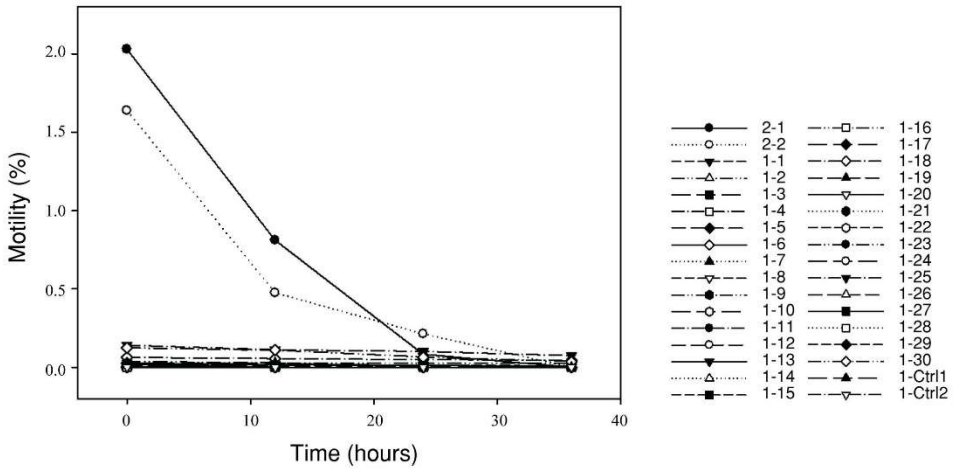

Figure 3. Motility changes in frozen-thawed spermatozoa from the primary and secondary semen cryopreservation tests (SCT-1, 2). Motility after the initial 36 h was plotted. The results of SCT-1 (from 1-1 to 1-Ctrl2) and SCT-2 (2-1 and 2-2) are presented together.

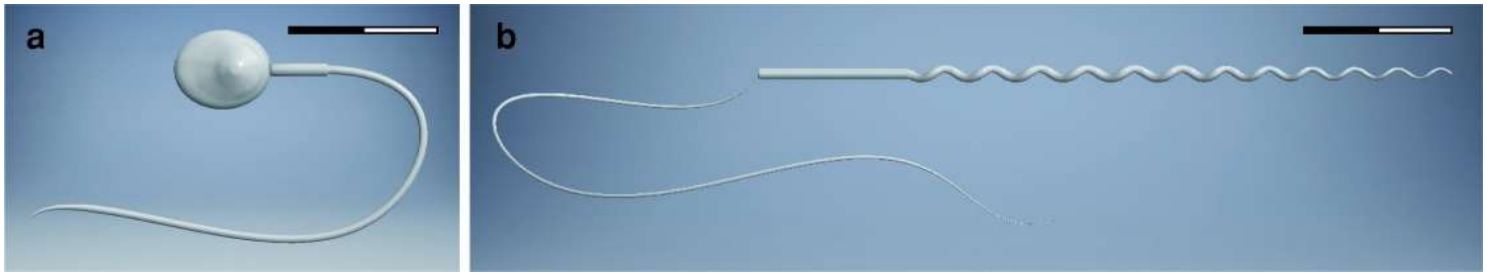

Figure 4. Three-dimensional modeling of the spermatozoon for the surface-area-to-volume ratio calculation. (a) Human spermatozoon; (b) *Triakis scyllium* spermatozoon. Scale bars: 8 μm.

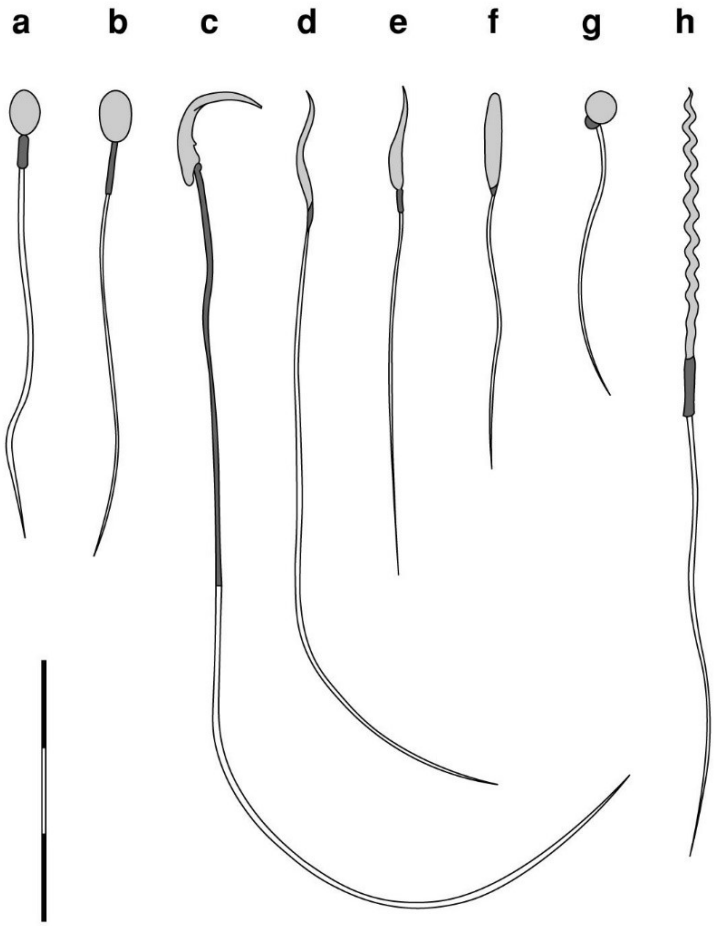

Figure 5. Spermatozoa morphologies of diverse vertebrates. Grey: head region; dark grey: midpiece region; white: flagellum region. All spermatozoa are drawn in proportion (Bousseau et al., 1998; Frandson et al., 2009; Pitnick et al., 2009). (a) Human; (b) Dog; (c) Rat; (d) Chicken; (e) Turtle; (f) Frog; (g) Zebrafish; (h) Shark. Scale bar: 20 μm.

References

Aas, G.H., Refstie, T., Gjerde, B. (1991). Evaluation of milt quality of Atlantic salmon. *Aquaculture*. 29, 101–110.

Alvarez, B., Arenal, A., Fuentes, R., Pimentel, R., Abad, Z., Pimentel, E. (2008). "Use of post-thaw silver carp (*Hypophtalmichthys molitrix*) spermatozoa to increase hatchery productions" in Methods in Reproductive Aquaculture: Marine and Freshwater Species, ed. E. Cabrita, V. Robles, M. P. Herraez (FL: CRCPress), 345–350.

Barber, J. (2016). "Canine semen collection and evaluation" in Proceedings of the CVC, 2016 April 1 (Washington DC, US).

Blanco, J.M., Wildt, D.E., Hofle, U., Voelker, W., Donoghue, A.M. (2009). Implementing artificial insemination as an effective tool for ex situ conservation of endangered avian species. *Theriogenology*. 71(1), 200–213.

Bousseau. S., Billard, J.P., Marguant-Le Guienne, B., Guerin, B., Camus, A., Lechat, M. (1998). Comparison of bacteriological qualities of various egg yolk sources and the *in vitro* and *in vivo* fertilizing potential of bovine semen frozen in egg yolk or lecithin based diluents. *Theriogenology*. 50(5), 699–706.

Cabrita, E., Sarasquete, C., Martinez-Paramo, S., Robles, V., Beirao, J., Perez-Cerezales, S., et al. (2010). Cryopreservation of fish sperm: applications and perspectives. *J. Appl. Ichthyol.* 26(2010), 623–635.

Clark, E., Von Schmidt, K. Sharks of the Central Gulf Coast of Florida. (1965). *Bull. Mar. Sci.* 15, 13–83.

Compagno, L.J.V. (1984). Sharks of the world: an annotated and illustrated catalogue of shark species known to date. *FAO Species Catalogue*. 4(2), 432.

Dadras, H., Dzyuba, B., Cosson, J., Golpour, A., Siddique, M.A.M., Linhart, O. (2017). Effect of water temperature on the physiology of fish spermatozoon function: a brief review. *Aquac. Res.* 48, 729–740.

Daly, J., Holland, M., Galloway, E. (2011). "Preliminary investigations on sperm cryopreservation of a stingray, the sparsely spotted stingaree" in Cryopreservation in Aquatic Species, ed. T. R. Tiersch, C. C. Green (World Aquaculture Society), 334–337.

Daly, J., Jones, R. (2017). "The use of reproductive technologies in breeding programs for elasmobranchs in aquaria" in Elasmobranch husbandry manual II: recent advances in the care of sharks, rays and their relatives, ed. M. Smith, D. Warmolts, D. Thoney, R. Hueter, M. Murray, J. Ezcurra (Ohio Biological Survey) 363–374.

Devi, G.A., Devi, G.S., Singh, O.B., Munilkumar, S., Reddy, A.K. (2009). Induced spawning and hatching of *Osteobrama belangeri* (Valenciennes) using Ovatid, an ovulating agent. *Asian Fish. Sci.* 22, 1107–1115.

Frandson, R.D., Wilke, W.L., Fails, A.D. (2009). "Physiology of male reproduction" in Anatomy and Physiology of Farm Animals. (NJ: Wiley-Blackwell), 413–420.

Fujinami, Y., Tanaka, S. (2013). Age, growth and reproduction of the banded houndshark *Triakis scyllium* around the tip of the Izu Peninsula, Japan. Nippon Suisan Gakk. 79(6), 968–976.

Gilbert, P.W., Heath, G.W. (1972). The clasper-siphon sac mechanism in Squalus acanthias and Mustelus canis. *Comp. Biochem. Physiol. A Physiol.* 42(1), 97–100.

Glogowski, J., Kolman, R., Szczepkowski, M., Horvath, A., Urbanyi, B., Sieczynski, P., et al. (2002). Fertilization rate of Siberian sturgeon (*Acipenser baeri*, Brandt) milt cryopreserved with methanol. *Aquaculture*. 211, 367–373.

Gwo, J.C., Ohta, H. (2008). "Cryopreservation of grouper semen" in Methods in Reproductive Aquaculture: Marine and Freshwater Species. Biology Series, ed. E. Cabrita, V. Robles, M. P. Herraez (FL: CRCPress) 469–474.

Hamlett, W.C. (2005). Reproductive Biology and Phylogeny of Chondrichthyes. Sharks, Batoids, and Chimaeras, Volume 3. (NH: Science Publishers Inc).

Hermes, R., Göritz, F., Streich, W.J., Hildebrandt, T.B. (2007). Assisted reproduction in female rhinoceros and elephants - current status and future perspective. *Reprod. Domest. Anim.* 42, 33–44.

Hildebrandt, T.B., Hermes, R., Walzer, C., Sós, E., Molnar, V., Mezösi, L., et al. (2007). Artificial insemination in the anoestrous and the postpartum white rhinoceros using GnRH analogue to induce ovulation. *Theriogenology*. 67, 1473–1484.

Horvath, A., Wayman, W.R., Dean, J.C., Urbanyi, B., Tiersch, T.R., Mims, S.D., et al. (2008). Viability and fertilizing capacity of cryopreserved sperm from three North American Acipenseriform species: a retrospective study. *J. Appl. Ichthyol.* 24, 443–449.

IUCN (International Union for Conservation of Nature). The IUCN Red List of Threatened Species 2019. http://www.iucnredlist.org [Accessed March 23, 2020]

Kim, S.W., Hong, W.H., Han, S.J., Kwon, J., Ko, H., Lee, S.B., et al. (2020). Use of synthetic salmon GnRH and domperidone (Ovaprim®) in sharks: preparation for *ex situ* conservation. *Front. Mar. Sci.* 7, 571741.

Kumar, S. (2012). Extinction need not be forever. Nature. 492, 9.

Lack, M., Sant, G. (2011). The future of sharks: a review of action and inaction. *TRAFFIC International and the Pew Environment Group*. https://www.pewtrusts.org/~/media/legacy/uploadedfiles/peg/publications/report/the20future20of20sharkspdf.pdf

Lockwood, A.P.M. (1961). “Ringer” solutions and some notes on the physiological basis of their ionic composition. *Comp. Biochem. Physiol.* 2(4), 241–289.

Mansour, N., Richardson, G.F., McNiven, M.A. (2006). Effect of extender composition and freezing rate on post-thaw motility and fertility of Arctic char, Salvelinus alpinus (L.), spermatozoa. *Aquac. Res.* 37, 862–868.

Martínez-Páramo, S., Pérez-Cerezales, S., Gómez-Romano, F., Blanco, G., Sánchez, J.A., Herráez, M. (2009). Cryobanking as tool for conservation of biodiversity:

Effect of brown trout sperm cryopreservation on the male genetic potential. *Theriogenology*. 71, 594–604.

Martínez-Páramo, S., Horvath, A., Labbe, C., Zhang, T., Robles, V., Herraez, P., et al. (2017). Cryobanking of aquatic species. *Aquaculture*. 472, 156–177.

Masuda, M., Izawa, Y., Kametsuta, S., Ikuta, H., Isogai, T. (2003). Artificial insemination of the cloudy catshark. *J. Japan. Assoc. Zoo. Aquar.* 44, 39–43.

Masuda, M., Izawa, Y., Kametsuta, S., Ikuta, H., Isogai, T. (2005). Artificial insemination of the white-spotted bamboo shark, *Chiloscyllium plagiosum*. *J. Japan. Assoc. Zoo. Aquar.* 46, 91–96.

Mijkherjee, M., Praharaj, A., Das, S. (2002). Conservation of endangered fish stocks through artificial propagation and larval rearing technique in West Bengal, India. *Aquac. Asia.* 7, 8–11.

Minamikawa, S., Morisawa, M. (1996). Acquisition, initiation and maintenance of sperm motility in the shark, *Triakis scyllia*. *Comp. Biochem. Physiol. A Physiol.* 113(4), 387–392.

Misro, M.M., Ramya, T. (2012). “Fuel/Energy Sources of Spermatozoa” in Male Infertility, eds. S. Parekattil, A. Agarwal. (NY: Springer-Verlag).

Morris, J.P. IV, Hagen, A., Kanki, J.P. (2008). “Zebrafish sperm cryopreservation with N,N-Dimethylacetamide” in Methods in Reproductive Aquaculture: Marine and Freshwater Species. Biology Series, ed. E. Cabrita, V. Robles, M. P. Herraez (FL: CRCPress), 329–338.

Morrison, M.L., Block, W.M., Strickland, M.D., Collier, B.A., Peterson, M.J. (2008). Wildlife Study Design. (NY: Springer-Verlag).

Myers, R.A., Baum, J.K., Shepherd, T.D., Powers, S.P., Peterson, C.H. (2007). Cascading effects of the loss of apex predatory sharks from a coastal ocean. *Science.* 315(5820), 1846–1850.

Nussdorfer, P., Cileňsek, I., Zorn, B., Petrovič, D. (2018). Adapted methods for scanning electron microscopy (SEM) in assessment of human sperm morphology. *Bosnian J. Basic Med.* 18(1), 43–48.

Ogale, S.N. (1997). Induced spawning and hatching of golden mahseer *Tor putitora* (Hamilton) at Lonavla, Pune District (Maharashtra) in Western Ghats. *Fish. Chimes.* 1997, 27–29.

Ogale, S.N. (2002). Mahseer breeding and conservation and possibilities of commercial culture. The Indian experience. *FAO Fisheries Technical Paper.* 431, 193–212.

Pitnick, S., Hosken, D.J., Birkhead, T.R. (2009). “Sperm morphological diversity” in Sperm Biology: An Evolutionary Perspective, ed. T. R. Birkhead, D. J. Hosken, S. Pitnick (MA: Academic Press), 69–149.

Rigby, C.L., Walls, R.H.L., Derrick, D., Dyldin, Y.V., Herman, K., Ishihara, H., et al. (2021). *Triakis scyllium*. *The IUCN Red List of Threatened Species 2021.* e.T161395A124476903.

Rowley, A., Locatello, L., Kahrl, A., Rego, M., Boussard, A., Garza-Gisholt, E., et al. (2019). Sexual selection and the evolution of sperm morphology in sharks. *J. Evol. Biol.* 32(10), 1027–1035.

Rurangwa, E., Kime, D.E., Ollevier, F., Nash, J.P. (2004). The measurement of sperm motility and factors affecting sperm quality in cultured fish. *Aquaculture.* 234, 1–28.

Schaller, P. (2006). Husbandry and reproduction of Whitetip reef sharks at Steinhart Aquarium, San Francisco. Int. Zoo Yearb. 40, 232–240.

Stevens, J.D., Bonfil, R., Dulvy, N.K., Walker, P.A. (2000). The effects of fishing on sharks, rays, and chimaeras (chondrichthyans), and the implications for marine ecosystems. *ICES J. Mar. Sci.* 57(3), 476–494.

Storrie, M.T., Walker, T.I., Laurenson, L.J., Hamlett, W.C. (2008). Microscopic organization of the sperm storage tubules in the oviducal gland of the female gummy shark (*Mustelus antarcticus*), with observations on sperm distribution and storage. *J. Morphol.* 269, 1308–1324.

Suquet, M., Dreanno, C., Fauvel, C., Cosson, J., Billard, R. (2000). Cryopreservation of sperm in marine fish. *Aquac. Res.* 31, 231–243.

Tanaka, S., Kurokawa, H., Hara, M. (1995). “Comparative morphology of the sperm in chondrichthyan fishes in Advances” in Spermatozoal Phylogeny and Taxonomy, ed. B. G. M. Jamieson, J. Ausio, J. L. Justine (Memoires du Museum National d’Histoire Naturelle), 313–320.

Temple-Smith, P.D., Ravichandran, A., Horta Nunez, F.E. (2018). “Sperm: comparative vertebrate” in Encyclopedia of Reproduction, ed. M. F. Skinner (MA: Academic Press) 210–220.

Thongtip, N., Mahasawangkul, S., Thitaram, C., Pongsopavijitr, P., Kornkaewrat, K., Pinyopummin, A., et al. (2009). Successful artificial insemination in the Asian elephant (*Elephas maximus*) using chilled and frozen-thawed semen. *Reprod. Biol. Endocrin.* 7, 75.

Tsvetkova, L.I., Cosson, J., Linhart, O., Billard, R. (1996). Motility and fertilizing capacity of fresh and frozen–thawed spermatozoa in sturgeons *Acipenser baeri* and *A. ruthenus*. *J. Appl. Ichthyol.* 12, 107–112.

Wildt, D.E., Rall, W.F., Crister, J.K., Monfort, S.L., Seal, U.S. (1997). Genome resource banks: ‘living collections’ for biodiversity conservation. *Bioscience*. 47, 689–698.

Xin, M., Sterba, J., Shaliutina-Kolesova, A., Dzyuba, B., Lieskovska, J., Boryshpolets, S., et al. (2018). Protective role of antifreeze proteins on sterlet (*Acipenser ruthenus*) sperm during cryopreservation. *Fish Physiol. Biochem.* 44, 1527–1533.

Xin, M., Niksirat, H., Shaliutina-Kolesova, A., Siddique, M.A.M., Sterba, J., Boryshpolets, S., et al. (2020). Molecular and subcellular cryoinjury of fish spermatozoa and approaches to improve cryopreservation. *Rev. Aquac.* 12, 909–924.

Yanong, R.P.E., Martinez, C., Watson, C.A. (2009). Use of Ovaprim in ornamental fish aquaculture. *University of Florida IFAS Extension*. 2009, FA161.

CHAPTER III

Use of synthetic salmon GnRH and domperidone (Ovaprim®) in sharks: preparation for *ex-situ* conservation

This manuscript has been published in *Front. Mar. Sci.* 7:571741 (2020).

Abstract

Shark populations are constantly decreasing owing to environmental destruction and overfishing; thus, sharks are now at a risk of extinction, with 27.9% of shark species classified as endangered on the International Union for Conservation of Nature's Red List. Sharks are apex predators and a keystone species in balancing the marine food chain; their extinction will create an imbalance of the entire marine ecosystem. Assisted reproductive technology is the last resort for protecting animals facing severe extinction. Here, as a proactive effort toward building a hormone-induced artificial insemination protocol for endangered wild sharks, the possibility of germ cell maturation by administration of Ovaprim®, a commercially produced synthetic salmon gonadotropin-releasing hormone, and its optimum dosage and injection timing were identified. The experiment was conducted on two shark species—*Triakis scyllium* and *Triaenodon obesus*. It was found that intramuscular injections of 0.2 mL/kg of Ovaprim® for male *T. scyllium* and *T. obesus*, 0.2 mL/kg + 0.5 mL/kg at a 24 h interval for female *T. scyllium*, and 0.2 mL/kg + 0.2 mL/kg or 0.2 mL/kg + 0.3 mL/kg at a 24 h interval for female *T. obesus* were optimal dose protocols. These doses effectively induced the maturation and ovulation of oocytes and the release of semen. Current study results confirm that Ovaprim® is a suitable tool for shark hormone-induced artificial insemination and indicate that this method may enable the conservation of the endangered shark species.

Key words: *Triakis scyllium*, *Triaenodon obesus*, synthetic salmon GnRH, Ovaprim®, hormone-induced artificial insemination

1. Introduction

Shark populations have been severely threatened by indiscriminate hunting over the last 40–50 years (Lack et al., 2011). Of the species identified on the International Union for Conservation of Nature (IUCN) Red List, 27.9% of shark species are listed as “vulnerable,” “endangered,” or “critically endangered” (IUCN, 2019). Sharks are apex predators and keystone species of the ocean food chain. If their populations are excessively reduced or become extinct, there will be a rapid imbalance in the marine ecosystem (Ferretti et al., 2010) and the quantity of marine food sources will also drop sharply. Protecting endangered shark species is imperative for humanity and for nature (Myers et al., 2007).

However, sharks have very slow reproduction rate owing to their long gestation period, slow sexual maturation, and small litter size (Ferretti et al., 2010). Introduction of assisted reproductive technology is necessary for securing genetic diversity and to accelerate breeding rates (Comizzoli et al., 2000). Artificial insemination, one of the most important techniques of assisted reproductive technology, is a method of mixing spermatozoa and oocytes by artificial means. In animals that undergo internal fertilization, it entails direct injection of spermatozoa into the vagina/uterus at the time of ovulation. Artificial insemination has been conducted on various endangered species, ranging from terrestrial animals such as whooping crane (*Grus americana*), Przewalski’s horses (*Equus ferus*), Asian elephants (*Elephas maximus*), and northern white rhinoceros (*Ceratotherium simum*

cottoni) to aquatic animals including lake sturgeon (*Acipenser fulvescens*), Mahseer, *Osteobrama belangeri*, Padba (*Ompok pabo*), Tangra (*Mystus guillo*), etc. (Ogale, 1997; Mijkherjee et al., 2002; Ogale, 2002; Hermes et al., 2007; Hildebrandt et al., 2007; Blanco et al., 2009; Devi et al., 2009; Thongtip et al., 2009).

Thus far, only two papers have been published on shark artificial insemination in the white-spotted bamboo shark (*Chiloscyllium plagiosum*) and cloudy catshark (*Scyliorhinus torazame*) (Masuda et al., 2003; Masuda et al., 2005). These sharks are mesopredators of the marine food web as they regulate populations of mollusks, crustaceans, and bony fishes and serve as suitable prey for larger elasmobranchs meeting their metabolic requirements (Taniuchi, 1988; Ferretti et al., 2010; Tambling et al., 2018). As these species have small body sizes and can store spermatozoa in the female reproductive tracts, their artificial insemination strategies can be simplistic (Masuda et al., 2003; Masuda et al., 2005). Some artificial insemination studies, which have not been officially reported in the academic literature, have been performed in aquariums using large apex predator sharks. They used the shark's natural hormonal cycle, for which blood is collected and the hormone concentration changes are tracked periodically for at least one year. The biggest drawback of this strategy is that it can only be carried out on shark species that are safe and accessible to humans. Most endangered sharks in the wild may have very limited access to human beings either owing to their numbers or temper and applying the existing method to them is simply not possible.

Hormone-induced artificial insemination is a method of increasing the number of germ cells sampled by inducing gamete maturation and controlling the timing of fertilization through artificial hormone administration. The biggest advantage of hormone-induced artificial insemination is that the timing of reproduction can be artificially adjusted; it has been commonly used in teleost owing to its commercial efficiency as it effectively increases the productivity of a fish farm (Hill et al., 2009; Karami et al., 2011; Hoga et al., 2018). If the hormone-induced artificial insemination method can be established in sharks, it would minimize shark-human contact by inducing reproduction at the desired timepoint. This advantage could significantly increase the chances of artificial insemination success in endangered shark species.

For hormone-induced artificial insemination, the hypothalamus-pituitary-gonadal axis that has been used in Osteichthyes were used in this study (Rottmann et al., 1991; Cardinaletti et al., 2010; Genz et al., 2014; Yom-Din et al., 2016; Shanthanagouda et al., 2018). The hypothalamus secretes gonadotropin-releasing hormone (GnRH), the pituitary secretes gonadotropic hormones, and the gonads secrete gonadal steroids. This results in the maturation and release of germ cells in both males and females. Ovaprim® is one of the most popular agents that induces reproduction using the hypothalamus-pituitary-gonadal axis in fish. It has been used successfully for various species, proving its effectiveness and safety on fish, which

are important criteria in hormone-induced artificial insemination (Yanong et al., 2009).

Ovaprim® is composed of a salmon gonadotropin-releasing hormone analog (20 μg/mL) and domperidone (10 mg/mL) (USFDA, 2020). The salmon gonadotropin-releasing hormone analog elicits the release of gonadotropins from the pituitary and domperidone acts as a Dopamine D2 receptor antagonist, negating other mechanisms of GnRH release inhibition (Yanong et al., 2009). Ovaprim® facilitates gonadotropin release and eventually induces maturation and release of germ cells, which is conducive to artificial insemination. However, since there is no official record of Ovaprim® application to elasmobranchs yet, it is not known whether Ovaprim® will work on sharks. To confirm whether it works, experiments using two shark species: the banded houndshark (*Triakis scyllium*) and the whitetip reef shark (*Triaenodon obesus*) were performed.

Triakis scyllium and *T. obesus* belong to the order Carcharhiniformes (the former to the family Triakidae and the latter, to Carcharhinidae). *Triakis scyllium* inhabits the Northwest Pacific Ocean and shows aplacental viviparity with internal fertilization (Compagno, 1984). They are relatively easier to handle by aquarists when bred in aquariums, thanks to their small body size (less than 1.5 m). *Triakis scyllium* is classified into the group of "least concern" by the IUCN Red List (IUCN, 2019) and is one of the most accessible shark species in the Republic of Korea. *Triaenodon obesus* lives in the warm waters of the Indo-Pacific Ocean. This species

also fertilizes its gametes internally but shows placental viviparity. Although the IUCN Red List classifies this species into the "near threatened" group (IUCN, 2019), it is also a species commonly seen in aquariums. These two species were chosen owing to their accessibility, abundance in the aquarium, and their smaller size in which both are thought to be sexually mature if the body length is longer than ~1 m. Another important reason is that both show a synchronous reproduction strategy, which makes it meaningful to induce reproduction at the desired time point. A group of sharks showing reproductive synchrony have same stage of the reproduction cycle at a time, manifesting seasonal breeding (Castro et al., 2009).

Herein, to the best of my knowledge, Ovaprim® was administrated for the first time to *T. scyllium* and *T. obesus*, confirming its effect on oocyte maturation, ovulation, and semen production. Based on this, a platform where artificial insemination in endangered sharks becomes practically possible, was constructed.

2. Materials and methods

2.1. Sharks for the experiment

As a result of selecting sharks with a total body length of approximately 90 centimeters or more, a total of five male and seven female *T. scyllium*, and three male and three female *T. obesus* individuals were collected from Hanwha Aqua Planet Jeju,

Jeju-do, Republic of Korea. More adult sharks were sought in large aquariums and fish markets in Korea for a sufficiently large experimental population. There were many immature sharks, but fully-grown ones were not available. In other words, the sharks used in this experiment were virtually the best cohort available in the country. *Triakis scyllium* males were named M001–M005 and *T. obesus* WM001–WM003. Females were named F001–F007 and WF001–WF003, respectively. For identification, punch biopsy (Kai Medical, Japan) was done at the tip of the left pectoral fin of the sharks using a binary numbering system.

Body length and body weight were measured in all sharks and clasper calcification, elongation, bending, and rhipidion formation were checked in male sharks to judge sexual maturity and suitability for experimentation (Clark and Von Schmidt, 1965; Fujinami and Tanaka, 2013) (**Table 1**). As all males met the stand`ards, all were utilized for experimentation.

Abdominal ultrasonography of the uterus and ovaries was performed on all female sharks to judge sexual maturity and for pregnancy detection using an Aloka ProSound 2 (Hitachi-Aloka Medical Ltda., Tokyo, Japan) with a convex probe set to a frequency of 26 MHz (Madigan et al., 2015; Swider et al., 2017; Anderson et al., 2018). Only F003 among the female *T. scyllium* displayed an ovarian follicle during ultrasonography and F001 and F002 were confirmed as pregnant. Blood sampling was carried out to check the hormone level baseline of the pregnant sharks, and they were excluded from the rest of the experiments. Ultrasounds conducted for over a

month confirmed that the other individuals were not pregnant and showed differences in their blood hormone levels compared to those that were obviously pregnant (F001 and F002) (**Table 2**). Since the other females (F004–F007) did not show any follicle in their ovaries, it was highly likely that they were sexually immature. Despite this, the possibility of an Ovaprim® administration triggering the first ovarian cycle in the sharks was tested since they were approaching the body length of sexually matured specimens. So, every non-pregnant female *T. scyllium* (F003 – F007) was used as an experimental candidate.

The sharks' breeding history was examined and according to it the *T. scyllium* have shown irregular pregnancy regardless of the season, and the *T. obesus* did not show any pregnancy at all throughout the exhibition. Since there was little change in water temperature and circadian rhythm throughout the year in the facility, their loss of seasonality is explainable (Schaller, 2006; George et al., 2017).

A physical examination, including swimming status, food response, and respiratory rate, was done to screen overall health status after more than a month of the acclimatization period. Blood examinations including hematology, blood chemistry tests, and blood gas analysis were performed. Packed cell volume was determined by centrifugation of whole blood. Plasma was separated from whole blood in a lithium heparin tube for testing Na^+, K^+, Cl^-, Ca^+, P, Mg_2^+, blood urea nitrogen, creatinine, uric acid, total protein, albumin, glucose, total bilirubin, direct bilirubin, total cholesterol, glutamic-pyruvate transaminase, glutamic-oxaloacetic

transaminase, gamma-glutamyl transferase, lactate dehydrogenase, creatine phosphokinase, alkaline phosphatase, amylase, lipase, triglyceride, and NH_3 using a Fuji Dri-Chem 4000i analyzer (Fujifilm, Tokyo, Japan). Blood gas analysis was also performed to determine TCO_2, pCO_2, pO_2, sO_2, pH, glucose, HCO_3^-, base excess, Na^+, K^+ and ionized Ca_2^+ using whole blood without anticoagulants with a CG8+ cartridge and VetScan i-STAT (Abaxis, CA, USA).

No anomalies were detected in complete blood count, blood chemistry, and blood gas analysis of the experimental candidates (**Table 3**). All sharks were judged to have a body condition score of 3/5, and no abnormalities were identified by ultrasonography. All sharks showed normal swimming, good vitality, and good appetite throughout the experiment. Based on all these data, veterinarians (WHH and SWK) judged that all sharks were healthy and available for experimentation. Water quality of the shark tanks was maintained consistently throughout the experiment (**Table 4**).

2.2. Water quality and environmental management

Male and female sharks were contained separately in two sea water tanks in the Hanwha Aqua Planet Jeju. Both tanks were supplied with filtered water siphoned directly from the coastal sea around Jeju Island. Concentrations of dissolved oxygen (DO), nitrite (NO_2^-), nitrate (NO_3^-), ammonia (NH_3), water temperature, salinity, gravity, and pH were maintained constant and checked at least once a week in both

tanks. The sharks were target-fed mackerel, whiteleg shrimp, and squid thrice a week, and Mazuri Vita-Zu® Shark/Ray II Tablet (Purina Mills LCC, USA) once a week.

2.3. Reproductive hormone levels before Ovaprim® administration

Since only minimally invasive procedures were used in this study, sharks were sedated for every step. Tricaine methanesulfonate (MS-222) in 50–60 ppm concentration was used to induce sedation for the experiments. To determine the hormone level before Ovaprim® (Syndel Laboratories, Vancouver, Canada) injection, 3 mL of blood was collected from all 16 sharks from their tail vein and placed in BD Vacutainer® SSTTM II Advance (BD, NJ, USA) tubes for serum separation. Serum estradiol, progesterone, and testosterone concentrations were measured by electrochemiluminescence immunoassay (ECLIA) using Elecsys® progesterone III assay, Elecsys® estradiol III assay, and Elecsys® testosterone II assay on the Cobas 8000 modular analyzer series (Roche Diagnostics Corp., Indianapolis, IN, USA; Neodin Veterinary Laboratory, Seoul, Republic of Korea). Blood collection and blood hormone analysis were carried out in the same manner for all subsequent experiments. The hormone concentration analyses were repeated four times per a shark over a one-month period. These data were used as the basis values for later experiments. In order to establish an accurate control group, it was necessary to administer a biologically ineffective fluid instead of Ovaprim® for each experiment,

but due to a lack of population size, using this basis value was chosen as an alternative.

2.4. Dose optimization of Ovaprim® and its effects in male T. scyllium

The final purpose of this study was to determine if Ovaprim® could draw biological reactions through the shark's hypothalamus-pituitary-gonadal axis, and if confirmed, to find out the optimum dose for performing artificial insemination in the sharks. In the case of male sharks, the criterion of judgment was quantity and quality of collected semen. For females, the administered dose should induce follicular maturation and ovulation but should not result in egg dropping. This is described schematically in **Figure 1**, and the doses falling under the shaded area indicate the optimum range for female sharks. Too high a dose will result in egg dropping, and too little cannot induce follicular maturation. Throughout this study, diverse doses were tested and according to their biological reactions in the tested sharks, the experiments were marked on the schematic graph (**Figure 1**). Optimized doses were assessed through this process for *T. scyllium* and *T. obesus*.

After testing the basic hormone level of the sharks, dose optimization experiments were performed using *T. scyllium*, which had a larger population size than *T. obesus*. The experiment was first performed on male sharks. Female doses were tested in another experiment, based on the determined male dose.

As there was no reported information about Ovaprim® dosage in sharks, experimental doses based on the amounts previously administered to Osteichthyes were set (Nandeesha et al., 1990; Khan et al., 2006; Genz et al., 2014; Paul et al., 2014). Male sharks were used for this experiment as divided into three groups as follows: Group A: M004; Group B: M001 and M002; Group C: M003 and M005. Although Group A contained only one shark, it was still designated as a 'Group' for ease of understanding. The sharks were grouped in this manner because both small and large specimens were intended to be distributed evenly in each group. Ovaprim® was injected intramuscularly (IM) at the doses of 0.1 mL/kg, 0.2 mL/kg, and 0.4 mL/kg to the Groups A, B, and C, respectively, into the epaxial muscle (Yanong et al., 2009). The change in the concentration of blood estradiol, progesterone, and testosterone was monitored, and semen collection trials were performed at 10 min pre-injection and at 1, 2, and 6 h post-injection. Semen was taken from the urogenital papilla of each shark using a syringe lacking the needle while the abdomen was massaged gently. The first transparent part of the ejaculated semen was discarded and only the subsequent cloudy part was taken, thereby excluding urine and maximizing the concentration of spermatozoa. After collection, semen volume was measured and stored at 21℃ for subsequent experiments. Semen was diluted with activating solution and checked using an optical microscope for motile spermatozoa. Through this step, it was confirmed that if Ovaprim® affected the hormonal system in sharks and determined the effective dosage for males.

After dose optimization, injection tests were performed using the optimized dose (0.2 mL/kg) to observe the timing for semen collection and blood hormone level changes up to 48 h post-injection. In total, three experiments were performed in a row with more than a month interval between experiments to allow the hormone concentrations to return to baseline levels. Semen collection was performed at 1, 12, and 36 h post-injection in each experiment. The blood-concentration of estradiol, progesterone, and testosterone were checked at 10 min pre-injection and at 1, 12, 24, 36, and 48 h post-injection in all three experiments.

2.5. Dose optimization of Ovaprim® and its effects in female T. scyllium

In females, Ovaprim® was administered twice in every experiment. The primary injection was to trigger follicular maturation and the second was for induction of ovulation. This strategy is commonly used in bony fish (Nandeesha et al., 1990; Khan et al., 2006; Genz et al., 2014; Paul et al., 2014).

For dose optimization in females, four different dosages were tried. The first trial dose was deduced from the optimum dose in males based on Osteichthyes protocols (Nandeesha et al., 1990; Khan et al., 2006; Genz et al., 2014; Paul et al., 2014). Based on the biological reactions following the injection, optimization was performed in serial, controlling the dose in the experiments. As the optimum dose for males was concluded to be 0.2 mL/kg IM in the epaxial muscle in the previous experiment, doses used in each of the four experiments were as follows: First: 0.6

mL/kg + 0.6 mL/kg; Second: 0.2 mL/kg + 0.4 mL/kg; Third: 0.2 mL/kg + 0.6 mL/kg; and Fourth: 0.2 mL/kg + 0.5 mL/kg. Blood estradiol, progesterone, and testosterone concentration analysis, follicular size change and ovulation checks with ultrasonography, and egg dropping checks were carried out at 10 min pre-injection and at 12, 24, and 36 h post-injection. Axes lengths and area of the follicle's largest cross section at every time points were measured using the embedded tool from the ultrasonography device. Eccentricity was calculated manually with the long and short axis values. The time gap between the primary and the secondary injections in the first trial was set to 6 h, following protocols commonly used in other species (Nandeesha et al., 1990; Paul et al., 2014). As the hormone level graph and biological reactions from each experiment were being monitored, the timings for the second injection were adjusted and applied throughout the experiments as follows: First: 6 h; Second: 12 h; Third: 24 h; and Fourth: 24 h. To perform the following experiment after the hormone concentration returned to baseline, a time interval of more than one month was set between each experiment.

2.6. Dose optimization of Ovaprim® and its effects in T. obesus

Based on the experimental outcome in *T. scyllium*, 0.2 mL/kg Ovaprim® was administered to *T. obesus* males. As the biological reaction to the injection was thought to be appropriate, three replicate experiments were performed without further dose optimization for males. The concentration of estradiol, progesterone, and testosterone was assessed in blood drawn 10 min pre-injection and 12, 24, 36,

and 48 h post-injection. Semen collection was performed at 15 min, and 1, 12, 24, 36, and 48 h post-injection.

In females, 0.2 mL/kg Ovaprim® was administered twice at a 24 h interval for the first experiment, extrapolating the results of female *T. scyllium* and male *T. obesus*. Two experimental doses were administered in the female group with more than a month interval between the trials. Administered doses were as follows: First: 0.2 mL/kg + 0.2 mL/kg; Second: 0.2 mL/kg + 0.3 mL/kg at a 24 h interval. Blood collection for hormone analyses, ovary ultrasonography for follicular growth measurement, and egg drop checking were carried out 10 min pre-injection and at 12, 24, 36, and 48 h post-injection, using the same methodologies that were applied to *T. scyllium.*

2.7. Ethical approval

This study was approved by the Seoul National University Institutional Animal Care and Use Committee (approval number: SNU-181218-2) and all the experiments were performed in accordance with relevant guidelines and regulations.

3. Results

3.1. Reproductive hormone levels before Ovaprim® administration

Results of blood hormone levels are shown in **Table 2**. In females, it was possible to distinguish between pregnant and non-pregnant individuals based on their estradiol concentration. An average estradiol level of 9159.80 pg/mL for the pregnant group, and 1018.68 pg/mL for the non-pregnant group was recorded, showing more than a nine-fold difference between the two (**Table 2**). There were evident interspecific differences, especially in estradiol and testosterone concentrations in females and males, respectively. Male *T. obesus* showed a more than six times higher testosterone level than that in male *T. scyllium*. Female *T. scyllium*, however, showed a more than 400 times higher estradiol concentration than that in female *T. obesus*. This suggests that the baseline data must be established separately for each species. As there is no previously published information on hormone levels for both *T. scyllium* and *T. obesus*, the data presented in **Table 2** merits academic use in other studies and by clinicians.

3.2. Dose optimization of Ovaprim® and its biological effects in male T. scyllium

The results from the hormone level analysis of male *T. scyllium* are shown in **Figure 2**. All three Ovaprim® concentrations administered to Groups A, B, and C induced hormonal reactions in sharks. This was the first time that Ovaprim® has been confirmed to be effective physiologically in the shark. Among the three hormones tested, testosterone level fluctuations were the most obvious, and thus, it was chosen as one of the bases for monitoring the biological reaction of the male sharks. The initial fluctuation was greatest in group B at 59.6 ng/mL, whereas the fluctuation of

testosterone was 34.3 ng/mL in group A and 13.0 ng/mL in group C. The results from group B and C confirmed that a 0.2 mL/kg dose was effective to elicit in vivo reactions, as the fluctuation was larger in group B, even though similar baseline concentrations at 0 h (Group B: 94.8 ng/mL; Group C: 98 ng/mL) were evident.

Semen from all sharks was sampled. It was most easily sampled at 1 h post-injection. The average volume of semen sampled at 1 h post-injection was 1.9 mL for Group A; 7.7 mL for Group B; and 2.8 mL for Group C. No semen could be sampled from any of the experiments in any group at 6 h post-injection and at 10 min pre-injection. Thus, all three doses triggered semen emissions, of which the dosage of 0.2 mL/kg resulted in the largest volume of ejaculate. It also confirmed that 1 h post-injection was an appropriate interval at which to procure semen samples. Based on these observations, it was concluded that the optimum Ovaprim® dose in male *T. scyllium* was 0.2 mL/kg.

To check the biological influence of this optimum dose in *T. scyllium*, 0.2 mL/kg Ovaprim® was injected into all five male sharks. This experiment was performed in triplicate and the resulting hormone level data are shown in Figure 3A. Up to 48 h of observation showed that testosterone levels decreased in the beginning, recovered, and then increased, reaching peak values at 36 h. In addition, semen sampling was attempted at 1 h, 12 h, and 36 h post-injection. The average volume of the five semen samples was 4.6 mL at 1 h; 2.0 mL at 12 h; and 0 mL at 36 h post-injection. It was

confirmed that 1 h post-injection was the most optimum time for semen sampling in *T. scyllium*.

3.3. Dose optimization of Ovaprim® and its effects in female T. scyllium

In females, dose optimization was performed in four steps, which resulted in the blood hormone concentration graph in **Figure 3B**. Of the three hormones, progesterone showed the clearest form of fluctuation, reaching its peak at 24 h. Optimum dosage was judged based on biological reactions. As the purpose of Ovaprim® administration in females is to successfully induce follicular maturation and artificial insemination-performable conditions, the goal was to isolate safe zones that would avoid the two undesirable phenomena for artificial insemination: immature follicles and egg dropping (**Figure 3**). The aim of this experiment was to find the doses that would coincide with the shaded area. It was determined that it would only be possible to perform artificial insemination when the experimental conditions fell into this area.

In the first experiment, Ovaprim® was administered to all female *T. Scyllium* sharks (F003–F007). As a result, the average hormone concentration change graph was as shown in **Figure 3B**. However, data showed a large gap between the hormonal levels in F003 and the rest of the female sharks. The hormone concentration graph for F003 is shown in **Figure 3C**. In F003, the basic concentration of hormones itself was higher than in the other sharks. In addition, the change in progesterone

concentration itself was significantly greater in F003 than in the other sharks (F003: 12.0 ng/mL; F004: 3.1 ng/mL; F005: 2.3 ng/mL; F006: 3.4 ng/mL; F007: 1.7 ng/L).

There was another clue differentiating F003 from the other females: the changes in the ovary follicle size before and after Ovaprim® administration using ultrasonography. In F003, it was possible to identify the presence of ovarian follicles both before and after administration, and the observed size change of the follicle was apparent. However, for F004–F007, no visible follicles were observed on ultrasonography, both before and after hormone administration. Comparing the ultrasound reports of F003 before and after Ovaprim® administration, the increase in follicle size could be clearly discerned not only through measured figures (**Figure 4A**), but also with the naked eye (**Figure 4B, 4C**).

Collectively, F003 was the most and the only mature shark, and thus, further examinations were done with F003 only. Therefore, three more dose optimization experiments were conducted only on F003. The optimum time interval between the first and second injections in each experiment had to be decided, and the first experiment using the time gap of 6 h resulted in peak values of hormone concentration change (**Figure 3B**) and in increased follicle size (**Figure 4A**) at 24 h post-injection. Based on these observations, the time interval between injections was set at 24 h for the third and fourth experiments.

The biological reactions in the experiments on F003 are shown in **Figure 5A**: first experiment (0.6 mL/kg + 0.6 mL/kg): both follicle maturation and egg dropping occurred; second experiment (0.2 mL/kg + 0.4 mL/kg): neither follicle maturation nor egg dropping occurred; third experiment (0.2 mL/kg + 0.6 mL/kg): both follicle maturation and egg dropping occurred; fourth experiment (0.2 mL/kg + 0.5 mL/kg): follicle maturation occurred but egg dropping did not. As *T. scyllium* is an aplacental viviparous species, or ovoviviparous species, the fact that the eggs were dropped means these were not conducive conditions for artificial insemination. Around 15–20 eggs were found on the bottom of the female tank during the first and third experiments. As a result of all four experiments, the optimum protocol for female *T. scyllium* was concluded to be two injections of 0.2 mL/kg and 0.5 mL/kg of Ovaprim® at a 24 h interval.

3.4. Dose optimization of Ovaprim® and its effects in T. obesus

Changes in blood hormone levels after administration of 0.2 mL/kg Ovaprim® in males are as shown in **Figure 3D**. Overall, testosterone levels after salmon gonadotropin-releasing hormone analog administration were significantly higher in *T. obesus* than those in *T. scyllium*, although these decreased at 24 h post-injection. Progesterone, however, showed peak concentrations at 24 h compared to at 12 h in *T. scyllium*, thus showing different increments between species. Estradiol remained constant at very low levels. Unlike *T. scyllium*, semen was not sampled at both 1 h

and 12 h post-injection. The sampling time point was further reduced to 15 min post-injection and as a result, sufficient amounts of semen could be collected with an average volume of 6.5 mL. Semen sampling was found to be effective if carried out almost immediately after Ovaprim® administration in *T. obesus*. Semen sampling at later stages could result in the loss of semen to the surrounding environment.

In females, both the first (0.2 mL/kg + 0.2 mL/kg) and second (0.2 mL/kg + 0.3 mL/kg) experiments showed follicular maturation (**Figure 4D, 4E, 4F**) and no egg dropping (**Figure 5B**). Follicular size change could be recognized clearly both by the naked eyes in ultrasonography and through measurements in the figures (**Figure 4D**). No egg dropping suggested that the sharks were in a suitable state for artificial insemination. Overall, hormone levels after Ovaprim® administration were lower than those in female *T. scyllium* (**Figure 3E**). Estradiol and testosterone levels remained constant, whereas progesterone concentrations showed a steady increase. As there was no peak within 48 h, it was thought that the progesterone level would increase after 48 h.

4. Discussion

4.1. Biological reactions following Ovaprim® administration in sharks

For seasonally breeding sharks, natural ovarian follicular maturation occurs gradually throughout the year concomitant with a gradual increase in follicular diameter (Sulikowski et al., 2007; George et al., 2017). Therefore, the follicular maturation that was observed over 1 or 2 days in the current study is not a natural phenomenon. Follicular diameters increased by more than 1.5–2.0 cm within only 48 h in response to the administration of Ovaprim®, thereby confirming that this salmon gonadotropin-releasing hormone can effectively induce follicular maturation in both *T. scyllium* and *T. obesus*.

The observation that sharks lost their seasonality during the captive period also supports the argument that the follicular maturation was due to Ovaprim® administration (Schaller, 2006; George et al., 2017). The loss of seasonality, as a consequence of a reduction in water temperature and circadian rhythm changes over seasons, has been observed in sharks maintained in some aquaria, and indeed, maintaining constant water temperatures year-round is suggested as a method for reducing reproductive activity (Schaller, 2006; Henningsen et al., 2008; George et al., 2017). Consequently, taking into consideration the fact that the sharks lose seasonality and thereby undergo a reduction in reproductive activity, it can be assumed that their ovarian follicular growth observed in the present study is more likely to have been a response to the administration of Ovaprim®, rather than a manifestation of the natural reproductive cycle.

Given that reproduction is the most important aspect of conservation efforts, the loss of seasonality phenomenon in captive-bred sharks can represent a major hurdle in *ex-situ* conservation programs. Accordingly, the observations that Ovaprim® can induce follicular maturation in sharks that have lost their seasonality highlight the potential utility of this agent in overcoming the reproductive hurdle. In this regard, numerous previous studies on bony fish have demonstrated the successful promotion of reproduction via hormone induction, even during periods other than the natural breeding seasons of these fish. For example, in carp, in which the administration of Ovaprim® is a commonly used treatment, breeding can be induced more than twice annually during non-breeding periods. Thus, if Ovaprim® can be used to overcome natural patterns in fish reproductive cycles, it could become a potentially useful tool in the ex-situ conservation of a range of endangered species.

In this study, Ovaprim® could induce biological reactions only when the sharks matured sexually to some extent—confirmed by both hormone concentration analyses and Ovaprim® injection experiments using sharks F003–F007. The basal hormonal concentrations in shark F003 were higher than those observed in the six other sharks. Given the significant differences in physique between sharks F004–F007 and F003 (**Table 1**), current study results, with respect to differences in hormonal concentrations, are consistent with those reported in previous studies showing that the levels of gonadal hormones increase as an animal matures (Lutton et al., 2005). The other four sharks (F004–F007) did not have active follicles prior

to the administration of Ovaprim®, indicating that these sharks were not sufficiently mature. As observed previously in bony fish, the lack of response to Ovaprim® administration in the sharks confirms that the gamete developmental stage is an important factor influencing the response to exogenous hormonal stimulation (Anderson et al., 2013).

Accordingly, it is important to determine sexual maturity accurately in sharks prior to using Ovaprim®. In this study, especially in the case of females, it was the ultrasonography images of the ovarian follicles that played a decisive role in determining sexual maturity—only the sharks that had follicles before administration of Ovaprim® were mature enough to be used in the experiment. Data on the baseline concentrations of sex hormones has not been established for most shark species; thus, it is very important to check the existence, size change, and ovulation of follicles using ultrasonography. In various piscine species, ultrasound is commonly used to determine sexual maturity, maximizing the efficiency of AI (Petochi et al., 2011; Du et al., 2017; Kujawa et al., 2019). As artificial intervention is much more difficult for sharks than other fish, accurate ultrasonography use is important for successful conservational attempt.

Based on measured gonadal hormone concentrations, current findings indicate that both female and male sharks showed responses to the administration of Ovaprim®. These observations indicate that the hypothalamus-pituitary-gonadal axis, which has previously been identified in bony fishes, including sturgeons, might also

exist in sharks (Yom-Din et al., 2016). Although the roles of salmon gonadotropin-releasing hormone analog and gonadal steroids have been identified, the pituitary levels of hormones were not determined directly, including gonadotropic hormones, in the present study. However, as the basic role of gonadotropic hormones is to induce fluctuations in gonadal steroid levels in each sex and to induce the maturation and release of germ cells, their roles were being carried out effectively in the sharks examined in the present study.

Finally, current observations that salmon gonadotropin-releasing hormone analog functions in two species from different genera, i.e., species showing different types of reproductive strategies based on the presence or absence of the placenta, indicate that Ovaprim® could also induce similar biological reactions in other shark species. These findings are consistent with those of Lovejoy et al. (1992), who identified molecules similar to salmon GnRH and chicken GnRH in sharks. Further studies are required to ascertain whether these two different forms of GnRH act similarly.

4.2. Necessity and possibility of Ovaprim® usage for hormone-induced artificial insemination in wild shark conservation

Populations of a diverse range of piscine species are being threatened by human activities, and accordingly, efforts are being made to conserve some of these species (Halpern et al., 2008; Arthington et al., 2016). Induced reproduction is one of the

important tools for the *ex-situ* conservation of endangered Osteichthyes species (Ogale, 1997; Mijkherjee et al., 2002). For example, Ogale (2002) and Devi et al. (2009) have reported the breeding and conservation of Mahseer and Osteobrama belangeri, respectively, and hormone-induced artificial reproduction has been conducted using sturgeon (Anderson et al., 2013). Furthermore, in India, the West Bengal Government is making active use of induced breeding techniques and shares the culture methods used for endangered species with local farmers (Mijkherjee et al., 2002). They also have professed their plans to study and share induced breeding techniques in other endangered species.

Among the different classes of fish, the Chondrichthyes are characterized as having the highest proportion of threatened species (30.39%). Although the risk of extinction among these cartilaginous fish is more serious than that of Actinopterygii (16.77%), Chondrichthyes conservation tends to rank low on the international conservation agenda (Dulvy et al., 2008; Jacques, 2010), which presumably reflects the fact that few Chondrichthyes species are of direct commercial importance. Accordingly, the importance of their conservation is recognized to a greater extent from an ecological perspective rather than from an economic imperative (Jacques, 2010). However, marked declines in the populations of apex predators can potentially precipitate the collapse of marine food chains, and thus in many instances may result in a reduction of food resources for humans (Myers et al., 2007; Ferretti

et al., 2010). Consequently, although Chondrichthyes conservation may not seem to be of direct economic benefit, the opposite may in fact be true.

The conservation of Chondrichthyes species includes both *in-situ* and *ex-situ* initiatives (Friedrich et al., 2014; Fox et al., 2018), the former of which includes establishing marine reserves or regulating fishing, and thereby maintaining populations of animals in their native habitats, whereas the latter preserves animals using facilities external to their native ranges (Arthington et al., 2016; Fox et al., 2018). Although most of the conservation efforts for Chondrichthyes are *in-situ*, some *ex-situ*-managed breeding and monitoring programs are being conducted by several aquaria (Fox et al., 2018). However, to the best of my knowledge, none of these programs have employed hormone-induced breeding for the purposes of Chondrichthyes conservation.

In the case of wild sharks, aquaria could potentially serve as sites for *ex-situ* conservation. However, if water temperatures and circadian rhythms at the facilities are not precisely controlled, there is a high probability that reproductive activity would be reduced, as indicated by the findings of the present study (Henningsen et al., 2008). Furthermore, when targeting large wild sharks, it is generally difficult to accurately determine the timing of the ovulation of mature eggs, as conventional artificial insemination methods involve frequent ultrasonography, blood collection, and hormone concentration analysis. Given these aforementioned factors, hormonal

triggering is deemed to be among the essential tools required for the ex-situ conservation of sharks.

Hormonal inducers such as Ovaprim® can be used for a number of different purposes, from inducing natural courtship behaviors to facilitating artificial reproduction (Viveiros et al., 2002; Zarski et al., 2009; Montchowui et al., 2011). Successful induction of reproduction in an internal fertilizer requires conditions such as the stable ovulation of mature eggs, acquisition of spermatozoa with good fertility and quantity, and artificial insemination at the appropriate time, and by manipulating the timing and number of reproduction events using hormonal inducers, the efficacy of reproduction can be maximized. As a hormonal inducer, Ovaprim® has commonly been used to induce spawning for successful fertilization and hatching in vulnerable wild species, and is also used in the establishment of ovulation protocols for introducing new species to the aquaculture industry (Sarkar et al., 2004; Zadmajid et al., 2017). These uses of Ovaprim® have been based on one common feature, namely, the successful induction of reproduction in wild fish. However, prior to the present study, it had not been established whether this product could be used to induce biological reactions in Chondrichthyes.

As a proactive step toward the development of a hormone-induced artificial insemination protocol for endangered wild sharks, Ovaprim® was used to induce germ cell maturation and to establish suitable injection protocol. A single 0.2 mL/kg Ovaprim® dose induced semen release in the males of both study species and that

the administration of two 0.2 mL/kg + 0.5 mL/kg doses (at a 24 h interval) in *T. scyllium*, and 0.2 mL/kg + 0.2 mL/kg or 0.3 mL/kg (at a 24 h interval) in *T. obesus* females induced follicular maturation without egg dropping. Accordingly, given that the basic conditions for hormone-induced artificial insemination can be established using Ovaprim®, it can be reasonably expected that hormone-induced reproduction can be achieved in sharks. Compared with the development of hormone-induced artificial insemination technology in other fish species, the research reported herein is in its infancy; however, the findings of the present study, which to the best of my knowledge, is the first to have demonstrated successful hormone-induced reproduction in sharks, can serve to guide the direction of further related studies (Nandeesha et al., 1990; Khan et al., 2006; Brzoska et al., 2008; Olumuji et al., 2012; Dhara et al., 2013). Considering the importance of hormone-induced reproduction techniques in the *ex-situ* conservation of wild sharks, the findings of the present study will make a potentially important contribution to the conservation of endangered shark species.

4.3. Study limitations and future perspectives

Studies on the populations of wild animals are often constrained by sample scarcity, limited study periods, and insufficient funding, inter alia (Morrison et al., 2008). Sharks as species representative of marine wildlife are notably difficult targets for sampling, and the small sample sizes typically obtained invariably impose certain experimental limitations: only simple comparison between groups was possible, and

different conditions were tested on an animal with temporal intervals of more than a month between experiments. Therefore, further studies designed to augment population size are inevitable.

Nevertheless, even given such limitations, the findings of the present study provide a clear direction for further research on shark hormone-induced artificial insemination. Ovaprim® was found to induce biological reactions in the shark, and as expected, the induced reactions were confirmed to be related to germ cell maturation and release. General dose range and appropriate administration protocol were possible to be established in this study. Although fewer experiments were carried out for *T. obesus* than for *T. scyllium*, the desired biological responses could be induced, thereby indicating that the protocol developed in this study has potentially broad applicability in sharks.

Although Ovaprim® was found to induce ovulation and semen release, only the maturity or quantity of the germ cells were examined, and consequently, further studies will be necessary to verify whether there are any negative effects of synthetic salmon gonadotropin-releasing hormone analog administration on the quality of these germ cells. Aside from volume, other metrics of semen quality—morphology (normal spermatozoa), motility (progressive spermatozoa), viability, and concentration—should be evaluated in further studies to confirm the time to collect quality samples. Furthermore, given that an actual artificial insemination experiment was not conducted in the present study, the fertilization rate of the artificially

maturated germ cells was not possible to be determined. Moreover, the pituitary hormones were not analyzed, and thus, further studies are required to verify the presence, changes in concentration, and interactions of pituitary-level hormones in the hypothalamus-pituitary-gonadal axis of sharks.

Table 1. Body measurement traits of *Triakis scyllium* and *Triaenodon obesus*. C: calcified; NC: not calcified; E: elongated, longer than pelvic fin; NE: not elongated, not longer than pelvic fin; B: bending; NB: not bending; R: rhipidion formed; RN: rhipidion not formed.

Species	Sex	ID	Body weight (kg)	Body length (cm)	Clasper			
					Calcification	Elongation	Bending	Rhipidion formation
T. scyllium	Male	M001	14.8	160.0	C	E	B	R
		M002	3.1	98.0	C	E	B	R
		M003	1.6	78.0	NC	NE	NB	RN
		M004	3.4	100.0	C	E	B	R
		M005	3.1	100.0	C	E	B	R
		M006	8.9	137.5	C	E	B	R
	Female	F001	16.4	152.5	-	-	-	-
		F002	12.5	137.5	-	-	-	-
		F003	13.8	137.0	-	-	-	-
		F004	2.6	86.5	-	-	-	-
		F005	3.7	92.8	-	-	-	-
		F006	4.0	92.6	-	-	-	-
		F007	3.0	95.0	-	-	-	-
T. obesus	Male	WM001	17.8	163.0	C	E	B	R
		WM002	13.9	153.0	C	E	B	R
		WM003	15.1	155.0	C	E	B	R
	Female	WF001	20.0	156.0	-	-	-	-
		WF002	11.8	134.0	-	-	-	-
		WF003	14.5	146.0	-	-	-	-

Table 2. Hormone concentrations of *Triakis scyllium* and *Triaenodon obesus* prior to Ovaprim® administration. Concentrations are the average values of four measurements. M: mean; SE: standard error.

Species	Sex	Hormone	Concentration (M ± SE)
T. scyllium	Male (n = 5)	Estradiol (pg/mL)	12.68 ± 3.31
		Progesterone (ng/mL)	1.37 ± 0.30
		Testosterone (ng/mL)	70.03 ± 8.23
	Female, non-pregnant (n = 5)	Estradiol (pg/mL)	1018.68 ± 477.61
		Progesterone (ng/mL)	0.38 ± 0.08
		Testosterone (ng/mL)	0.93 ± 0.53
	Female, pregnant (n = 2)	Estradiol (pg/mL)	9159.80 ± 424.10
		Progesterone (ng/mL)	0.85 ± 0.12
		Testosterone (ng/mL)	2.78 ± 0.11
T. obesus	Male (n = 3)	Estradiol (pg/mL)	17.08 ± 1.59
		Progesterone (ng/mL)	0.76 ± 0.34
		Testosterone (ng/mL)	424.79 ± 172.81
	Female (n = 3)	Estradiol (pg/mL)	22.51 ± 1.73
		Progesterone (ng/mL)	0.09 ± 0.03
		Testosterone (ng/mL)	0.04 ± 0.01

Table 3. Average blood test results of *Triakis scyllium* and *Triaenodon obesus*. CBC: complete blood count; WE blood cell; RBC: red blood cell; mPCV: manual packed cell volume; BUN: blood urea nitrogen; ALKP: alkaline pho AST: aspartate transaminase; ALT: alanine transferase; GGT: gamma-glutamyl transferase; CK: creatinine kina lactate dehydrogenase; TCO_2: total CO_2; T: temperature; NT: not tested.

		Triakis scyllium				*Triaenodon obesu*
	Unit	**Pregnant female (n=2)**	**Non-pregnant female (n=3)**	**Male (n=5)**	**Female (n=3)**	**M (n**
CBC						
WBC	(10^9/L)	10.46	30.86	33.76	NT	
RBC	(10^{12}/L)	0.35	0.44	0.48	NT	
Hemoglobin	g/dL	9.25	8.80	9.52	10.13	8
mPCV	%	32.00	28.40	31.20	45.50	28
Chemistry						
Na^+	mmol/L	279.00	282.60	283.60	293.00	28
K^+	mmol/L	3.45	3.66	3.26	3.60	3
Cl^-	mmol/L	222.00	225.60	234.60	230.00	24
Calcium	mg/dL	18.00	18.28	17.92	18.73	19
Phosphorus-Inorganic	mg/dL	6.85	5.28	5.26	5.47	5
Magnesium	mg/dL	3.75	3.40	4.22	4.23	4
BUN	mg/dL	1135.45	1081.12	1097.44	940.90	10
Creatinine	mg/dL	0.10	0.10	0.22	0.01	0

Uric Acid	mg/dL	0.35	0.34	0.58	0.57	0.40
Ammonia	µmol/L	40.00	17.40	62.20	124.67	33.00
Protein-Total	g/dL	2.95	2.66	2.92	3.70	4.37
Albumin	g/dL	1.30	1.18	1.28	1.63	1.93
Globulin	g/dL	1.65	1.48	1.64	2.07	2.43
Glucose	mg/dL	87.00	92.00	95.60	100.67	98.00
Bilirubin-Total	mg/dL	0.10	0.10	0.10	0.13	0.10
Bilirubin-Direct	mg/dL	0.10	0.10	0.10	0.10	0.10
Cholesterol-Total	mg/dL	103.00	120.60	101.20	81.67	87.33
Triglyceride	mg/dL	287.50	230.40	322.60	22.33	42.00
Lipase	U/L	53.00	109.80	218.00	50.00	37.00
Amylase	U/L	18.00	53.60	13.60	5.67	5.33
ALKP	U/L	113.50	105.00	87.60	19.33	32.67
AST	U/L	29.50	14.00	19.20	12.33	12.00
ALT	U/L	13.50	11.60	12.60	5.33	6.33
GGT	U/L	1.00	1.60	1.00	1.00	1.00
CK	U/L	942.00	74.80	220.20	599.33	214.00
LDH	U/L	181.50	25.80	96.80	97.67	35.00
Gas Analysis						
pH		7.53	7.59	7.48	NT	NT
PCO_2	mmHg	9.25	7.40	10.14	NT	NT
PO_2	mmHg	8.00	19.20	11.80	NT	NT
BEecf	mmol/L	-16.50	-16.80	-23.20	NT	NT
HCO_3	mmol/L	9.20	8.22	9.08	NT	NT
TCO_2	mmol/L	9.50	8.40	9.80	NT	NT
SO_2	%	35.00	78.00	54.40	NT	NT
T	℃	22.50	22.26	21.60	NT	NT

Table 4. Water quality of the shark tanks during experiments. Total eight criteria were measured regularly. Each value indicates average ± standard deviation of the measurements.

Tank	pH	Temperature (℃)	Salinity (ppt)	Specific gravity	Dissolved oxygen (ppm)	NO_2^- (ppm)	NO_3^- (ppm)	NH_3 (ppm)
Male tank	7.0 ± 0.0	21.3 ± 0.6	40.8 ± 1.1	1.0 ± 0.0	7.8 ± 0.5	0.0 ± 0.0	2.6 ± 0.9	0.0 ± 0.0
Female tank	7.0 ± 0.0	22.0 ± 0.2	40.2 ± 1.0	1.0 ± 0.0	8.6 ± 0.3	0.0 ± 0.0	2.3 ± 0.3	0.0 ± 0.0

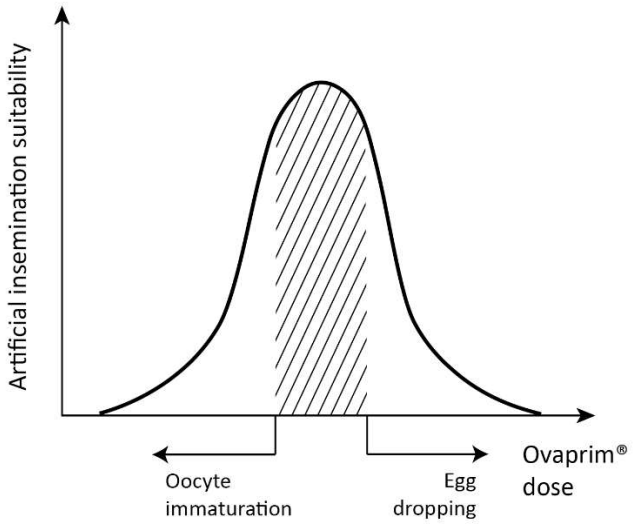

Figure 1. Schematic graph of dose optimization in female sharks. A conceptual graph showing the correlation between biological phenomena (x-axis) and artificial insemination suitability (y-axis) that change depending on the total dose of Ovaprim® administered. The shaded area denotes mature oocytes after follicle growth but prior to egg dropping, which is the targeted area for females in this study.

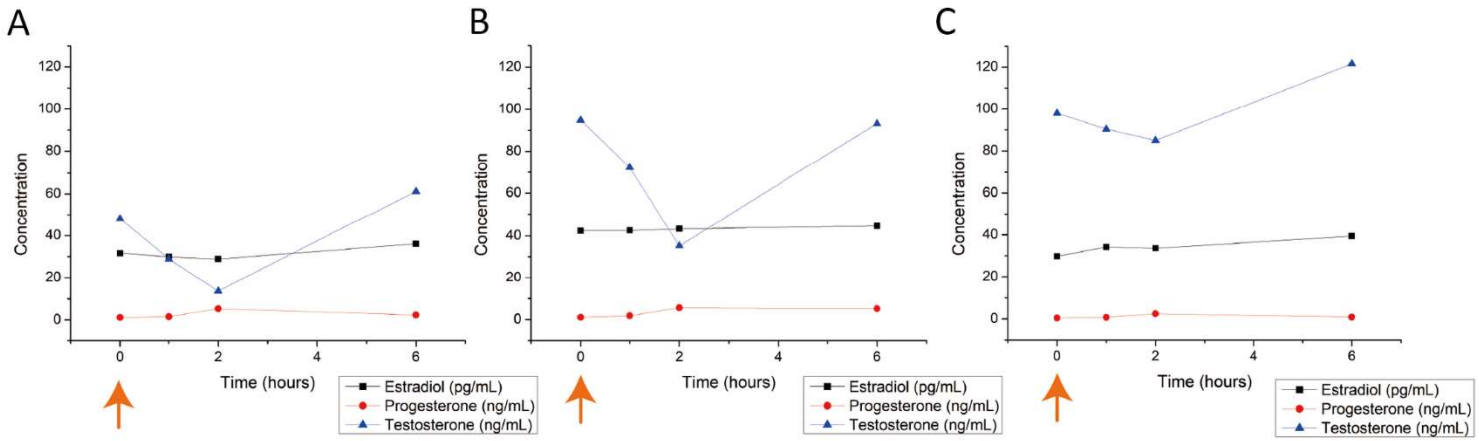

Figure 2. Blood hormone level changes after Ovaprim® injection in male *Triakis scyllium*. Ovaprim® was injected intramuscularly into the epaxial muscle. A: average hormone concentration changes of Group A (0.1 mL/kg). B: average hormone concentration changes of Group B (0.2 mL/kg). C: average hormone concentration changes of Group C (0.4 mL/kg). The orange arrows indicate the time points of Ovaprim® injection.

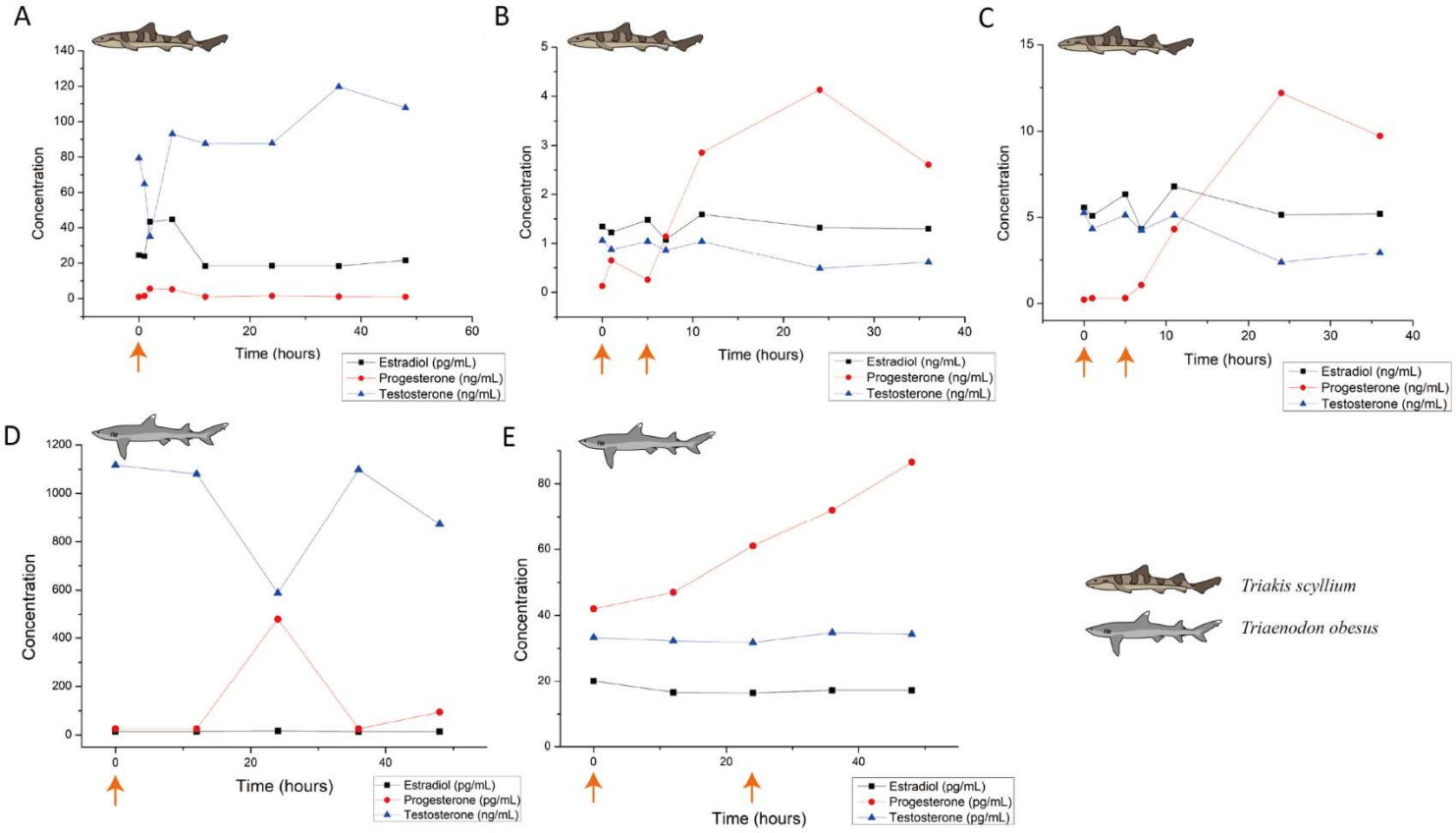
A
B
C
D
E
Concentration
Time (hours)
Estradiol (pg/mL)
Progesterone (ng/mL)
Testosterone (ng/mL)
Estradiol (ng/mL)
Progesterone (pg/mL)
Triakis scyllium
Triaenodon obesus

Figure 3. Blood hormone level changes after Ovaprim® injection in *Triakis scyllium* and *Triaenodon obesus*. A: average hormone concentration changes in male *T. scyllium*. Ovaprim® was injected at 0.2 mL/kg dose at the orange arrowed time point. B: average hormone concentration changes of female *T. scyllium*. Ovaprim® was injected at 0.6 mL/kg dose at the orange arrowed time points. C: average hormone concentration changes of *T. scyllium* (Female #3; F003). Ovaprim® was injected at 0.6 mL/kg dose at the orange arrowed time point. D: average hormone concentration changes of male *T. obesus*. Ovaprim® was injected at 0.2 mL/kg dose at the orange arrowed time point. E: average hormone concentration changes in female *T. obesus*. Ovaprim® was injected at 0.2 mL/kg and 0.3 mL/kg doses in serial at the orange arrowed time points.

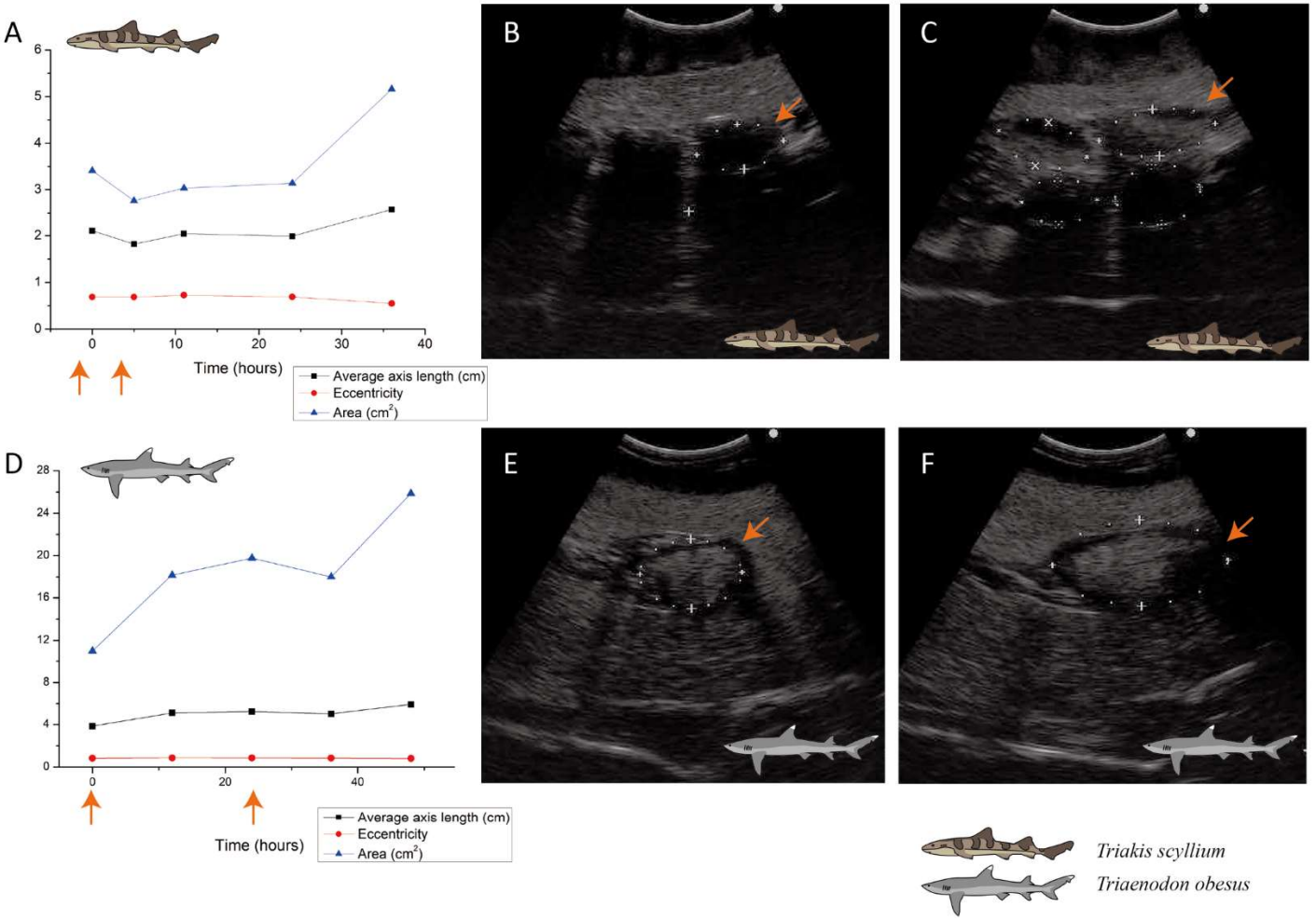
A
B
C
D
E
F
Time (hours)
Average axis length (cm)
Eccentricity
Area (cm²)
Triakis scyllium
Triaenodon obesus

Figure 4. Ovarian follicle size change after Ovaprim® injection in *Triakis scyllium* and *Triaenodon obesus.* A: Ovarian follicle size changes after Ovaprim® injection in female *T. scyllium*. Axis length and area values were measured directly on ultrasonography. Eccentricity was calculated with the long and short axis values. The orange arrows indicate the time points of Ovaprim® administration. B: Ultrasonography of left ovary before Ovaprim® injection in *T. scyllium* (F003). The orange arrows indicate the same follicle in panel C at different time point. Size of the follicle with the orange arrow was 3.7 cm × 1.9 cm (5.45 cm^2). C: Ultrasonography of left ovary after Ovaprim® injection in *T. scyllium* (F003). Follicles showed distinct size increase. The orange arrows indicate the same follicle in panel B at different time point. Size of the follicle with the orange arrow was 4.9 cm × 2.0 cm (7.60 cm^2). D: Ovarian follicle size changes after Ovaprim® injection in female *T. obesus*. Axis length and area values were measured directly on ultrasonography. Eccentricity was calculated with the long and short axis values. The orange arrows indicate the time points of Ovaprim® injection. E: Ultrasonography of left ovary before Ovaprim® injection in WF002 (*T. obesus*). The orange arrows indicate the same follicle in panel F at different time point. Size change of the follicles can be recognized by ultrasonography. Size of the follicle with the orange arrow was 4.4 cm × 3.0 cm (10.27 cm^2). F: Ultrasonography of left ovary after Ovaprim® injection in WF002 (*T. obesus*). The orange arrows indicate the same follicle in panel E at different time point. Size of the follicle with the orange arrow was 7.4 cm × 3.7 cm (21.77 cm^2).

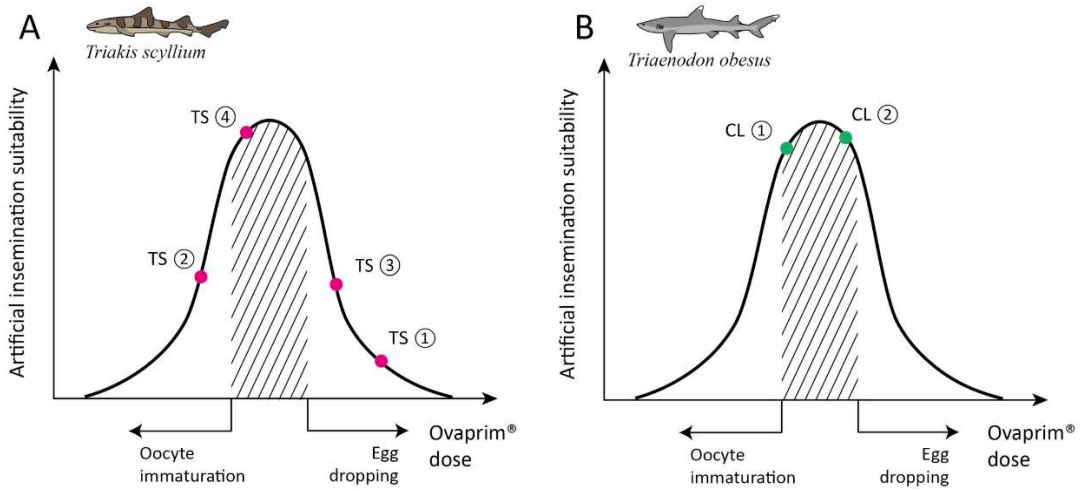

Figure 5. Schematic graph of dose optimization in *Triakis scyllium* and *Triaenodon obesus*. A conceptual graph showing the correlation between biological phenomena (x-axis) and artificial insemination suitability (y-axis) that change depending on the total dose of Ovaprim® administered. The shaded area denotes mature oocytes after follicle growth but prior to egg dropping, which is the targeted area for females in this study. A: Ovaprim® experimental doses for female *T. scyllium*. TS①: 0.6 mL/kg + 0.6 mL/kg, 6 h time gap; TS②: 0.2 mL/kg + 0.4 mL/kg, 12 h time gap; TS③: 0.2 mL/kg + 0.6 mL/kg, 24 h time gap; TS④: 0.2 mL/kg + 0.5 mL/kg, 24 h time gap. B: Ovaprim® experimental doses for female *T. obesus*. CL①: 0.2 mL/kg + 0.2 mL/kg, 24 h time gap; CL②: 0.2 mL/kg + 0.3 mL/kg, 24 h time gap.

References

Anderson, B., Belcher, C., Slack, J., Gelsleichter, J. (2018). Evaluation of the use of portable ultrasonography to determine pregnancy status and fecundity in bonnethead shark *Sphyrna tiburo*. *J. Fish Biol.* 93, 1163–1170.

Anderson, W.G., Genz, J., and McDougall, C. (2013). Using Ovaprim™ as a conservation tool for lake sturgeon, *Acipenser fulvescens*: The short and long term effects of endocrine manipulation during the reproductive cycle. Winnipeg, University of Manitoba.

Arthington, A.H., Dulvy, N.K., Gladstone, W., and Winfield, I.J. (2016). Fish conservation in freshwater and marine realms: status, threats and management. *Aquatic Conserv.* 26, 838–857.

Blanco, J.M., Wildt, D.E., Hofle, U., Voelker, W., and Donoghue, A.M. (2009). Implementing artificial insemination as an effective tool for *ex situ* conservation of endangered avian species. *Theriogenology* 71, 200–213.

Brzoska, E., and Adamek, J. (2008). Artificial spawning of European catfish, *Silurus glanis* L.: stimulation of ovulation using LHRH-a, Ovaprim and carp pituitary extract. *Aquac. Res*. 30, 59–64.

Cardinaletti, G., Franzoni, M.F., Palermo, F.A., Cottone, E., Mosconi, G., Guastalla, A., et al. (2010). "Environmental and neuroendocrine control of fish reproduction" in Recent Advances in Fish Reproduction Biology, ed. A. G. Ayala, J. M. Penalver, and E. C. Pozo (NY: Research Signpost), 67–87.

Castro, J.I. (2009). Observations on the reproductive cycles of some viviparous North American sharks. Aqua, *Int. J. Ichthyol*. 15, 4–15.

Clark, E., and Von Schmidt, K. (1965). Sharks of the Central Gulf Coast of Florida. *Bull. Mar. Sci.* 15, 13–83.

Comizzoli, P., Mermillod, P., and Mauget, R. (2000). Reproductive biotechnologies for endangered mammalian species. *Reprod. Nutr. Dev.* 40, 493–504.

Compagno, L.J.V. (1984). Sharks of the world: an annotated and illustrated catalogue of shark species known to date. *FAO Species Catalogue.* 4, 432.

Devi, G.A., Devi, G.S., Singh, O.B., Munilkumar, S., and Reddy, A.K. (2009). Induced spawning and hatching of *Osteobrama belangeri* (Valenciennes) using Ovatid, an ovulating agent. *Asian Fish. Sci.* 22, 1107–1115.

Dhara, K., and Saha, N.C. (2013). Controlled breeding of Asian catfish *Clarias batrachus* using pituitary gland extracts and Ovaprim at different temperatures, latency periods and their early development. *J. Aquac. Res*. Dev. 4, 186.

Du, H., Zhang, X., Leng, X., Zhang, S., Luo, J., Liu, Z., et al. (2017). Gender and gonadal maturity stage identification of captive Chinese sturgeon, *Acipenser sinensis*, using ultrasound imagery and sex steroids. *Gen. Comp. Endocrinol.* 245. 36–43.

Dulvy, N.K., Baum, J.K., Clarke, S., Compagno, L.J.V., Cortés, E., Domingo, A., et al. (2008). You can swim but you can′t hide: the global status and conservation of oceanic pelagic sharks and rays. *Aquat. Conserv.: Mar. Freshwater. Ecosyst.* 18, 459–482.

Ferretti, F., Worm, B., Britten, G.L., Heithaus, M.R., and Lotze, H.K. (2010). Patterns and ecosystem consequences of shark declines in the ocean. *Ecol. Lett.* 13, 1055–1071.

Fox, G., Darolti, I., Hibbitt, J., Preziosi, R.F., Fitzpatrick, J.L., and Rowntree, J.K. (2018). Bespoke markers for ex-situ conservation: application, analysis and challenges in the assessment of a population of endangered undulate rays. *J. Zoo Aquar. Res.* 6, 50–56.

Friedrich, L.A., Jefferson, R., and Glegg, G. (2014). Public perceptions of sharks: gathering support for shark conservation. *Mar. Policy* 47, 1–7.

Fujinami, Y. and Tanaka, S. (2013). Age, growth and reproduction of the banded houndshark *Triakis scyllium* around the tip of the Izu Peninsula, Japan. *Nippon Suisan Gakk*. 79, 968–976.

Genz, J., McDougall, C.A., Burnett, D., Arcinas, L., Khetoo, S., and Anderson, W.G. (2014). Induced spawning of wild-caught adult lake sturgeon: assessment of hormonal and stress response, gamete quality, and survival. *J. Appl. Ichthyol.* 30, 1565–1577.

George, R.H., Steeil, J., and Baine, K. (2017). “Diagnosis and treatment of common reproductive problems in elasmobranchs” in The Elsmobranch Husbandry Manual II: Recent Advances in the Care of Sharks, Rays and their Relatives, ed. M. Smith, D. Warmolts, D. Thoney, R. Hueter, M. Murray, and J. Ezcurra (Columbus, OH: The Ohio State University Printing Servicies), 363–374.

Halpern, B.S., Walbridge, S., Selkoe, K.A., Kappel, C.V., Micheli, F., D'Agrosa, C., et al. (2008). A global map of human impact on marine ecosystems. *Science* 319, 948–952.

Henningsen, A.D., Murru, F.L., Rasmussen, L.E.L., Whitaker, B.R., and Violetta, G.C. (2008). Serum levels of reproductive steroid hormones in captive sand tiger sharks, *Carcharias taurus* (Rafinesque), and comments on their relation to sexual conflicts. *Fish Physiol. Biochem.* 34, 437–446.

Hermes, R., Göritz, F., Streich, W.J., and Hildebrandt, T.B. (2007). Assisted reproduction in female rhinoceros and elephants - current status and future perspective. *Reprod. Domest. Anim.* 42, 33–44.

Hildebrandt, T.B., Hermes, R., Walzer, C., Sós, E., Molnar, V., Mezösi, L., et al. (2007). Artificial insemination in the anoestrous and the postpartum white rhinoceros using GnRH analogue to induce ovulation. *Theriogenology*. 67, 1473–1484.

Hill, J.E., Kilgore, K.H., Pouder, D.B., Powell, J.F.F., Watson, C.A., and Yanong, R.P.E. (2009). Survey of Ovaprim use as a spawning aid in ornamental fishes in the United States as administered through the University of Florida tropical aquaculture laboratory. *N. Am. J. Aquacult.* 71, 206–209.

Hoga, C.A., Almeida, F.L., and Reyes, F.G.R. (2018). A review on the use of hormones in fish farming: Analytical methods to determine their residues. *CyTA. J. Food.* 16, 679–691.

IUCN (International Union for Conservation of Nature). The IUCN Red List of Threatened Species 2019. http://www.iucnredlist.org [Accessed September 10, 2020]

Jacques, P.J. (2010). The social oceanography of top oceanic predators and the decline of sharks: a call for a new field. *Prog. Oceanogr.* 86, 192–203.

Karami, A., Christianus, A., Zokaeifar, H., Saad, K.Z., Imraan, F.T.J., Shakibazadeh, S., et al. (2011). Ovaprim treatment promotes oocyte development and milt fertilization rate in diploid and triploid African catfish (*Clarias gariepinus*). *Aquac. Int.* 19, 1025–1034.

Khan, A.M., Shakir, H.A., Ashraf, M., and Ahmad, Z. (2006). Induced spawning of Labeo rohita using synthetic hormones. *Punjab Univ. J. Zool.* 21, 67–72.

Kujawa, R., Nowosad, J., Biegaj, M., Cejko, B.I., and Kucharczyk, D. (2019). Use of ultrasonography to determine sex in sexually immature European river lamprey *Lampetra fluviatilis* (L.). *Anim. Reprod. Sci.* 204, 95–100.

Lack, M., and Sant, G. (2011). The future of sharks: a review of action and inaction. TRAFFIC International and the Pew Environment Group 44.

Lovejoy, D.A., Ashmead, M.B., Coe, I.R., and Sherwood, N.M. (1992). Presence of gonadotropin-releasing hormone immunoreactivity in dogfish and skate brains. *J. Exp. Zool.* 263, 272–283.

Lutton, B.V., George, J., Murrin, C.R., Fileti, L.A., and Callard, I.P. (2005). “The Elasmobranch Ovary” In Reproductive Biology and Phylogeny of

Chondrichthyes: Sharks, Batoids, and Chimaeras, ed. W. C. Hamlett (UK: Science Publishers), 237–282.

Madigan, D.J., Brooks, E.J., Bond, M.E., Gelsleichter, J., Howey, L.A., Abercrombie, D.L., et al. (2015). Diet shift and site-fidelity of oceanic whitetip sharks *Carcharhinus longimanus* along the Great Bahama Bank. *Mar. Ecol. Prog. Ser.* 529, 185–197.

Masuda, M., Izawa, Y., Kametsuta, S., Ikuta, H., and Isogai, T. (2003). Artificial insemination of the cloudy catshark. *J. Japan. Assoc. Zoo. Aquar*. 44, 39–43.

Masuda, M., Izawa, Y., Kametsuta, S., Ikuta, H. and Isogai, T. (2005). Artificial insemination of the white-spotted bamboo shark, *Chiloscyllium plagiosum*. *J. Japan. Assoc. Zoo. Aquar*. 46, 91–96.

Mijkherjee, M., Praharaj, A., and Das, S. (2002). Conservation of endangered fish stocks through artificial propagation and larval rearing technique in West Bengal, India. Aquaculture Asia. 7, 8–11.

Montchowui, E., Laleye, P., Philippart, J.C., and Poncin, P. (2011). Reproductive behaviour in captive African carp, *Labeo parvus* Boulenger, 1902 (Pisces: Cyprinidae). *J. Fish. Int.* 6, 6–12.

Morrison, M. L., Block, W. M., Strickland, M. D., Collier, B. A., Peterson, M. J. (2008). Wildlife Study Design (New York: Springer-Verlag).

Myers, R.A., Baum, J.K., Shepherd, T.D., Powers, S.P., and Peterson, C.H. (2007). Cascading Effects of the Loss of Apex Predatory Sharks from a Coastal Ocean. *Science*. 315, 1846–1850.

Nandeesha, M.C., Rao, K.G., Jayanna, R.N., Parker, N.C., Varghese, T.J., Keshavanath, P., et al. (1990). “Induced spawning of Indian major carps through single application of Ovaprim-C” in The Second Asian Fisheries Forum, ed. R. Hirano and I. Hanvu (Manila, Philippines: Asian Fisheries Society), 581–585.

Ogale, S.N. (1997). Induced spawning and hatching of golden mahseer *Tor putitora* (Hamilton) at Lonavla, Pune District (Maharashtra) in Western Ghats. *Fishing Chimes*. 27–29.

Ogale, S.N. (2002). Mahseer breeding and conservation and possibilities of commercial culture. The Indian experience. *FAO Fisheries Technical Paper*. 431, 193–212.

Olumuji, O.K., and Mustapha, M.K. (2012) Induced breeding of African mud catfish, *Clarias gariepinus* (Burchell 1822), using different doses of normal saline diluted Ovaprim. *J. Aquac. Res. Dev.* 3, 133. doi: 10.4172/2155-9546.1000133

Paul, M., and Chanda, M. (2014). Induced breeding of carps. University of Calcutta. https://www.researchgate.net/publication/261994048.

Petochi, T., Di Marco, P., Donadelli, V., Longobardi, A., Corsalini, D., Bertotto, D., et al. (2011). Sex and reproductive stage identification of sturgeon hybrids (*Acipenser naccarii* × *Acipenser baerii*) using different tools: ultrasounds, histology and sex steroids. *J. Appl. Ichth.* 27, 637–642.

Rottmann, R.W., Shireman, J.V., and Chapman, F.A. (1991). Introduction to hormone-induced spawning of fish. SRAC publication No. 421.

Sarkar, U.K., Negi, R.S., Deepak, P.K., Singh, S.P., Srivastava, S.M., and Roy, D. (2004). Captive breeding of vulnerable Indian carp *Cirrhinus reba* with Ovaprim for conservation of wild populations. *Aquac. Asia*. 9, 5–7.

Schaller, P. (2006). Husbandry and reproduction of Whitetip reef sharks at Steinhart Aquarium, San Francisco. *Int. Zoo Yearb.* 40, 232–240.

Shanthanagouda, A.H., and Khairnar, S.O. (2018). Breeding and spawning of fishes: Role of endocrine gland. *Int. J. Fish. Aquat. Stud*. 6, 472–478.

Sulikowski, J.A., Driggers III, W.B., Ford, T.S., Boonstra, R.K., and Carlson, J.K. (2007). Reproductive cycle of the blacknose shark *Carcharhinus acronotus* in the Gulf of Mexico. *J. Fish Biol.* 70, 428–440.

Swider, D.A., Corwin, A.L., Kamerman, T.Y., Zimmerman, S.L., Violetta, G.C., Davis, J., et al. (2017). "Reproduction of spotted eagle rays, *Aetobatus narinari*, in aquaria" in Elasmobranch Husbandry Manual II: Recent Advances in the Care of Sharks, Rays and their Relatives, ed. M. Smith, D. Warmolts, D. Thoney, R. Hueter, M. Murray, and J. Ezcurra (Columbus, OH: The Ohio State University Printing Servicies), 433–442.

Taniuchi, T. (1988). Aspects of Reproduction and Food Habits of the Japanese Swellshark *Cephaloscyllium umbratile* from Choshi, Japan. *Nippon Suisan Gakk.* 54, 627–633.

Tambling, C.J., Avenant, N.L., Drouilly, M., Melville, H.I. (2018). "The role of Mesopredators in ecosystems: Potential effects of managing their populations on ecosystem processes and biodiversity" in the Livestock Predation and its

Management in South Africa: a Scientific Assessment, ed. G.I.H. Kerley, S.L. Wioson and D. Balfour (Port Elizabeth, South Africa: Centre for African Conservation Ecology, Nelson Mandela University), 205–227.

Thongtip, N., Mahasawangkul, S., Thitaram, C., Pongsopavijitr, P., Kornkaewrat, K., Pinyopummin, A., et al. (2009). Successful artificial insemination in the Asian elephant (*Elephas maximus*) using chilled and frozen-thawed semen. *Reprod. Biol. Endocrin*. 7, 75.

U.S.FDA. FOI Summary Ovaprim. https://www.fda.gov/animal-veterinary/minor-useminor-species/foi-summary-ovaprim [Accessed September 9, 2020]

Viveiros, A.T.M., Fessehaye, Y., Veld, M., Schulz, R.W., and Komen, J. (2002). Hand-stripping of semen and semen quality after maturational hormone treatments, in African catfish *Clarias gariepinus*. *Aquaculture*. 213, 373–386.

Yanong, R.P.E., Martinez, C., and Watson, C.A. (2009). Use of Ovaprim in ornamental fish aquaculture. *University of Florida IFAS Extension.* FA161.

Yom-Din, S., Hollander-Cohen, L., Aizen, J., Boehm, B., Shpilman, M., Golan, M., et al. (2016). Gonadotropins in the Russian Sturgeon: Their Role in Steroid Secretion and the Effect of Hormonal Treatment on Their Secretion. *PLoS One.* 11, e0162344.

Zadmajid, V., Mirzaee, R., Hoseinpour, H., Vahedi, N., and Butts, I.A.E. (2017). Hormonal induction of ovulation using Ovaprim™[(D-Arg6, Pro9NEt)-sGnRH + domperidone] and its impact on embryonic development of wild-caught

Longspine scraper, *Capoeta trutta* (Heckel, 1843). *Anim. Reprod. Sci.* 187, 79–90.

Zarski, E., Kucharczyk, D., Targonska, K., Jamroz, M., Krejszeff, S., and Mamcarz, A. (2009). Application of Ovopel and Ovaprim and their combinations in controlled reproduction of two reophilic cyprinid fish species. *Pol. J. Nat. Sci.* 24, 235–244.

GENERAL CONCLUSION

Sharks are keystone species of great importance both ecologically and academically. However, due to difficulties in access, not many studies have been conducted on this animal. To improve this lack of information and to contribute to their conservation, in this study, basic radiology data on sharks was set up, and based on this, the assisted reproductive technologies including semen cryopreservation, hormone-induced follicular maturation and ovulation, and hormone-induced semen release on sharks were established.

1. The detailed atlas of banded houndshark (*Triakis scyllium*) was set up using CT, MRI, and cryosection in transverse, sagittal, and dorsal sections. Organs and tissues of musculoskeletal system, cardiovascular system, digestive system, excretory system, and nervous system, of banded houndshark were able to be differentiated in detail. This study provides a basis for accurate anatomy identification while clinical approaching in the future studies.

2. Activating extender for banded houndshark (*Triakis scyllium*) semen was optimized and designated as SSAE-1. A preliminary protocol for semen cryopreservation, which is one of the most important techniques consisting ARTs, was established using SSAE-1. Though the Kim's protocol set up during this study did not show high post-thaw motility (2.03%), it clearly suggested the direction of further studies for semen cryopreservation protocol optimization for sharks, by identifying the factors that contribute

or hinder the motility of spermatozoa.

3. Normal blood concentrations of testosterone, progesterone, and estradiol were set up in banded houndshark (*Triakis scyllium*) and whitetip reef shark (*Triaenodon obesus*) and used as the standard for further experimental analysis. The applicability of sGnRHa (Ovaprim®) to the sharks was firstly looked up. After confirming that the Ovaprim® elicits a biological reaction from the shark species, proper injection dose and period were elicited. As a result, follicular maturation and ovulation in females and semen release in males were successfully induced by the Ovaprim® applications, showing the possibility of hormone-induced artificial insemination trial in the shark species.

Since all data were the world's first reports to sharks, this study could contribute to enhancing the understanding of Selachimorpha biology, specifically in the fields of anatomy and reproductive physiology. Detailed anatomy description in sharks using imaging tools increased the accuracy of clinical approaches, and the application of Ovaprim® showed the existence of hypothalamus-pituitary-gonad axis in sharks and the possibility that they could be stimulated by sGnRHa. These studies can serve as the basis for ARTs development that can practically contribute to shark conservation. Further studies need to optimize semen cryopreservation protocol to have improved post-thaw motility, decide post-thaw motility of cryopreserved semen by AI, and eventually be able to conduct HAI successfully.

국문 초록

상어에서의 기초 보조생식기술 연구

김 상 화

서울대학교 대학원
수의학과 수의병인생물학 및 예방수의학 전공

상어는 판새아강 상어상목에 속하는 어종들의 총칭으로, 초기 척추동물 중 현재까지 성공적으로 생존해 있는 대표적인 동물군이다. 척추동물 형성 초기에 나타나 진화의 역사를 고스란히 담고 있는 만큼, 상어는 면역체계, 번식 전략, 암 저항성 등 다양한 측면에서 중요한 진화생물학적 연구의 대상이다. 뿐만 아니라 상어는 생태학적으로도 중요한 역할을 하는데, 해양 생태계 먹이사슬의 최상위 포식자로서 해당 생태계가 균형 있고 안정적으로 유지될 수 있도록 기여하고 있기 때문이다. 상어 개체 수에 이상이 생기면 먹이사슬 전체가 무너질 수 있다는 점은 이미 여러 선행연구를 통해 밝혀진 바, 그 중요성이 높기 때문에 핵심종이라고도 불린다.

문제는 이들이 현재 심각한 멸종위기에 처해있다는 점이다. IUCN Red List 에 따르면, 연골어류의 37%가량이 취약 (VU), 절멸 위기 (EN), 절멸 위급 (CR)군으로 분류되고 있어 심각한 멸종위기 상태를 마주하고 있다. 이러한 양상은 이미 1970 년대부터 확인되어 왔으며, 그 가장 큰 요인으로는 샥스핀 산업을 필두로 하는 어업이 지적되어 왔다. 이에 전세계적으로 상어 어획량을 줄이고자 하는 환경운동이 수행되어 왔으나, 상어 특유의 느린 번식속도에 기인하여 이들의 멸종위기 상태가 쉽게 개선되지는 않고 있는 실정이다.

심각한 멸종위기 상태의 동물 종 보전을 위해서는 사람의 인위적인 개입이 필수불가결하다. 이미 재두루미, 몽고말, 코끼리, 북부흰코뿔소 등 다양한 멸종위기 동물종에서 종 구제 및 보호를 위하여 보조생식기술이 개발 적용되고 있다. 그러나 상어의 경우 동물 자체에 대한 접근이 쉽지 않아 사실상 연구 되어있는 바가 거의 없다. 이에 본 논문에서는 상어 종 보전에 기여하고자 일련의 연구들을 수행하였다. 우선적으로 기초적인 영상의학 아틀라스를 확립하였으며, 이후 보조생식기술 개발을 위하여 상어 정액 동결보존 프로토콜 및 호르몬 유도 배란 프로토콜, 호르몬 유도 정액 샘플링 프로토콜을 개발하였다.

1. 영상의학적 분석 기반 확립은 모든 수의학적 접근 방식의 기본이

되는 만큼, 본 연구는 최초로 컴퓨터 단층촬영 (CT) 및 자기공명영상진단 (MRI) 방식을 이용하여 상어에서의 세밀한 영상의학 아틀라스를 확립하였다. 체장 1 m 안팎의 어린 까치상어 (*Triakis scyllium*) 세 마리의 전신 CT 및 MRI 스캔을 수행했으며, 각 개체들을 냉동 후 transverse, sagittal, dorsal 단면으로 잘라 실제 단면 모습과 CT, MRI상의 단면을 비교분석 하였다. 다양한 장기 및 조직들을 세밀하게 구분하여 아틀라스를 확립하였다. 다만 미성숙 개체들을 대상으로 연구를 수행하였던 만큼 생식계통에 대한 확인은 불가하였다.

2. 까치상어 (*Triakis scyllium*) 수컷 다섯 마리를 대상으로 실험을 수행하였다. Ovaprim®을 0.2 mL/kg 투여 후 1시간 뒤, 상어의 복부를 부드럽게 마사지하여 urogenital papilla를 통해 나오는 정액의 secondary cloudy portion을 샘플링 하여 실험에 이용하였다. 정지상태 정자의 motility를 최대로 만들 수 있는 활성화 용액 조성을 확립하였으며 이를 SSAE-1로 명명하였다. 까치상어 정자에 최적화된 동결보존 프로토콜을 확립하기 위하여 총 8종의 extender solution, 3종류의 extension ratio, 15종의 cryoprotectants, 4종의 equilibration periods, 3종의 cooling rates, 3종의 thawing temperature를 테스트 하였다. 결과적으로

정립된 Kim’s protocol은 다음과 같다: extender, filtered seawater; extension ratio, 1:3; cryoprotectant, egg yolk 10% + ethylene glycol 10%; equilibration period, 10 min; cooling rate, 3 cm, 3 min; thawing temperature, 30℃, 10 s. 프로토콜을 이용했을 때 최종적으로 확인된 정자의 해동 후 운동능은 2.03%로 확인되었다.

3. 난태생 상어인 까치상어 (*Triakis scyllium*)와 태반성 태생 상어인 화이트팁 상어 (*Triaenodon obesus*)에서 실험을 수행하여 다양한 번식전략을 지닌 상어 종 전반에 걸쳐 연어 유래 gonadotropin-releasing hormone (GnRH, Ovaprim®) 적용 가능성을 확인하였다. 실험에 앞서 두 상어종에서 암컷과 수컷의 정상 혈중 성호르몬 농도를 각각 확인하여 추후 실험 분석의 base line으로 이용하였다. 두 종 모두에서 Ovaprim®이 혈중 에스트로겐, 프로게스테론, 테스토스테론의 농도 변화를 성공적으로 유도하였으며, 암컷에서는 난포 성숙 및 배란을, 수컷에서는 정액 사출을 유도함을 확인하였다. 추후 인공수정에 적용할 수 있도록 Ovaprim®의 농도 및 투여 주기를 최적화한 결과는 다음과 같았다: 까치상어 수컷: 0.2 mL/kg 투여 1시간 뒤 정액 샘플링; 까치상어 암컷: 0.2 mL/kg 투여 24시간 뒤 0.5 mL/kg 2차

투여; 화이트팁 상어 수컷: 0.2 mL/kg 투여 직후 정액 샘플링; 화이트팁 상어 암컷: 0.2 mL/kg 투여 24시간 뒤 0.2 mL/kg 또는 0.3 mL/kg 2차 투여.

주요어 : 상어, 보조생식기술, 컴퓨터 단층촬영, 자기공명영상, 정액 동결보존, 호르몬유도 배란, *Triakis scyllium, Triaenodon obesus.*

학 번 : 2019-39492

PUBLISHED ARTICLES

2021

1. **Sang Wha Kim**, Won Hee Hong, Seunghwan Choi, Seong Soo Lim, Jun Kwon, Sib Sankar Giri, Sang Guen Kim, Jeong Woo Kang, Sung Bin Lee, Su Jin Jo, Won Joon Jung, Young Min Lee, Goo Jang, Byeong Chun Lee, Byung Yeop Kim, Dong Wan Kim, Se Chang Park*. Preliminary study for banded houndshark (*Triakis scyllium*) semen cryopreservation: preparing for the *ex-situ* conservation of endangered shark species. *Biology.* (Under review)

2. **Sang Wha Kim**, Adams Hei Long Yuen, Cherry Tsz Ching Poon, Joon Oh Hwang, Chang Jun Lee, Moon Kwan Oh, Ki Tae Kim, Hyoun Joong Kim, Sib Sankar Giri, Sang Guen Kim, Jun Kown, Sung Bin Lee, Min Cheol Choi, Se Chang Park*. Cross-sectional anatomy, computed tomography, and magnetic resonance imaging of the banded houndshark (*Triakis scyllium*). *Scientific Reports*. doi: 10.1038/s41598-020-80823-y

3. Won Joon Jung, **Sang Wha Kim**, Sib Sankar Giri, Hyoun Joong Kim, Sang Guen Kim, Jeong Woo Kang, Jun Kwon, Sung Bin Lee, Woo Taek Oh, Jin Woo Jun, Se Chang Park*. *Janthinobacterium tructae* sp. nov., isolated from kidney of rainbow trout (*Oncorhynchus mykiss*). *Pathogens*. 10(2):229. doi: 10.3390/pathogens10020229

4. **Sang Wha Kim**, Seon Young Park, Hyemin Kwon, Sib Sankar Giri, Sang Guen Kim, Jeong Woo Kang, Jun Kwon, Sung Bin Lee, Won Joon Jung, Jun Mo Lee, Se Chang Park*, Ji Hyung Kim. Complete mitochondrial genome and phylogenetic analysis of the copper shark *Carcharhinus brachyurus* (Gunther, 1870). *Mitochondrial DNA Part B.* 6(6):1659–1661, doi: 10.1080/23802359.2021. 1920863

5. Jun Kwon, **Sang Wha Kim**, Sang Guen Kim, Jeong Woo Kang, Won Joon Jung, Sung Bin Lee, Young Min Lee, Sib Sankar Giri, Cheng Chi, Se Chang Park*. The characterization of a novel phage, pPa_SNUABM_DT01, infecting *Pseudomonas aeruginosa*. *Microorganisms*. 9(10): 2040, doi: 10.3390/microorganisms9102040

6. Jun Kwon, Sang Geun Kim, Hyoun Joong Kim, Sib Sankar Giri, **Sang Wha Kim**, Sung Bin Lee, Se Chang Park*. Isolation and characterization of

Salmonella jumbo-phage pSal-SNUABM-04. *Viruses*. 13(1): 27. doi: 10.3390/v13010027

7. Jun Kwon, Sang Geun Kim, Hyoun Joong Kim, Sib Sankar Giri, **Sang Wha Kim**, Sung Bin Lee, Se Chang Park*. Bacteriophage as an alternative to prevent reptile-associated *Salmonella* transmission. *Zoonoses And Public Health*. doi: 0.1111/zph.12804

8. Sib Sankar Giri, Sang Guen Kim, Jeong Woo Kang, **Sang Wha Kim**, Jun Kwon, Sung Bin Lee, Won Joon Jung, Se Chang Park. Applications of carbon nanotubes and polymeric micro-/nano-particles in fish 2 vaccine delivery: progress and future perspectives. *Reviews in Aquaculture*. doi: 10.1111/raq.12547

9. Won Joon Jung, Hyoun Joong Kim, Sib Sankar Giri, Sang Guen Kim, **Sang Wha Kim**, Jeong Woo Kang, Jun Kwon, Sung Bin Lee, Woo Taek Oh, Jin Woo Jun, Se Chang Park*. *Citrobacter tructae* sp. nov. isolated from kidney of diseased rainbow trout (*Oncorhynchus mykiss*). *Microorganisms*. 9(2): 275, doi: 10.3390/microorganisms9020275

10. Sang Guen Kim, Sib Sankar Giri, Saekil Yun, Hyoun Joong Kim, **Sang Wha Kim**, Jeong Woo Kang, Sung Bin Lee, Won Joon Jung, Se Chang Park*. Strategy for mass production of lytic *Staphylococcus aureus* bacteriophage pSa-3: contribution of multiplicity of infection and response surface methodology. *Microbial Cell Factories*. 2021(20):56, doi: 10.1186/s12934-021-01549-8

11. Sang Guen Kim, Sib Sankar Giri, Saekil Yun, **Sang Wha Kim**, Se Jin Han, Jun Kwon, Woo Teak Oh, Sung Bin Lee, Yong Ho Park, Se Chang Park*. Two novel bacteriophages control multidrug- and methicillin-resistant *Staphylococcus pseudintermedius* biofilm. *Frontiers in Medicine*. 2021(8):524059, doi: 10.3389/fmed.2021.524059

12. Sib Sankar Giri, Min Jung Kim, Sang Guen Kim, **Sang Wha Kim**, Jeong Woo Kang, Jun Kwon, Sung Bin Lee, Won Joon Jung, Venkatachalam Sukumaran, Se Chang Park*. Role of dietary curcumin against waterborne lead toxicity in common carp *Cyprinus carpio*. *Ecotoxicology and Environmental Safety*. 2021(219):112318, doi: 10.1016/j.ecoenv.2021.112318

13. Sang Guen Kim, Eunjung Roh, Jungkum Park, Sib Sankar Giri, Jun Kwon, **Sang Wha Kim**, Jeong Woo Kang, Sung Bin Lee, Won Joon Jung, Young Min

Lee, Kevin Cho, Se Chang Park*. The bacteriophage pEp_SNUABM_08 is a novel singleton Siphovirus with high host specificity for *Erwinia pyrifoliae*. *Viruses*. 13(7):1231. doi: 10.3390/v13071231

14. Sib Sankar Giri, Hyoun Joong Kim, Sang Guen Kim, **Sang Wha Kim**, Jun Kwon, Sung Bin Lee, Kang Jeong Woo, Won Joon Jung, Min Jung Kim, Venkatachalam Sukumaran, Se Chang Park*. Effects of Dietary *Lactiplantibacillus plantarum* subsp. plantarum L7, alone or in combination with *Limosilactobacillus reuteri* P16, on growth, mucosal immune responses, and disease resistance of *Cyprinus carpio*. *Probiotics and Antimicrobial Proteins*. doi: 10.1007/s12602-021-09820-5

2020

1. **Sang Wha Kim**, Won Hee Hong, Se Jin Han, Jin Woo Jun, Heejun Ko, Sung Bin Lee, Sib Sankar Giri, Sang Guen Kim, Byung Yeop Kim, Goo Jang, Byeong Chun Lee, Dong Wan Kim, Se Chang Park*. Use of synthetic salmon GnRH and domperidone (Ovaprim®) in sharks: preparation for *ex-situ* conservation. *Frontiers in Marine Science*. 7: 571741. doi: 10.3389/fmars.2020.571741

2. **Sang Wha Kim**, Sib Sankar Giri, Sang Guen Kim, Jun Kwon, Woo Taek Oh, Se Chang Park*. Carp edema virus and cyprinid herpesvirus-3 coinfection is associated with mass mortality of koi (*Cyprinus carpio haematopterus*) in the Republic of Korea. *Pathogens*. 9(3): 222. doi: 10.3390/pathogens9030222

3. Jessica A. Weber, Seung Gu Park, Victor Luria, Sungwon Jeon, Hak-Min Kim, Yeonsu Jeon, Youngjune Bhak, Je Hun Jun, **Sang Wha Kim**, Won Hee Hong, Semin Lee, Yun Sung Cho, Amir Karger, John W. Cain, Andrea Manica, Soonok Kim, Jae-Hoon Kim, Jeremy S. Edwards, Jong Bhak, and George M. Church. The whale shark genome reveals how genomic and physiological properties scale with body size. *PNAS*. 117(34): 20661-20671. doi: 10.1073/pnas.1922576117

4. Saekil Yun, Seung-Jun Lee, Sib Sankar Giri, Hyoun Joong Kim, Sang Geun, Kim, **Sang Wha Kim**, Se Jin Han, Jun Kwon, Woo Taek Oh, Se Chang Park*. Vaccination of fish against *Aeromonas hydrophila* infections using the novel approach of transcutaneous immunization with dissolving microneedle patches in aquaculture. *Fish and Shellfish Immunology*. 2020(97): 34-40. doi: 10.1016/j.fsi.2019.12.026

5. Sib Sankar Giri, Jin Woo Jun, SaekilYun, Hyoun Joong Kim, Sang Guen Kim, **Sang Wha Kim**, Jeong Woo Kang, Se Jin Han, Woo Taek Oh, Jun Kwon, Venkatachalam Sukumaran, Se Chang Park*. Effects of dietary heat-killed *Pseudomonas aeruginosa* strain VSG2 on immune functions, antioxidant efficacy, and disease resistance in *Cyprinus carpio*. *Aquaculture*. 514: 734489. doi: 10.1016/j.aquaculture.2019.734489

6. Jun Kwon, Sang Guen Kim, **Sang Wha Kim**, Saekil Yun, Hyoun Joong Kim, Sib Sankar Giri, Se Jin Han, Woo Teak Oh, Se Chang Park*. A case of mortality caused by *Aeromonas hydrophila* in wild-caught red-eyed crocodile skinks (*Tribolonotus gracilis*). *Veterinary Sciences*. 2020, 7(1), 4. doi: 10.3390/vetsci7010004

7. Sang Guen Kim, Sib Sankar Giri, Saekil Yun, Hyoun Joong Kim, **Sang Wha Kim**, Jeong Woo Kang, Se Jin Han, Woo Taek Oh, Se Chang Park*. Genomic characterization of bacteriophage pEt-SU, a novel phiKZ-related virus infecting *Edwardsiella tarda*. *Archives of Virology*. 2020(165): 219-222. doi: 10.1007/s00705-019-04432-5

8. Woo Taek Oh, Jin Woo Jun, Hyoun Joong Kim, Sib Sankar Giri, SaekilYun, Sang Geun Kim, **Sang Wha Kim**, Jung Woo Kang Se Jin Han, Jun Kwon, Se Chang Park*. Characterization and pathological analysis of a virulent *Edwardsiella anguillarum* strain isolated from Nile tilapia (*Oreochromis niloticus*) in Korea. *Frontiers in Veterinary Science*. 7: 14. doi: 10.3389/fvets.2020.00014

9. Woo Taek Oh, Jin Woo Jun, Sib Sankar Giri, SaekilYun, Hyoun Joong Kim, Sang Geun Kim, **Sang Wha Kim**, Jung Woo Kang Se Jin Han, Jun Kwon, Se Chang Park*. Morganella psychrotolerans as a possible opportunistic pathogen in rainbow trout (*Oncorhynchus mykiss*) fisheries. *Aquaculture*. 520: 735021. doi: 10.1016/j.aquaculture.2020.735021

10. Woo Taek Oh, Jin Woo Jun, Sib Sankar Giri, SaekilYun, Hyoun Joong Kim, Sang Geun Kim, **Sang Wha Kim**, Se Jin Han, Jun Kwon, Se Chang Park*. Isolation of *Chryseobacterium siluri* sp. nov., from liver of diseased catfish (*Silurus asotus*). *Heliyon*. 6(2): e03484. doi: 10.1016/j.heliyon.2020.e03454

11. Saekil Yun, Sung Young Yoon, Eun Jeong Hong, Sib Sankar Giri, Sang Geun Kim, **Sang Wha Kim**, Se Jin Han, Jun Kwon, Woo Taek Oh, Sung Bin Lee, Se Chang Park*. Effect of plasma-activated water, used as a disinfectant, on the

hatch rate of dormant cysts of the *Artemia salina*. *Aquaculture*. 523: 735232. doi: 10.1016/j.aquaculture.2020.735232

12. Hyoun Joong Kim, Jin Woo Jun, Sib Sankar Giri, Cheng Chi, Saekil Yun, Sang Guen Kim, **Sang Wha Kim**, Se Jin Han, Jun Kwon, Woo Taek Oh, Hyung Bae Jeon, Ji Hyung Kim, Se Chang Park*. Identification and genome analysis of *Vibrio coralliilyticus* causing mortality of Pacific oyster (*Crassostrea gigas*) Larvae. *Pathogens*. 9(3): 206. doi: 10.3390/pathogens9030206

13. Jin Woo Jun, Jeong Woo Kang, Sib Sankar Giri, SaekilYun, Hyoun Joong Kim, Sang Geun Kim, **Sang Wha Kim**, Se Jin Han, Jun Kwon, Woo Taek Oh, Se Chang Park*. Immunostimulation by starch hydrogel-based oral vaccine using formalin-killed cells against edwardsiellosis in Japanese eel, *Anguilla japonica*. *Vaccine*. 38(22): 8. doi: 10.1016/j.vaccine.2020.03.046

14. Sang Guen Kim, Sib Sankar Giri, Saekil Yun, Hyoun Joong Kim, **Sang Wha Kim**, Jeong Woo Kang, Se Jin Han, Jun Kown, Woo Taek Oh, Jin Woo Jun, Se Chang Park*. Synergistic phage-surfactant combination clears IgE-promoted *Staphylococcus aureus* aggregation *in vitro* and enhances the effect *in vivo*. *International Journal of Antimicrobial Agents*. 56(1): 105997. doi: 10.1016/j.ijantimicag. 2020.105997

15. Sang Guen Kim, Sib Sankar Giri, **Sang Wha Kim**, Jun Kown, Sung Bin Lee, Se Chang Park*. First isolation and characterization of *Chryseobacterium cucumeris* SKNUCL01, isolated from diseased pond loach (*Misgurnus anguillicaudatus*) in Korea. *Pathogens*. 9(5): 397. doi: 10.3390/ pathogens9050397

16. Hyoun Joong Kim, Sib Sankar Giri, Sang Guen Kim, **Sang Wha Kim**, Jun Kwon, Sung Bin Lee, Se Chang Park*. Isolation and characterization of two bacteriophages and their preventive effects against pathogenic *Vibrio coralliilyticus* causing mortality of Pacific oyster (*Crassostrea gigas*) larvae. *Microorganisms*. 8(6): 926. doi: 10.3390/microorganisms8060926

17. Sib Sankar Giri, Hyoun Joong Kim, Sang Guen Kim, **Sang Wha Kim**, Jun Kwon, Sung Bin Lee Venkatachalam Sukumaran, Se Chang Park*. Effectiveness of the guava leaf extracts against lipopolysaccharide-induced oxidative stress and immune responses in *Cyprinus carpio*. *Fish and Shellfish Immunology*. 2020(105): 164-176. doi: 10.1016/j.fsi.2020.06.004

18. Sib Sankar Giri, Hyoun Joong Kim, Sang Guen Kim, **Sang Wha Kim**, Jun Kwon, Sung Bin Lee, Se Chang Park*. Immunomodulatory role of microbial surfactants, with special emphasis on fish. *International Journal of Molecular Sciences*. 21(19): 7004. doi: 10.3390/ijms21197004

19. Hyoun Joong Kim, Jin Woo Jun, Sib Sankar Giri, Sang Guen Kim, **Sang Wha Kim**, Jun Kwon, Sung Bin Lee, Cheng Chi, Se Chang Park*. Bacteriophage cocktail for the prevention of multiple-antibiotic-resistant and mono-phage-resistant *Vibrio coralliilyticus* infection in Pacific oyster (*Crassostrea gigas*) Larvae. *Pathogen*. 9: 831. doi: 10.3390/pathogens9100831

20. Sang Guen Kim, Sung Bin Lee, Sib Sankar Giri, Hyoun Joong Kim, **Sang Wha Kim**, Jun Kown, JungKum Park, Eunjung Roh, Se Chang Park*. Characterization of novel *Erwinia amylovora* jumbo bacteriophages from *Eneladusvirus* Genus. *Viruses*. 12: 1373. doi: 10.3390/v12121373

21. Jun Kwon, **Sang Wha Kim**, Geun Kim, Hyoun Joong Kim, Sib Sankar Giri, Se Chang Park*. Bacterial osteomyelitis induced by *Morganella morganii* in a bearded dragon (*Pogona vitticeps*). *Journal of Veterinary Clinics*. 37(6), 342-344. doi:10.17555/jvc.2020.12.37.6.342

2019

1. **Sang Wha Kim**, Se Jin Han, Young Ran Lee, Byung Yeop Kim, Se Chang Park*. First report of a Risso's dolphin (*Grampus griseus*) stranded in Jeju Island, Republic of Korea: findings from necropsy, histopathology and microbiome analysis. *Veterinary Record Case Reports*. 7 :e000860. doi: 10.1136/vetreccr-2019-000860

2. Deok-Soo Kim*, Joonghyun Ryu, Youngsong Cho, Mokwon Lee, Jehyun Cha, Chanyoung Song, **Sang Wha Kim**, Roman A. Laskowski, Kokichi Sugihara, Jong Bhak, and Seong Eon Ryu. MGOS: A library for molecular geometry and its operating system. *Computer Physics Communications*. 251: 107101. doi: 10.1016/j.cpc.2019.107101

3. Saekil Yun, Jin Woo Jun, Sib Sankar Giri, Hyoun Joong Kim, Cheng Chi, Sang Geun, Kim, **Sang Wha Kim**, Jung Woo Kang, Se Jin Han, Jun Kwon, Woo Taek Oh, Se Chang Park*. Immunostimulation of *Cyprinus carpio* using phage lysate of *Aeromonas hydrophila*. *Fish and Shellfish Immunology*. 86: 680-687. doi: 10.1016/j.fsi.2018.11.076

4. Sib Sankar Giri, Jin Woo Jun, Saekil Yun, Hyoun Joong Kim, Sang Guen Kim, Jeong Woo Kang, **Sang Wha Kim**, Se Jin Han, Se Chang Park*. V. Sukumaran. Characterisation of lactic acid bacteria isolated from the gut of *Cyprinus carpio* that may be effective against lead toxicity. *Probiotics and Antimicrobial Proteins*. 11(1), 65-73. doi: 10.1007/s12602-017-9367-6

5. Jin Woo Jun, Jeong Woo Kang, Sib Sankar Giri, SaekilYun, Hyoun Joong Kim, Sang Guen Kim, **Sang Wha Kim**, Se Jin Han, Jun Kwon, Woo Taek Oh, Dal sang Jeong, Se Chang Park*. Superiority of PLGA microparticle-encapsulated formalin-killed cell vaccine in protecting olive flounder against *Streptococcus parauberis*. *Aquaculture*. 509: 67-71. doi: 10.1016/j.aquaculture.2019.04.079

6. Saekil Yun, Sib Sankar Giri, Hyoun Joong Kim, Sang Geun Kim, **Sang Wha Kim**, Jung Woo Kang Se Jin Han, Jun Kwon, Woo Taek Oh, Cheng Chi, Jin Woo Jun, Se Chang Park*. Enhanced bath immersion vaccination through microbubble treatment in the cyprinid loach. *Fish and Shellfish Immunology*. 91: 12-18. doi: 10.1016/j.fsi.2019.05.021

7. Cheng Chi, Sib Sankar Giri, Jin Woo Jun, Hyoun Joong Kim, Saekil Yun, **Sang Wha Kim**, Jeong Woo Kang, Se Chang Park*. Detoxification, apoptosis, and immune transcriptomic responses of the gill tissue of bay scallop following exposure to the algicide thiazolidinedione 49. *Biomolecules*. 9(8): 310. doi: 10.3390/biom9080310

8. Woo Taek Oh, Sib Sankar Giri, SaekilYun, Hyoun Joong Kim, Sang Geun Kim, **Sang Wha Kim**, Jung Woo Kang, Se Jin Han, Jun Kwon, Jin Woo Jun, Se Chang Park*. Emergence of rickettsial infection in rainbow trout (*Oncorhynchus mykiss*) fry displaying the appearance of red mark syndrome in Korea. *Microorganisms*. 7(9): 302. doi: 10.3390/microorganisms7090302

9. Woo Taek Oh, Jin Woo Jun, Sib Sankar Giri, SaekilYun, Hyoun Joong Kim, Sang Geun Kim, **Sang Wha Kim**, Jung Woo Kang Se Jin Han, Jun Kwon, Ji Hyung Kim, THM Smits, Se Chang Park*. *Pseudomonas tructae* sp. nov., novel species isolated from rainbow trout kidney. *International Journal of Systematic and Evolutionary Microbiology*. 69: 3851-3856. doi: 10.1099/ijsem.0.003696

10. Woo Taek Oh, Jin Woo Jun, Sib Sankar Giri, SaekilYun, Hyoun Joong Kim, Sang Geun Kim, **Sang Wha Kim**, Se Jin Han, Jun Kwon, Se Chang Park*. *Staphylococcus xylosus* infection in rainbow trout (*Oncorhynchus mykiss*) as a primary pathogenic cause of eye protrusion and mortality. *Microorganisms*. 7(9):

330. doi: 10.3390/microorganisms7090330

11. Woo Taek Oh, Sib Sankar Giri, SaekilYun, Hyoun Joong Kim, Sang Geun Kim, **Sang Wha Kim**, Jung Woo Kang, Se Jin Han, Jun Kwon, Jin Woo Jun, Se Chang Park*. *Janthinobacterium lividum* as an emerging pathogenic bacterium affecting rainbow trout (*Oncorhynchus mykiss*) fisheries in Korea. *Pathogens*. 8(3): 146. doi: 10.3390/pathogens8030146

12. Hyoun Joong Kim, Jin Woo Jun, Sib Sankar Giri, Cheng Chi, Saekil Yun, Sang Guen Kim, **Sang Wha Kim**, Jeong Woo Kang, Se Jin Han, Jun Kwon, Kw Hun On, Woo Taek Oh, Se Chang Park*. Application of the bacteriophage pVco-14 to prevent *Vibrio coralliilyticus* infection in Pacific oyster (*Crassostrea gigas*) larvae. *Journal of Invertebrate Pathology*. 11: 107244. doi: 10.1016/j.jip.2019.107244

13. Cheng Chi, Saekil Yun, Sib Sankar Giri, Hyoun Joong Kim, **Sang Wha Kim**, Jeong Woo Kang, Se Chang Park*. Effect of the algicide thiazolidinedione 49 on immune responses of bay scallop *Argopecten irradians*. *Molecules*. 24(19): 3579. doi: 10.3390/molecules24193579

14. Woo Taek Oh, Ji Hyung Kim, Jin Woo Jun, Sib Sankar Giri, Saeki lYun, Hyoun Joong Kim, Sang Geun Kim, **Sang Wha Kim**, Se Jin Han, Jun Kwon, Se Chang Park*. Genetic characterization and pathological analysis of a novel bacterial pathogen, *Pseudomonas tructae*, in rainbow trout (*Oncorhynchus mykiss*). *Microorganisms*. 7(10): 432. doi: 10.3390/microorganisms7100432

15. Woo Taek Oh, Jin Woo Jun, Sib Sankar Giri, Saekil Yun, Hyoun Joong Kim, Sang Geun Kim, **Sang Wha Kim**, Se Jin Han, Jun Kwon, Se Chang Park*. Genome and phylogenetic analysis of infectious hematopoietic necrosis virus strain SNU1 isolated in Korea. *Pathogens*. 8(4): 200. doi:10.3390/pathogens8040200

16. Sang Guen Kim, Sib Sankar Giri, Saekil Yun, Hyoun Joong Kim, **Sang Wha Kim**, Jeong Woo Kang, Se Jin Han, Woo Taek Oh, Se Chang Park*. Genomic characterization of bacteriophage pEt-SU, a novel phiKZ-related virus infecting *Edwardsiella tarda*. *Archives of Virology*. 165: 219-222. doi: 10.1007/s00705-019-04432-5

CONFERENCE PROCEEDINGS

2021

1. Jun Kwon, Sang Guen Kim, **Sang Wha Kim**, Sung Bin Lee, Won Joon Jung, Jeong Woo Kang, Sib Sankar Giri, Se Chang Park*. Topical bacteriophage application, a promising alternative against dog otitis externa. Oxford Bacteriophage Conference – Phages 2021. Virtual conference, 7th September – 8th September, 2021.

2. Jun Kwon, Sang Guen Kim, Sib Sankar Giri, Hyoun Joong Kim, **Sang Wha Kim**, Jung Woo Kang, Sung Bin Lee, Won Jun Jeong, Se Chang Park*. Genomic characterization of bacteriophage pSal-SNUABM-01, a novel elongated head phage infecting *Salmonella sp*. The Korean Society of Veterinary Science Autumn Conference 2021. GSCO Gunsan, North Jeolla Province, Republic of Korea, 28th October – 30th October, 2021.

2020

3. **Sang Wha Kim**, Won Hee Hong, Hyoun Joong Kim, Sang Guen Kim, Jun Kwon, Sung Bin Lee, Won Joon Jung, Jeong Woo Kang, Byung Yeop Kim, Se Chang Park*. Assisted reproductive technologies in shark: First report of hormone-induced artificial insemination and sperm cryopreservation in Chondrichthyes. The Korean Society of Veterinary Science Autumn Conference 2020. Hongcheon, Gangwon-do, Republic of Korea, 19th November – 21st November, 2020.

4. **Sang Wha Kim**, Jun Kwon, Hyoun Joong Kim, Sang Guen Kim, Sung Bin Lee, Won Joon Jung, Jeong Woo Kang, Se Chang Park*. Bacteriophage phage topical, a promising alternative against dog otitis externa. The Korean Society of Veterinary Science Autumn Conference 2020. Hongcheon, Gangwon-do, Republic of Korea, 19th November – 21st November, 2020.

2019

1. **Sang Wha Kim**, Won Hee Hong, Jun Kwon, Se Jin Han, Byung Yeop Kim, Se Chang Park*, 2019. First report of Ovaprim™ application in shark: Induction of oocyte development, ovulation, and semen release by Ovaprim™ injection in

banded houndshark (*Triakis scyllium*). Marine Biotechnology Converence 2019. Shizuoka, Japan, 9th September – 13th September, 2019.

2. **Sang Wha Kim**, Won Hee Hong, Jun Kwon, Se Jin Han, Byung Yeop Kim, Se Chang Park*, 2019. First report of Ovaprim™ application in shark: Induction of oocyte development, ovulation, and semen release by Ovaprim™ injection in banded houndshark (*Triakis scyllium*). 2019 Education, Research & Development Day. Seoul, Korea, 11st November – 13th November, 2019.

3. Woo Taek Oh, Jin Woo Jun, **Sang Wha Kim**, Se Jin Han, Se Chang Park*, 2019. Emergence of rickettsial infection in rainbow trout (*Oncorhynchus mykiss*) fry displaying the appearance of red mark syndrome in Korea. Marine Biotechnology Converence 2019. Shizuoka, Japan, 9th September – 13th September, 2019.

4. Sib Sankar Giri, Saekil Yun, Hyoun Joong Kim, Sang Guen Kim, **Sang Wha Kim**, Se Jin Han, Woo Taek Oh, Jun Kwon, V. Sukumaran, Se Chang Park*, 2019. Effects of dietary heat-killed *Pseudomonas aeruginosa* strain VSG2 on immune functions, antioxidant efficacy, and disease resistance of *Cyprinus carpio*. Marine Biotechnology Converence 2019. Shizuoka, Japan, 9th September – 13th September, 2019.

감사의 글

제가 하고싶은 연구를 마음껏 할 수 있었던, 감사하고도 황송한 박사과정 기간이었습니다. 많은 분들께 도움을 받았기에 학위를 무사히 마칠 수 있었던 만큼, 감사의 말씀을 전하고 싶은 분들이 많습니다.

원하는 대로 도전하며 연구를 할 수 있도록 넓은 울타리를 쳐 주신 박세창 교수님께 누구보다 큰 감사의 말씀을 전하고 싶습니다. 현실과 이상 사이에서 절묘한 가이드를 잡아 주셨기에 제가 큰 좌절 없이, 그러나 도전적인 태도를 잃지 않으면서 학위과정을 지나올 수 있었습니다. 긴 기간동안 균형 잡힌 삶을 살 수 있는 삶의 지혜와, 연구를 추진해 나갈 수 있는 힘을 심어 주셨던 바, 진심으로 감사드립니다. 야생 상어와 사육 상어를 찾아 제주도를 제 집처럼 드나들며 연구했던 학위 기간은 제 인생에서 가장 자유롭고 행복했던 기간이었기에 평생 잊지 못할 것 같습니다. 저를 믿어 주시고, 자유롭게 연구에 매진할 수 있는 환경을 만들어 주셔서 감사드립니다. 부족한 점이 많은 저를 한 명의 박사로 키워내 주신 이 은혜, 평생토록 잊지 않겠습니다.

제주도의 야생 상어 샘플링은 김병엽 교수님이 계셨기에 가능했던 일이었습니다. 필드를 접하지 않는 형태의 야생동물 연구는 탁상공론과 같아질 수 있다고 생각합니다. 교수님께서 물심양면으로 도와 주신 덕분에 논문에서만 보던 수많은 상어들을 실제로 접하며 연구를 수행할 수 있었고, 제가 성장할 수 있는 기회를 얻을 수 있었습니다. 제 박사학위의 주 무대로 제주도를 선택할 수 있게 여건을 마련해 주셔서

진심으로 감사드립니다. 교수님께서 기울여 주신 노고가 정말 크다는 것을 잘 알고 있는 바, 은혜를 잊지 않겠습니다.

상어를 대상으로 하는 큰 스케일의 실험을 실제로 수행할 수 있었던 것은 아쿠아리움과의 협업을 이끌어내 주신 홍원희 수의사님의 노력이 있었기 때문임을 잘 알고 있습니다. 가장 힘들었던 시기에, 제게 '이대로 꾸준히 연구해서 상어 전문가가 되었으면 좋겠다'고 담담히 말씀해 주셨던 날의 기억이 아직도 제 마음에 따뜻하게 남아있습니다. 다정함과 지혜로움으로 곁에서 저를 응원해 주셨던 것 잊지 않겠습니다. 정말 감사드립니다.

부족한 제 글을 박사 졸업논문에 합당한 수준으로 끌어 올려 주신 심사위원분들께도 감사의 말씀을 전하고 싶습니다. 바쁘신 와중에 흔쾌히 심사위원장을 맡아 주신 윤화영 교수님께 진심으로 감사의 말씀을 드립니다. 대학원 입학 직후부터 제 연구에 다양한 조언을 아끼지 않으셨던 김지형 박사님, 여쭙고 싶고 닮고 싶은 점이 너무 많아 제가 꾸준히 귀찮게 연락 드려 온 한지은 교수님, 같은 실험실에서 생활하면서 연구하시는 모습을 직접 보고 배울 수 있었던 전진우 교수님 모두 감사드립니다. 아직 부족한 점이 많다는 것을 잘 알고 있기에, 일러주신 방향으로 더 나은 연구자가 되기 위해 최선을 다해 노력하겠습니다.

비슷한 시기에 학위 과정을 함께 하며 동고동락했던 최지은, 김다현에게도 정말 고맙다는 말을 전하고 싶습니다. 학자로서 존경스러운 면모를 갖춘 두 친구의 조언과 위로가 함께 했기에 박사과정 기간을 지혜롭게 지나갈 수 있었습니다. 때로는 공감해 주며, 때로는 실질적으로 연구에 도움을 주며 제게 힘이 되어 주었던 두 분에게 큰

감사를 드립니다. 능력적으로도 출중하고 마음도 넓은 두 사람과 함께 이 시기를 지낼 수 있었던 것은 제게 큰 행운이었습니다. 앞으로 각자 더 성장하여, 언젠가 함께 멋진 연구를 할 수 있는 날이 오기를 기원합니다.

긴 시간 실험실 생활을 함께 하며 성장해 온 김상근, 강정우, 권준, 이성빈, 정원준에게 고마웠다는 말을 전하고 싶습니다. 지금은 졸업하고 제주도에 있는 김현중 박사님과, 한결같은 모습으로 실험실에서 열일하고 계신 기리 박사님께도 고마움을 전하고 싶습니다. 합력해서 연구를 수행해가는 과정을 좋은 사람들과 함께 할 수 있어서 감사했습니다. 발리, 코타키나발루, 칭다오, 시즈오카 등 세계 곳곳을 함께하며 쌓은 추억들이 눈앞에 선합니다. 코로나의 끝에 한 번 더 함께 추억을 쌓을 기회가 닿기를 진심으로 기원합니다. 또 입학한지 얼마 되지 않은 영민이와 수진이에게는 응원의 말을 전하고 싶습니다. 두 분 다 학위기간동안 잘 해낼 것을 믿어 의심치 않습니다.

학자가 되고 싶은 제 삶에 가장 소중한 롤모델은 제 아버지, 김덕수 교수님 이셨습니다. 아버지의 인생은 그 자체로 제게 가능성을 보여주고, 용기를 불어넣어주었습니다. 박사과정 내내 다양한 어려움을 맞닥뜨렸었지만, 되돌아보면 이런 상황을 정면으로 돌파해 나가셨던 아버지의 모습을 저는 이미 어릴 때부터 지켜봐 왔더군요. 평생에 걸쳐 도전하고, 증명해 내고, 일궈내며 인류의 지식에 공헌해 오신 아버지 곁에서 배울 수 있음에 그저 감사할 따름입니다. 인생 자체가 하나의 작품이 될 수 있음을, 아버지의 삶을 바라보면서 배웠습니다. 은하수를 여행하려는 제 삶의 원동력이자 가이드가 되어 주셔서 감사하고, 사랑합니다.

이 세상에서 가장 사랑하는 사람, 나의 어머니 이해진, 말로 표현할 수 없이 감사드립니다. 소울메이트 마냥 하는 생각과 느끼는 바가 비슷한 어머니가 있어서 제가 지금처럼 굳건히 설 수 있었습니다. 너무나 쉽게 휘어지는 마음이, 휘어질진대 꺾일 필요는 없다는 것을 인생에 걸쳐 제게 가르쳐 주신 어머니 덕분에 제가 이리 굳게 서있을 수 있었습니다. 짧은 풀포기일 지언정 뿌리는 저 깊숙이까지 내딛고 있는 제 삶이 이제는 참 안정적입니다. 어머니가 계셨기에 제 마음에 그늘짐 없이, 이 세상 곳곳으로 제 꿈을 좇아 날아다닐 수 있었습니다. 내가 아는 그 누구보다 강인하고 지혜로운 사람, 이해진이 내 어머니라서 하나님께 감사합니다.

마지막으로, 박사학위 과정 중 저와 평생을 함께 하기로 결심하고 제 남편이 되어준 유정하에게 고맙다는 말을 전하고 싶습니다. 제 삶을 있는 그대로 인정하고 존중해 주는 당신이 있기에 안정적으로, 그리고 전력을 다해서 꿈을 좇을 수 있었습니다. 학위과정동안 흔들림 없이 보내준 지지에 진심으로 감사드립니다. 저 또한 당신의 삶을 존중하고 존경합니다. 이 우주에 남은 시간만큼 사랑합니다.

2021 년 10 월

김 상 화